DOCTOR OF PHILOSOPHY

Novel complexes of Molybdenum and Tungsten in materials chemistry

Parker, Emma Elizabeth

Award date:
1996

Awarding institution:
University of Wales, Bangor

Link to publication

NOVEL COMPLEXES OF

MOLYBDENUM AND TUNGSTEN

IN MATERIALS CHEMISTRY

A thesis submitted to the

University of Wales

by

Emma Elizabeth Parker
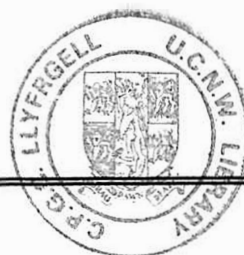
In candidature for the degree of

Philosophiae Doctor

University of Wales

Bangor

1996

For my Grandad,

Eddie Umpleby.

Abstract

The reactions of $[MI_2(CO)_3(NCMe)_2]$ {M = Mo or W} with two equivalents of the fluorescent ligand, 4,5-dihydro-($2H$)-1-phenyl-3-(p-cyanophenyl)-5-(p-benzoic acid)-pyrazole ($C_{23}H_{17}N_3O_2$), gave the new seven co-ordinate complexes $[MI_2(CO)_3(C_{23}H_{17}N_3O_2)_2]$ {M = Mo or W}. The fluorescence of the complexes was found to be very similar to that of the free ligand. The reaction of $[Mo(CO)_6]$ with one equivalent of $C_{23}H_{17}N_3O_3$ gave the new six co-ordinate fluorescent complex, $[Mo(CO)_5(C_{23}H_{17}N_3O_2)]$. The complexes $[Mo(CO)_5(L)]$ and $[MoI_2(CO)_3(L)_2]$ {L fluorescent ligand} exhibited third-order nonlinear optical effects.

The novel 1,2-dithiolene complexes, $[W(X)(CO)_2(L)]$ {X = dmit, mnt or bdt, L = $(PEt_3)_2$, $(PPh_3)_2$ or dppe; X = TTFS$_4$, L = $(PPh_3)_2$} were prepared and fully characterised. The structures of the complexes $[W(dmit)(CO)_2(L)]$ {L = $(PEt_3)_2$} and $[W(bdt)(CO)_2(L)]$ {L = $(PEt_3)_2$ and dppe} were determined by X-ray crystallography. The previously reported complex $[WI_2(CO)_3(PEt_3)_2]$ was synthesised by a new route and the structure determined by X-ray crystallography.

The reactions of 3-bromothiophene with a range of Grignard reagents of the type $[Ph(CH_2)_nMgBr]$ and $[PhO(CH_2)_nMgBr]$ {n = 1-6} were investigated. The subsequent reactions of the arene-substituted thiophenes with the complexes fac-$[M(CO)_3(NCMe)_3]$ were studied. The reaction of $[M(CO)_6]$ and fac-$[M(CO)_3(NCMe)_3]$ with thiophene-3-acetonitrile are also described.

The new seven co-ordinate complexes $[WI_2(CO)_3(3-NCCH_2\{SC_4H_3\})(L)]$ {L = PPh$_3$, or AsPh$_3$} were synthesised by the reaction of $[WI_2(CO)_3(NCMe)_2]$ with one equivalent of L {L = PPh$_3$ or AsPh$_3$} followed by the reaction with one equivalent of thiophene-3-acetonitrile. The reaction of $[WI_2(CO)_3(NCMe)_2]$ with two equivalents of thiophene-3-acetonitrile gave the complex, $[WI_2(CO)_3(3-NCCH_2\{SC_4H_3\})_2]$, which was galvanostatically electropolymerised, and the electrochemistry of both the monomer and the polymer were studied.

All the new complexes have been characterised by elemental analysis (C, H, N and S), infrared spectroscopy, ^{1}H NMR spectroscopy, and in selected cases, ^{13}C and ^{31}P NMR, UV / visible spectroscopy and cyclic voltammetry.

Acknowledgements

Contents

Abbreviations

acac	acetylacetonato
Ar	aryl
bdt	benzene-1,2-dithiol anion
bipy	bipyridyl
bzacac	benzylacetylacetonato
$C_{23}H_{17}N_3O_3$	4,5-dihydro-(*2H*)-1-phenyl-3-(*p*-cyanophenyl)-5-(*p*-benzoic acid)-pyrazole
Cp	cyclopentadienyl (C_5H_5)
Cy	cyclohexyl (C_6H_{11})
DFWM	Degenerate Four-Wave Mixing
DIOP	2,3-o-isopropylidene-2,3-dihydroxy-1,4-bis(diphenylphosphinobutane)
dmit	1,3-dithiole-2-thione-4,5-dithiolate anion
dppe	bis(diphenylphosphino)ethane
dppm	bis(diphenylphosphino)methane
dppp	bis(diphenylphosphino)propane
$Me_816[ane]S_4$	3,3,7,7,11,11,15,15-octamethyl-1,5,9,13-tetrathiacyclohexadecane
mnt	maleonitriledithiolate anion
NIR	Near Infrared
NLO	Nonlinear Optical
PMMA	polymethylmethacrylate
SHG	Second Harmonic Generation
TBA	tetrabutylammonium anion
TCNQ	tetracyano-7,7,8,8-quinodimethane
tdas	3,4-dichloro-1,2,5-thiadiazole
THG	Third Harmonic Generation
TMTSF	tetramethyltetraselenafulvalene
TTF	tetrathiafulvalene
$TTFS_4$	tetrathiafulvalenetetrathiolate
$3-SC_4H_3$	thiophene
$9[ane]S_3$	1,4,7-trithiacyclohexadecane

Chapter One

Introduction

1.1   MOLECULAR MATERIALS CHEMISTRY

The field of materials chemistry has become a flourishing research area for many scientists in a wide variety of disciplines for the last quarter of a century. Molecular electronics is a more specific term that may be applied to either the use of molecular materials in electronics or electronics at a molecular level [1]. Molecular electronics is poised at the intersection between chemistry, physics, electronic engineering, biochemistry and materials science [2].

The underpinning principle behind molecular electronics is the existence of an active molecule within the material. The active molecule can either be active in its own right, or be activated by association with other molecules. A great deal of work has been carried out on the design, preparation and study of materials that have the potential to exhibit the properties summarised in Figure 1.1. In all of the cases discussed in this introduction there is no 'set formula' for designing a molecule that will confer on a material the required properties; however there do seem to be certain attributes that make the chances of the molecule possessing these appropriate properties much greater.

MOLECULAR ELECTRONICS

| CONDUCTING MATERIALS | PHOTOCHROMIC MATERIALS | MOLECULAR MAGNETS | NON-LINEAR OPTICS | SUPRAMOLECULAR MATERIALS |
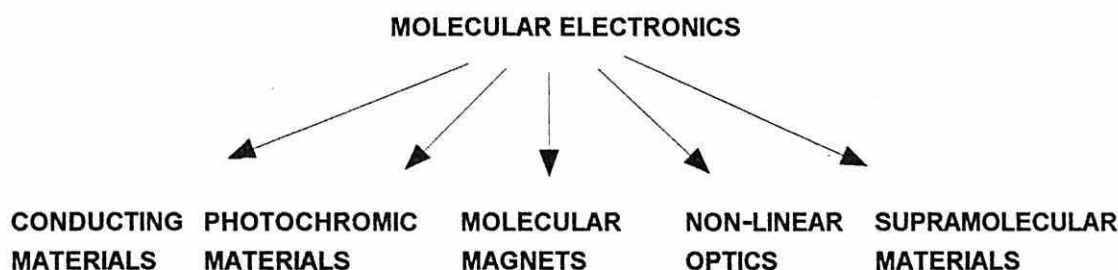
Figure 1.1 : Potential Properties associated with Molecular Electronics

2

1.1.1 Conducting Materials

The idea of organic and inorganic molecular materials functioning as molecular conductors and even superconductors, has led to a surge of research over the last twenty years since the first molecular conductor, TTF-TCNQ, see Figure 1.2, was prepared by Ferraris and Cowan in 1974 [3]. The class of compound known as molecular conductors can be envisaged as an assembly of molecules which exhibit metallic conductivity. Electron transport in these systems is usually highly anisotropic, that is the electrical conduction is several orders of magnitude higher in one or two preferred directions. Molecular conductors can be divided into three broad categories : C_{60} Fullerenes, Conducting Polymers and Molecular Metals. These classes can be further sub-divided, however this thesis is not directly concerned with molecular conductors and so they will not be discussed in great depth in this introduction.

Figure 1.2 : The Molecules TTF and TCNQ

Since the development of TTF-TCNQ, there has been a surge of research into these so-called charge transfer salts involving molecules that are based around a delocalised sulphur-containing heterocycle. It was envisaged that if molecules could be designed and synthesised that facilitated increased π-orbital overlap between the molecules then the delocalisation, and hence the conductivity, could be enhanced. This has led to the synthesis of complexes such as the metal-1,2-dithiolenes. A more detailed introduction to metal-1,2-dithiolenes is included in Chapter 3.

The essential difference between metals and non-metals lies in nature of the molecular

3

orbitals of the species. The high conductivities displayed by metals are characteristic of partially filled, spatially delocalised bands of molecular orbitals. The majority of molecular solids do not possess high conductivity and are insulators. To enable conduction to take place in molecular solids the following criteria should be satisfied :

- segregated stacks of donor and acceptor
- equidistant intrastack distances
- strong interstack interactions
- partial filling of the electronic band.

These requirements may be fulfilled by segregated stacks of planar, or almost planar, donor and acceptor molecules, as in TTF-TCNQ, see Figure 1.3.

```
D   A   D   A
D   A   D   A
D   A   D   A        Conduction Path
D   A   D   A
D   A   D   A
```
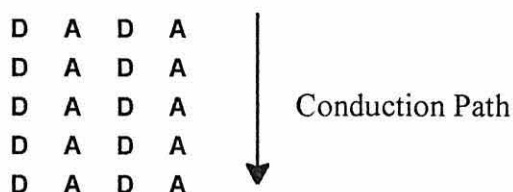
Figure 1.3 : Arrangement of Donor and Acceptors within a Molecular Conductor

As a chain of molecules are moved closer together, the molecular orbitals associated with them cease to remain discrete and effectively become an electronic band. The molecular orbitals of each individual molecule are not necessarily completely filled, for example in the case of lithium, the electronic configuration is $1s^2 2s^1$ so the highest occupied molecular orbital is only half-filled. If the constituent molecular orbitals are not completely filled, then there is the possibility the electronic band being only partially filled, this is known as 'Band Theory' [4 - 6]. Molecular materials often undergo Peierls Distortion [6, 7] of the electronic band structure and become insulators. A simplistic view of Peierls Distortion is the occurrence of distortions of the molecular structure that can induce distortions of the electronic structure, leading to the splitting of the electronic band at the Fermi level to form a filled and an unfilled band. Structures with a half-filled electronic band are succeptible to Peierls Distortion since there is a tendency for the

4

molecules to form dimers. In molecules such as TTF, see Figure 1.2, the planar structure enables the molecules to lie close together and create an electronic band, as a result the electron flow becomes uni-directional through the structure.

The first superconducting molecular charge transfer complex was reported by Bechgaard, Jerome and co-workers in 1980. The salt [TMTSF][PF$_6$] was found to be superconducting at 1K under 1.2 kbar (1200 atmospheres) pressure [8]. Since then the competition has been to develop materials that are superconductors closer to room temperature, for example β-[Me$_4$N][Pd(dmit)$_2$]$_2$ [9].

Conducting polymers come in the category of Molecular Conductors, however a detailed introduction to these materials is given in Chapter 4 and so they will not be discussed here.

1.1.2 Electrochromic Materials

The potential applications of coloured materials which have controllable absorption or transmission have generated immense interest. Electrochromic materials can be defined as materials that will reversibly change colour in response to an applied external potential. Many types of electrochromic substances have been reported and they may be divided into two classes : inorganic transition metal oxides and organic materials. The inorganic class of substances may be further subdivided into those that have reduced coloured states (cathodically colouring) and those with oxidised coloured states (anodically colouring). One of the most investigated and also more widely applied electrochromic material is tungsten trioxide, WO$_3$ [10]. A typical electrochromic device consists of two electrodes, at least one of which must be transparent, and an electrolyte. An applied voltage drives the charge into the electrochromic material causing a change in absorption. This phenomenon is observed in thin films of the material. The electrochromism of different materials is affected to a great extent by the structure, stoichiometry, bonding and water content in the films. All of these variables can be controlled in the preparation of the thin films.

5

The change in the colour of a thin film of an optically active material can also be affected by irradiating the film with at a certain frequency. Discolouration or bleaching of the film usually occurs. An early example of this was reported by Heller in the early 1980s. Heller *et al* investigated a series of photochromic organic molecules known as 'Aberchromes' [11]. These compounds undergo cyclisation when irradiated and change their colour. Exploitation of photochromic materials is most widely observed in light-reactive windows or spectacles [12 - 15].

1.1.3 Molecular Magnets

Magnets have been traditionally associated with metals and alloys such as iron. Molecular magnets, on the other hand, are identified as metal centres with magnetic properties that are 'linked' in some way by other ligands. A good example is the use of oxalato bridges in compounds such as $[NBu_4][MM'(ox)_3]$ {M = Ni, Fe, Mn or Zn; M' = Cr or Fe} [16, 17]. In a review of Molecular Magnetism, Gatteschi suggests that molecular magnets could have unusual optical properties as well as magnetic properties, since many crystallise in a non-centrosymmetric space group, and may therefore be of use in new combined applications [18].

1.1.4 Nonlinear Optical Materials

Materials that exhibit optical nonlinearity have the potential to be exploited in many ways. Not least of these is the development of all-optical communications networks which could operate at much faster switching speeds than conventional electronic based systems.

Every material possesses a refractive index, **n**, which can be defined as the ratio of the velocity of light in a vacuum, **c**, to the velocity of light through the material, **v**.

$$n = \frac{c}{v}$$

In general, the refractive index is constant at a fixed temperature. However, in some

6

instances the refractive index of a material will be altered by the application of an intense electromagnetic field, such that the propagation characteristics of the light in the material are changed. The changes that may be observed include alterations to the phase, polarisation, frequency and amplitude of the incident light. These changes in the refractive index resulting in the change of the physical properties of a material due to the application of an electromagnetic field are encompassed in the term 'nonlinear optics'.

A brief summary of the background to nonlinear optical effects is given below. When an oscillating electric field is applied to a material it will perturb the electron clouds causing the charges to redistribute, resulting in an oscillating dipole moment. A secondary field is generated by the dipole moment which interferes with the transient light and changes the refractive index of the material. The simplest case is when the applied field is of a low intensity. The behaviour of the molecule is dependent upon how easily the dipole moment can be induced by distorting the electron cloud. This is given by the equation below :

$$P = \alpha E$$

P = polarisation
α = linear polarisability
E = field strength

The relationship between the electric field and the polarisation is linear. If a more intense light field, such as that generated by a laser, is applied to a material then the relationship between the polarisation and the field intensity is no longer linear. The β and γ terms are much smaller than α, therefore if the applied electric field E, is large then the higher terms become more significant. This is then represented by the equation below :

$$P = \varepsilon_o(\alpha.E + \beta..E^2 + \gamma...E^3 + ...)$$

β and γ are known as the second- and third-order molecular hyperpolarisabilities. This equation applies to the molecular level. If the bulk material is considered, then the equation becomes :

7

$$P = \varepsilon_o(\chi.E + \chi^{(2)}..E^2 + \chi^{(3)}...E^3 + ...)$$

The $\chi^{(2)}$ and $\chi^{(3)}$ quantities are known as the 'second-order' and 'third-order' susceptibility terms respectively. These are the two main types of nonlinear properties that have been investigated in the field of molecular materials.

When an intense beam of laser light of frequency ω interacts with a second-order material a light at twice the input frequency 2ω is produced, this is known as second harmonic generation. Another second-order effect is the Pockel's effect which exploits the alteration in velocity of light by an applied DC electric current as the light passes through a second-order material. Theoretical studies have predicted that planar conjugated molecules with π-π* transitions that involve a large change in electron density, i.e. a dipole moment, are likely to show large effects. It is also necessary that the material crystallises with a non-centrosymmetric space group if the crystal is to be active. A good example of an organic molecule that exhibits a second-order nonlinear response is m-nitroaniline. Organometallic molecules such as $[FeCp((+)\text{-}DIOP)(p\text{-}NCC_6H_4R)][PF_6]$ {DIOP = chiral phosphine molecule; R = donor or acceptor} have been prepared and studied by Garcia et al [19]. The chiral centre (DIOP) ensures that the molecule will crystallise in a non-centrosymmetrical space group. The dipole moment in this molecule is facilitated by the incorporation of the p-substituted aniline group having a donor and an acceptor end to the ligand. The complex $[FeCp((+)\text{-}DIOP)(p\text{-}NCC_6H_4NO_2)][PF_6]$, see Figure 1.4, exhibits a second-order response 38 times greater than that of urea [19].

Materials that exhibit third-order nonlinear optical effects have also been the focus of much attention. A recent report of substituted dibenzamine compounds containing a metal centre illustrate just one of the many viable avenues of research that are being explored [20]. A more detailed introduction to third-order effects is given in Chapter 2.
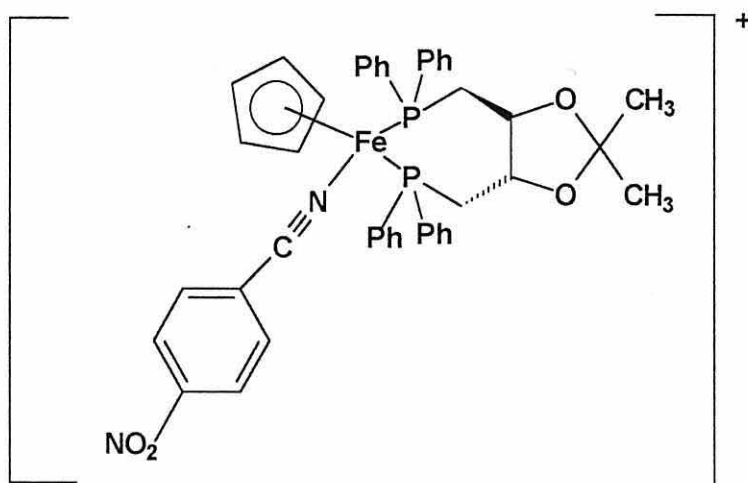
Figure 1.4 : [FeCp((+)-DIOP)(p-NCCH$_6$H$_4$NO$_2$)]$^+$

1.1.5 Supramolecular Materials

The first use of the term 'supramolecular chemistry' dates back to 1937 [21], however the phrase in its modern context is associated primarily with J-M. Lehn after his achievement of the Nobel Prize for Chemistry in 1987 [22]. Lehn made the comparison that "supermolecules are to molecules and the intermolecular bond what molecules are to atoms and the covalent bond". Supermolecules are essentially a combination of molecules that have properties and structures that are distinct from the aggregate properties of the constituent molecular species, see Figure 1.5. Self assembly, where molecules spontaneously associate to form stable, structurally well-defined composites joined by non-covalent bonds is frequently being employed in organic chemistry [23]. A natural progression from this is to employ self assembly in supramolecular chemistry. In 1992, Goulle and Lehn [24] reported an example of a molecular device that was essentially a supramolecular structure that was capable of switching a luminescent state on and off. The system comprises of a TTF moiety linked to a photosensitive unit. The photosensitive unit, [Ru^{II}(bipy)$_3$]$^{2+}$, is attached to the TTF centre *via* a vinyl link. The oxidation state of the TTF controls the luminescence by electron transfer to the ruthenium centre.

9
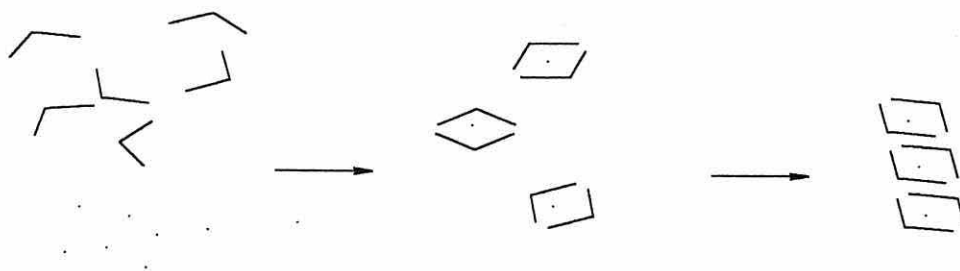
Figure 1.5 : Synthesis of Supermolecules

The rest of this introduction is concerned with molybdenum and tungsten chemistry, since new complexes of molybdenum and tungsten are described in Chapter 2 to 6 of this thesis.

1.2 MOLYBDENUM AND TUNGSTEN

Since the discovery of the elements in the mid-19th Century, the chemistry of molybdenum and tungsten compounds has been well documented. The similarity in their chemical behaviour has meant that they are often classed together in terms of properties and reactions. Chromium, although in the same group, does not exhibit the same diversity as molybdenum and tungsten, and so will not be mentioned in any great depth in this introduction.

Molybdenum is highly toxic, but despite this complexes of molybdenum are known to be important in many biological systems. For example, molybdenum is an integral part of the nitrogen fixing enzyme, nitrogenase [25], and also of many flavoproteins [26, 27]. Molybdenum is very important in the copper metabolism of ruminants. If the diets of cows or sheep are deficient in molybdenum, an excess of copper builds up and poisons the animal, similarly the reverse is true with a lack of copper in the diet causing molybdenum poisoning to occur. Conversely, tungsten is not poisonous and there is no evidence of biological activity. The main applications of tungsten are in tungsten filaments in lighting and heating.

1.3   ZERO-VALENT MOLYBDENUM AND TUNGSTEN COMPLEXES

There are many examples of zero-valent molybdenum and tungsten complexes and most are derived from the hexacarbonyl $[M(CO)_6]$ {M = Mo or W}. Aspects of the chemistry of zero-valent molybdenum and tungsten complexes more relevant to the work embodied in this thesis will be discussed.

1.3.1   Carbonyl Halides Complexes of Molybdenum(0) and Tungsten(0)

Anions of the type $[MX(CO)_5]^-$ {M = Mo or W; X = halogen} that contain molybdenum or tungsten in their zero-valent state are commonly prepared by displacement of a carbonyl ligand by a halide. For example, $[NR_4]X$ or KX [28] (Scheme 1.1).

$$[M(CO)_6] \ + \ X^- \ \longrightarrow \ [M(CO)_5X]^- \ + \ CO$$

M = Mo or W
X = Cl, Br or I
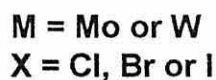
Scheme 1.1 : Preparation of the Anions $[MX(CO)_5]^-$

The resulting anions are diamagnetic, 18 electron complexes. They usually have octahedral geometries. The stability of the anions are a function of the halide ligand, X, with decreasing stability in the order I > Br > Cl > F. Greater stability is also achieved with larger cations such as $[Ph_4As]^+$ or $[R_4N]^+$ {R = Ph or alkyl group} as opposed to Na^+ or K^+.

The halide exerts a *cis*-labilising effect in $[MX(CO)_5]^-$ thereby facilitating the preparation of complexes such as *cis*-$[NEt_4][CrCl(CO)_4L]$ {L = PPh_3, $P(OPh)_3$ or $AsPh_3$} [29]. Buchner and Schenk [30] prepared a wide range of pseudo halide and alkene complexes from $[NEt_4][WCl(CO)_5]$, thus demonstrating the ease with which the halides can be removed from $[MX(CO)_5]^-$.

11

1.3.2 Nitrile and Phosphine Complexes of Molybdenum(0) and Tungsten(0)

Nitrile σ-donor complexes of the zero-valent metal species are invariably prepared by substitution reactions. Although nitriles are generally regarded as non-π-acceptors, it may be argued that they do have a limited π-acceptor ability similar to heterocyclic amines such as bipyridyl (bipy). There are many methods of synthesising zero-valent metal complexes containing σ-donor nitrile ligands, for example, the ubiquitous thermal substitution of the metal hexacarbonyl or ligand exchange with other nitrile complexes.

The degree of ligand π-acceptor character of the nitrogen ligands varies widely and is dependent upon the structure of the ligand. There have been a series of detailed reviews on carbonyl complexes of molybdenum and tungsten with monodentate phosphorus ligands [31, 32] including a more general review in 1990 of phosphorus chemistry by Regitz and Scherer [33]. Phosphines have empty d-orbitals of the right energy and symmetry to overlap with filled metal d-orbitals, thereby enabling the acceptance of π electrons by the phosphines. There are many examples of monodentate phosphorus donor ligands : phosphines PR_3, phosphites $P(OR)_3$, phosphorus halides PX_3, phosphorus amines, $P(NR)_3$. Not discussed here, but often considered are the analogous arsine, antimony and bismuth complexes which are much less stable. The π-acceptor ability of the ligands decreases in the order P > As > Sb > Bi. There are many routes to the formation of monodentate phosphine complexes, but the most common is the direct thermal or photochemical promoted substitution of $[M(CO)_6]$ or existing nitrile or phosphine derivatives.

Covey and Brown described a series of reactions in 1973 to compare the reactivity of complexes of σ-donor and π-acceptor ligands [34]. It was found that, as expected, the σ-donor ligands were more labile than the π-acceptor ligands. The *cis*-labilising effect of the non-carbonyl ligand may be observed when the complex is activated photochemically. These effects are summarised in Scheme 1.2.

12

$$[M(CO)_5L] + L \longrightarrow [M(CO)_4L_2] + CO$$

$$[M(CO)_5L] + N \longrightarrow [M(CO)_4LN] + CO$$

$$[M(CO)_5L] + N \longrightarrow [M(CO)_5N] + L$$
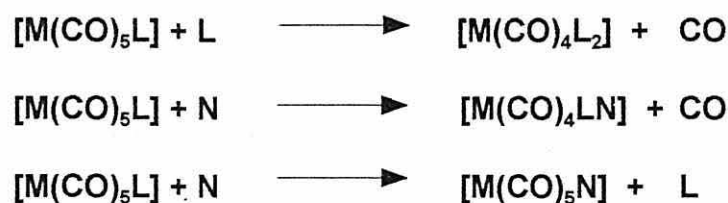
M = Mo or W
L = π-acceptor ligand
N = σ-donor nitrile

Scheme 1.2 : The Comparative Lability of σ-donor and π-acceptor Ligands and the *Cis*-Labilising Effect of the Nitrile Ligand

1.3.2.1 Bonding In PY_3 Phosphorus Donor Ligands

The length of the metal-phosphorus bond in the carbonyl phosphorus derivatives of zero-valent molybdenum and tungsten complexes is directly related to the cone angle of the phosphorus ligand. The cone angle is the area of rotation of the substituents, R, on the phosphine group, PR_3. Studies on the structures and reactivities of *cis*-$[Mo(CO)_4(PR_3)_2]$ complexes have shown that, in general, the PR_3 ligands with a larger cone angle result in increased Mo-P bond lengths, P-Mo-P angles and that they favour intramolecular rearrangement to the *trans*-isomer [35]. Similar conclusions have been drawn over *cis*-$[W(CO)_4(PR_3)_2]$, with investigations being carried out on the kinetic [36] and thermodynamic [37] aspects of the correlation between *cis* / *trans* isomerism and phosphine cone angle.

The electronic contribution of the tertiary phosphines, PR_3 to the metal-ligand bond is rather less clear cut than the steric properties. Many factors regarding the σ and the π components of the bonding have been considered and disputed. For example, the pK_a of the conjugate acid of the phosphorus ligand $(HPR_3)^+$ is a useful method of deriving the σ basicity and results in the traditional ordering $P(alkyl)_3 > P(aryl)_3$. Bancroft *et al*, adopting an alternative measure of the phosphorus σ base character using the gas-phase

13

photoelectron spectra of $[Mo(CO)_5(PMe_nPh_{3-n})]$ $\{n = 0-3\}$ complexes, confirmed the base ordering of $P(alkyl)_3 > P(aryl)_3$ [38].

However, whilst both steric and electronic properties taken individually affect the bonding in $[M(CO)_{6-n}L_n]$, the two factors interact strongly and therefore both need to be considered for an accurate assessment of the bonding in phosphines.

1.4 η^6-COMPLEXES OF MOLYBDENUM(0) AND TUNGSTEN(0)

Molybdenum(0) and tungsten(0) are known to react with unsaturated hydrocarbon compounds, such as alkenes, to give complexes containing the unsaturated hydrocarbon as a ligand with bonds to more than one carbon atom from the metal centre. The most common type of η^6-complexes of molybdenum and tungsten are the η^6-arene species of the type $[M(\eta^6\text{-arene})_2]$ and $[M(CO)_3(\eta^6\text{-arene})]$ $\{M = Mo \text{ or } W; \text{ arene } = R_nC_6H_{6-n}\}$. Work on η^6-arene complexes of molybdenum and tungsten is described in Chapter 4. The bis(arene) complexes will not be discussed here but these complexes are discussed in detail in Comprehensive Organometallic Chemistry, volume 3 [39].

Since the first reports of the complexes $[M(CO)_3(\eta^6\text{-}C_6H_6)]$ in 1958 $\{M = Mo$ [40]; W [41]$\}$, a wide variety of substituted benzene π-complexes of the general formula $[M(CO)_3(\eta^6\text{-}R_nC_6H_{6-n})]$ have been synthesised and characterised. Fischer *et al* first reported the synthesis of the complex $[M(CO)_3(\eta^6\text{-}R_nC_6H_{6-n})]$ by heating the appropriate metal hexacarbonyl directly with the arene [40, 41]. This gives the desired products $[M(CO)_3(\eta^6\text{-}R_nC_6H_{6-n})]$ but only in low yields of less than 10 %. The isolated tungsten and chromium products were reported to be reasonably stable in air at room temperature but there is some decomposition of the molybdenum complex over time under the same conditions. An alternative, and ultimately more successful, route of preparing the tungsten product was reported by King and Fronzaglia eight years later in 1966 [42]. The arene was heated in a solution of *fac*-$[W(CO)_3(NCMe)_3]$ giving yields of ca. 65 % of $[W(CO)_3(\eta^6\text{-}R_nC_6H_{6-n})]$. An improved synthesis of the molybdenum product was

described a few years later by Price and Sørensen [43] in which the arene was stirred at room temperature in a solution of *fac*-[Mo(CO)$_3$(py)$_3$] in the presence of a trifluoroboron-ether complex. This gave yields of ca. 70 % and proved to be a more successful route compared to that described by Fischer ten years previously.

1.5 MOLYBDENUM(II) AND TUNGSTEN(II) HALOCARBONYL COMPLEXES

The organometallic chemistry of the halocarbonyl complexes of molybdenum and tungsten in an oxidation state of +2 has been studied extensively since the mid-1950s. There have been several reviews on the six and seven co-ordinate halocarbonyl complexes of these metals, including two by Colton *et al* [44, 45]. The reviews in 1977 by Drew [46] on the structures of seven co-ordinate compounds and in 1985 by Melník and Sharrock [47] also provide a comprehensive overview of this field of chemistry. More recently, a review by Baker [48] gives a detailed account of the chemistry of halocarbonyl complexes of molybdenum(II) and tungsten(II) up to mid-1995.

The chemistry of molybdenum and tungsten is often viewed together with chromium since the three elements are all in the same group of the Periodic Table. However, in contrast to chromium(II), the larger molybdenum(II) and tungsten(II) can accommodate co-ordination by seven ligands, providing 14 electrons thereby enabling these complexes to obey the effective atomic number rule.

1.5.1 Synthesis of Molybdenum(II) and Tungsten(II) Halocarbonyl Complexes by Oxidation of the Zero-valent Complexes

The first dihalocarbonyl donor ligand complex of molybdenum, [MoI$_2$(CO)$_2$(diars)] was reported in 1957 by Nigam and Nyholm [49]. One of the most successful routes and therefore the most common method of preparing these halocarbonyl complexes involves the oxidation of the zero-valent species [M(CO)$_{6-n}$L$_n$] to M(II) {M = Mo or W} with halogens. For example, the oxidation of *fac*-[M(CO)$_3$(CNR)$_3$] {M = Mo or W; R = Et or Bu^t} with bromine yields the seven co-ordinate complexes [MBr$_2$(CO)$_2$(CNR)$_3$] [50].

In 1976 Tripathi *et al* reported the oxidation of the zero-valent complexes [W(CO)$_5$(amine)] and [W(CO)$_4$(amine)$_2$] {amine = butylamine, cyclohexamine, piperidine or morpholine} with an equimolar amount of X$_2$ {X = Br or I} to give the species [WX$_2$(CO)$_4$(amine)] [51] and [WX$_2$(CO)$_3$(amine)$_2$] [52] respectively.

Treatment of the monosubstituted molybdenum complexes [Mo(CO)$_5$(L)] {L = PPh$_3$, AsPh$_3$ or SbPh$_3$} with X$_2$ {X = Cl, Br or I} produces the six co-ordinate complexes [MoX$_2$(CO)$_3$(L)]. The seven co-ordinate complexes [MoX$_2$(CO)$_3$(L)$_2$] are formed if *cis*-[Mo(CO)$_4$(L)$_2$] {L = PPh$_3$, AsPh$_3$ or SbPh$_3$} is reacted with X$_2$ [53]. However, addition of X$_2$ {X = Br or I} to the monosubstituted tungsten analogue, [W(CO)$_5$(L)] {L = PMe$_3$, AsMe$_3$}, results in the seven co-ordinate products [WX$_2$(CO)$_4$(L)] [54]. This may suggest that the larger tungsten centre accepts seven ligands more readily than the molybdenum centre. Umland and Vahrenkamp [55] reported the carbonyl substitution reactions of [WX$_2$(CO)$_4$(L)] {X = Cl, Br or I; L= PMe$_3$, AsMe$_3$ or SbMe$_3$} with a second monodentate phosphine ligand L' to give the mixed phosphine products [WX$_2$(CO)$_3$(L)(L')]. Numerous seven co-ordinate complexes of molybdenum(II) and tungsten(II) containing a bidentate phosphine ligand have also been prepared by oxidation of complexes of the type [M(CO)$_4$(P^P)] {M = Mo or W; P^P = bidentate phosphine}. The simplest of the bidentate phosphine ligands are (Ph$_2$P(CH$_2$)$_n$PPh$_2$) and there have been many investigations into the preparation of seven co-ordinate complexes incorporating such ligands. Lewis and Whyman first gave an account of the oxidation by X$_2$ {X = Br or I} of [M(CO)$_4$(dppe)] to yield [MX$_2$(CO)$_3$(P^P)] in 1965 [56] and since then there has been a considerable amount of work done on this type of complex [57 - 59]. In summary, the seven co-ordinate complexes have been prepared by the general method of oxidising the zero-valent carbonyl complex containing the ligand L to give [MX$_2$(CO)$_3$(L)$_2$].

1.5.2   Synthesis and Reactions of the Complexes [MX$_2$(CO)$_3$(NCMe)$_2$]
{M = Mo or W; X = Br or I}

In 1962, Tate, Knipple and Augl reported the synthesis of *fac*-[M(CO)$_3$(NCMe)$_3$] {M = Cr, Mo or W} by refluxing [M(CO)$_6$] in acetonitrile [60]. Also described in this paper is

16

the reaction of *fac*-[W(CO)$_3$(NCMe)$_3$] with iodine in methanol. Three moles of gas, presumably carbon monoxide, were evolved to give a non-carbonyl containing product. In 1972, Westland and Muriithi investigated the reactions of the dimeric complexes first reported by Colton *et al* [44], namely, [{Mo(μ-X)X(CO)$_4$}$_2$] {X = Cl or Br} with weaker ligand-field ligands such as L {L = py, thf, NCMe etc.} to eliminate the carbonyl ligands to leave [MoX$_3$L$_3$] as the major products [61]. They implied that the product is formed *via* molybdenum(II) carbonyl halide intermediates. A proposed reaction scheme published fourteen years later [62], indicates that the bimetallic halocarbonyl seven co-ordinate complexes [MX$_2$(CO)$_3$(NCMe)$_2$] are produced in quantitative yield by the reaction scheme shown in Scheme 1.3, using acetonitrile as the solvent. The iodide derivatives are much more stable than the bromide complexes. Instead of using methanol as Tate, Knipple and Augl had done previously, Baker *et al* effectively used acetonitrile as the solvent by doing the reaction *in situ*. The resultant iodide complexes are red-brown crystalline solids. They are relatively stable in the solid state if stored under a blanket of argon or nitrogen. These complexes are excellent starting materials for the preparation of a variety of organometallic compounds because of the lability of the acetonitrile ligands.

$$[M(CO)_6] \xrightarrow[\Delta]{NCMe} \textit{fac-}[M(CO)_3(NCMe)_3] \xrightarrow[0\,C]{X_2} [MX_2(CO)_3(NCMe)_2]$$

M = Mo (reflux 24 hours) or W (reflux 72 hours)
X = Br or I

Scheme 1.2 : The Preparation of [MX$_2$(CO)$_3$(NCMe)$_2$]

The geometry of these complexes has been determined by X-ray crystallography as capped octahedral [63], with a carbonyl ligand capping the face of a halide ligand and two carbonyl ligands, see Figure 1.6. The iodide ligands in this structure are *trans* to each other (cf. [WI$_2$(CO)$_3$(PEt$_3$)$_2$] Chapter 3 and Figure 3.10). The geometry can be confirmed by low temperature ^{13}C NMR spectroscopy. At -70°C, the ^{13}C NMR spectrum of [WI$_2$(CO)$_3$(NCMe)$_2$] in CDCl$_3$ shows two peaks at 202 ppm and 228 ppm with a relative intensity of approximately 2:1. The smaller resonance at 228 ppm may be attributed to the capping carbonyl. The carbonyl groups in the seven co-ordinate complex are fluxional

17

at room temperature and as expected, at room temperature the ^{13}C NMR spectrum shows a single resonance at 200 ppm. A more successful method of preparing the dibromo complexes [MBr$_2$(CO)$_3$(NCMe)$_2$] {M = Mo or W} was reported ten years later in 1994 [64]. The complex *fac*-[M(CO)$_3$(NCMe)$_3$] was reacted with bromine at -78 °C, rather than at 0 °C as is the case with iodine. The higher reactivity of bromine means that the probability of formation of dimers or other side products in the reaction is higher. Lowering the temperature slows down the reaction and there is less chance of any side reactions taking place. The resultant complexes, [MBr$_2$(CO)$_3$(NCMe)$_2$] {M = Mo or W}, are less stable than the analogous iodide complexes. However, these complexes are stable enough to use as reagents in further reactions.
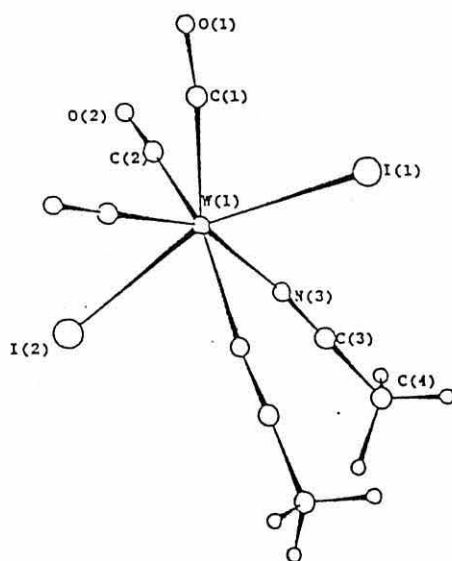
**Figure 1.6 : The Capped Octahedral Structure of the Seven
Co-ordinate Complex [WI$_2$(CO)$_3$(NCMe)$_2$] [63]**

The seven co-ordinate complexes [MI$_2$(CO)$_3$(NCMe)$_2$] {M = Mo or W} will react with many different kinds of ligands and this area of organometallic chemistry has attracted a great deal of attention over the last ten years. As this thesis is concerned mainly with the substitution of the acetonitrile groups by nitrile and phosphorus-based ligands, and the substitution of the iodide ligands with sulphur-based anions, these will be the only reactions discussed in any detail in this introduction. It should be noted, however, that there are many other types of reactions which these complexes may undergo, for example,

18

reaction with alkynes and alkenes. The development of the complexes $[MI_2(CO)_3(NCMe)_2]$ {M = Mo or W} has meant that ligands, such as nitriles, phosphines or other donor ligands can be reacted directly with the oxidised form of the metal, rather than with the zero-valent metal complex prior to oxidation by the halogen as was the case previously.

1.5.3 Displacement Reactions of $[MI_2(CO)_3(NCMe)_2]$

The complexes $[MI_2(CO)_3(NCMe)_2]$ react with an excess of the nitrile NCR to exchange the nitrile groups and give $[MI_2(CO)_3(NCR)_2]$ {M = Mo, R = Ph; M = W, R = Et, ^tBu, CH_2Ph, Ph}. These complexes can react further with one equivalent of L {L = PPh_3, $AsPh_3$ or $SbPh_3$} to give the mixed ligand complexes $[MI_2(CO)_3(NCR)(L)]$ [65]. The bis(nitrile) complexes can also react with two equivalents of the ligand L to eliminate the nitrile ligands completely and leave the products $[MI_2(CO)_3L_2]$. The synthetic work described in Chapter 2 concentrates mainly on the reactions of $[MI_2(CO)_3(NCMe)_2]$ {M = Mo or W} with highly substituted nitrile complexes. It should be noted that simple nitrile ligands are more labile than their phosphine equivalents. The degree of lability of such ligands may be summarised as NCR >> PR_3.

The reactions of $[MI_2(CO)_3(NCMe)_2]$ {M = Mo or W} with phosphorus, arsenic, antimony and bismuth donor ligands are comparable to those of the nitrogen donor ligands. The ligands PPh_3, $AsPh_3$ and $SbPh_3$ react with the complexes $[MI_2(CO)_3(NCMe)_2]$ to displace one acetonitrile ligand. If one equivalent of L {L = Group V donor ligand} is used, the complexes $[MI_2(CO)_3(NCMe)(L)]$ are initially afforded which dimerise to yield the iodide-bridged complexes $[M(\mu-I)I(CO)_3L]_2$ [66]. The complexes $[MI_2(CO)_3(NCMe)(L)]$ can subsequently be used to prepare a series of anionic complexes of the type $[^nBu_4N][MI_3(CO)_3L]$ {L = PPh_3, $AsPh_3$ or $SbPh_3$} [67]. If two equivalents of L are used, then both acetonitrile ligands are exchanged to yield the complexes $[MI_2(CO)_3(L)_2]$ [68]. The bis(triphenylphosphine) derivatives, $[MI_2(CO)_3(PPh_3)_2]$ were found to rearrange in solution in dichloromethane to give the salts $[PPh_3H][MI_3(CO)_3(PPh_3)]$.

[M(μ-I)I(CO)$_3$L]$_2$ [A][MI$_3$(CO)$_3$L]

↖ a(i)   ↗
                   a(ii)

[MI$_2$(CO)$_3$(NCMe)L]   [MI$_2$(CO)$_3$LL']   [MI$_2$(CO)$_3$(P^P]

↖   ↑   ↗
    a   b   c

[MI$_2$(CO)$_3$(NCMe)$_2$]

↙ f   ↓ e   d ↘

[MI$_2$(CO)$_3$(EPh$_3$)$_2$]   [MI$_2$(CO)$_3$(P(OR)$_3$}$_2$]   [MI$_2$(CO)$_3$(NCR)$_2$]

[MI$_2$(CO)$_3${P(OR)$_3$}$_2$]
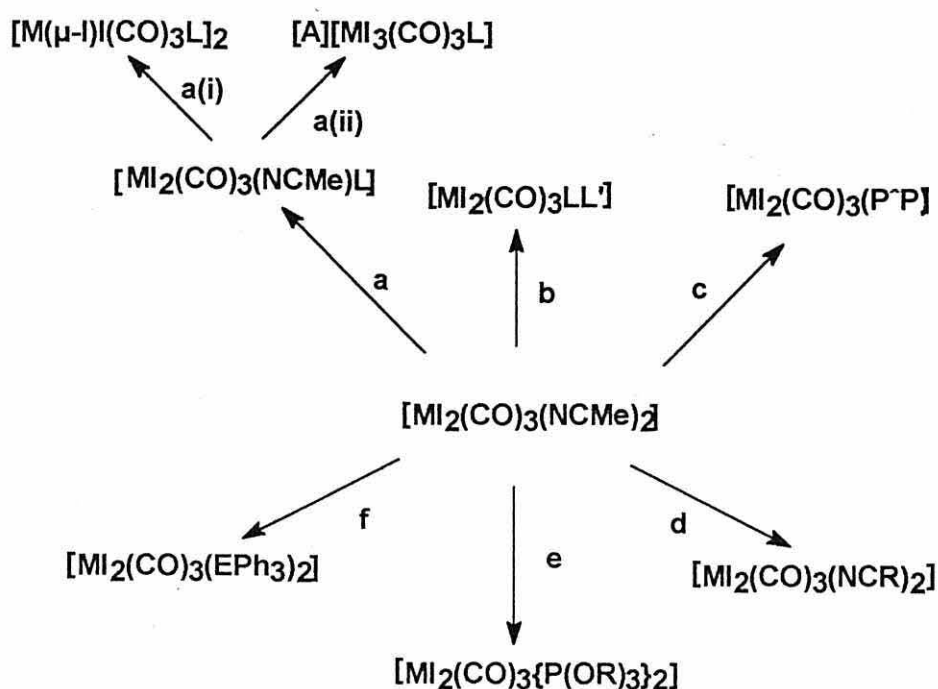
<u>Reaction with :</u>
a :   One equivalent L {L = Group V donor)
a(i) :   Dimerisation
a(ii) : YX {Y = cation; X = halogen}
b :   Equimolar amounts different phosphines {L and L'}
c :   Bidentate phosphine {P^P}
d :   Two equivalents nitrile {NCR}
e :   Two equivalents phosphite {P(OR)$_3$}
f :   Two equivalents of EPh$_3$ {E = P, As or Sb}

Scheme 1.4 : Reaction Scheme to Show Different Reactions

with Group V Donor Ligands

Mixed phosphine ligand complexes of molybdenum(II) or tungsten(II) are unusual,
however, in 1988 Baker *et al* synthesised complexes of the type [MI$_2$(CO)$_3$(L)(L')] by
reacting [MI$_2$(CO)$_3$(NCMe)$_2$] with one equivalent of L {L = PPh$_3$, AsPh$_3$ or SbPh$_3$},
followed by an equimolar quantity of L' {L' = PPh$_3$, AsPh$_3$ or SbPh$_3$ } [69]. Several
phosphine complexes of the type [MI$_2$(CO)$_3$L$_2$] also rearrange in dichloromethane at
room temperature to afford the salts [HL'][MI$_3$(CO)$_3$L] {M = Mo, L = PPh$_3$, L' = PPh$_2$Cy

or PPhCy$_2$; M = W, L = PPh$_3$ or SbPh$_3$, L' = PPh$_2$Cy or PPhCy$_2$}. The crystal structure of [(PPh$_2$Cy)H][WI$_3$(CO)$_3$(SbPh$_3$)] was found to be capped octahedral, with a carbonyl ligand in the unique capping position.

An equimolar quantity of a bidentate phosphine, (P^P) {for example, (P^P) = (Ph$_2$P(CH$_2$)$_n$PPh$_2$)}, when reacted with [MI$_2$(CO)$_3$(NCMe)$_2$] also replaces the nitrile ligands to give high yields of the complexes [MI$_2$(CO)$_3$(P^P)] [70]. The reactions of [MI$_2$(CO)$_3$(NCMe)$_2$] with phosphite ligands were first reported by Baker and Fraser in 1986 [71]. The products formed were the seven co-ordinate complexes [MI$_2$(CO)$_3${P(OR)$_3$}$_2$] which, when refluxed in chloroform, lose carbon monoxide to give the six co-ordinate, 16-electron complexes [MI$_2$(CO)$_2${P(OR)$_3$}$_2$].

1.5.4 Reactions with Other Ligands

The molybdenum(II) and tungsten(II) complexes are known to react with neutral oxygen and sulphur donor ligands by replacing the acetonitrile ligands. The complexes [MI$_2$(CO)$_3$(NCMe)$_2$] {M = Mo or W} react with one equivalent of thiourea (SC(NH$_2$)$_2$) in methanol to initially yield the monosubstituted complexes [MI$_2$(CO)$_3$(NCMe)(SC(NH$_2$)$_2$)] [72]. These rapidly dimerise to afford the iodide-bridged dimers [M(μ-I)I(CO)$_3$(SC(NH$_2$)$_2$)]$_2$ with the loss of an acetonitrile ligand. The reaction of [MI$_2$(CO)$_3$(NCMe)L] {M = Mo or W; L = PPh$_3$, AsPh$_3$ or SbPh$_3$} with one equivalent of thiourea gives the mixed ligand complexes [MI$_2$(CO)$_3$(L)(SC(NH$_2$)$_2$)] [73]. If the complexes [MI$_2$(CO)$_3$(NCMe)$_2$] react with two equivalents of thiourea then the complexes [MI$_2$(CO)$_3$(SC(NH$_2$)$_2$)$_2$] {M = Mo or W} are obtained, with displacement of both acetonitrile ligands.

When [MI$_2$(CO)$_3$(NCMe)$_2$] is treated with a slight excess of [RS(CH$_2$)$_2$SR] {R = Ph, 4-MeC$_6$H$_4$ or 4-FC$_6$H$_4$} the nitrile substituted complexes [MI$_2$(CO)$_3${RS(CH$_2$)$_2$SR}] are produced [74]. The structure of the complex for M = W and R = 4-MeC$_6$H$_4$ has been determined and has a capped octahedral geometry with a carbonyl in the unique capping position [74].

21

The reaction between molybdenum complexes and tridentate crown thioethers have been investigated mainly because of the interest in modelling the active site of the nitrogenase enzyme [74, 75]. These reactions are of particular significance because the reported molybdenum site in nitrogenase is bonded by three sulphur atoms [75, 76] together with an imidazole and two oxygens from other constituents of the active site. Reaction of $[MI_2(CO)_3(NCMe)_2]$ {M = Mo or W} with a slight excess of the crown thioether $9[ane]S_3$ {$9[ane]S_3$ = 1,4,7-trithiacyclononane} yields the seven co-ordinate cationic complexes $[MI(CO)_3(9[ane]S_3)][I]$ {M = Mo or W}. Further reaction with an excess of sodium tetraphenyl borate in methanol gave the seven co-ordinate anion exchanged products $[MI(CO)_3(9[ane]S_3)][BPh_4]$ {M = Mo or W} [78]. The structure of the tungsten derivative was determined by X-ray crystallography and the cation was found to have a 4:3 type geometry, see Figure 1.7. The reaction of two equivalents of $[WI_2(CO)_3(NCMe)_2]$ with a variety of tetradentate crown thioethers have produced seven co-ordinate, ionic complexes of the type $[WI(CO)_3(\eta^3\text{-CTE})][WI_3(CO)_4]$ and $[WI(CO)_2(\eta^4\text{-CTE})][WI_3(CO)_4]$ {CTE = crown thioether}. When the crown ether is $Me_8 16[ane]S_4$ {$Me_8 16[ane]S_4$ = 3,3,7,7,11,11,15,15-octamethyl-1,5,9,13-tetrathiacyclohexadecane}, the cations both have a 4:3 piano stool geometry similar to the structures of the cation of the tridentate crown thioether $[WI(CO)_3(9[ane]S_3)]^-$ which is illustrated in Figure 1.7, and the anion, $[WI_3(CO)_4]^-$ possesses an octahedral geometry with a capping carbonyl [79].
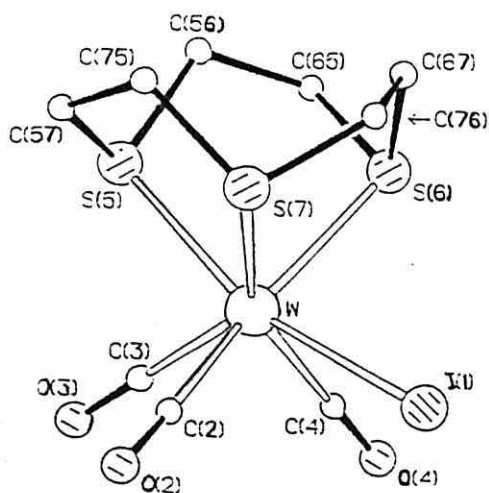
Figure 1.7 : The Structure of $[WI(CO)_3(9[ane]S_3)]^-$

The complexes $[MI_2(CO)_3(NCMe)_2]$, in addition to reacting with neutral oxygen or sulphur ligands to exchange with the acetonitrile groups, also react with anionic oxygen and sulphur donor ligands to eliminate the iodide ligands. Simple monoionic species such as $Na[O^{\wedge}O]$ {$O^{\wedge}O$ = acac, hfacac, bzacac etc.} react with the complexes $[MI_2(CO)_3(L)(L')]$ {M = Mo or W; $L = L'$ = NCMe, PPh_3 etc; L = NCMe, L' = PPh_3 etc.} to eliminate one iodide ligand and the most labile ligand L to afford the neutral complexes $[MI(CO)_3(L')(O^{\wedge}O)]$ [80]. Although the ligand is monoanionic, it coordinates in a bidentate manner. Various reactions with 1,1-dithiolene complexes, such as dithiocarbamates, proceed in a similar manner to give the products $[MI(CO)_3(L)(S^{\wedge}S)]$ [80 - 82]. These complexes are seven co-ordinate with the ligand bonding in a similar style to the oxygen based ligands ($O^{\wedge}O$) mentioned above.

In conclusion, it can be seen that in general the seven co-ordinate bis(acetonitrile) halocarbonyl complexes of molybdenum(II) and tungsten(II) are highly reactive. The acetonitrile ligands of the complexes $[MI_2(CO)_3(NCMe)_2]$ are very labile and are replaced by other neutral donor ligands with relative ease. Similarly, the iodide ligands can be replaced by anionic donor ligands to give uncharged seven co-ordinate products. These simple reactions have formed the basis for the work embodied in this thesis and in Chapter 3 of this thesis, the reactions of $[WI_2(CO)_3(L)]$ {L = $(PPh_3)_2$, $(PEt_3)_2$ or dppe} with dianionic 1,2-dithiolenes, $[A(S^{\wedge}S)]$ {A = H or Na; $S^{\wedge}S$ = 1,2-dithiolene}, to eliminate both iodide ligands are discussed in depth.

1.6   THE STRUCTURES OF SEVEN CO-ORDINATE COMPLEXES

In a comprehensive review of the structures of seven co-ordinate complexes in 1977, Drew assigned three basic arrangements to the ligands around a central metal atom [46]. The three structures are :

- pentagonal bipyramid
- capped octahedron
- capped trigonal prism

A fourth, less well-defined structure is the 4:3 'piano stool' geometry.

1.6.1 Pentagonal Bipyramid

The pentagonal bipyramid is depicted in Figure 1.8. It is found that in most complexes with seven equivalent ligands the axial ligand-metal bonds are slightly shorter than the equatorial ligand-metal bonds. The majority of seven co-ordinate complexes containing multiple bonds have pentagonal bipyramidial structures with the multiple bond in an axial site. Bonds that are *trans* to the multiple bond are weakened causing the metal atom to be raised above the equatorial plane. Bidentate ligands with a small bite angle are well suited to occupancy of the $L_{eq}...L_{eq}$ edge. The $L_{ax}...L_{eq}$ bite is only observed in [M(L-L)$_3$L] type complexes when two of the equatorial sites are occupied by chelates. Most complexes containing tri-, tetra- and pentadentate ligands have pentagonal bipyramidial geometries. The pentagonal bipyramid structure found throughout all of the monomers and dimers in the periodic table and is more due to the nature of the ligands than the stereochemical preference of the metal.
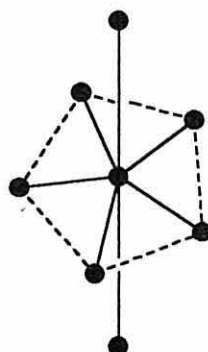
Figure 1.8 : Pentagonal Bipyramid

1.6.2 Capped Octahedron

The capped octahedral geometry can be seen in Figure 1.9. As opposed to the L-M-L angles in the pentagonal bipyramid, the angles in the capped octahedron are not fixed. The capped octahedral geometry is commonly found in molybdenum(II) and tungsten(II) carbonyl halides which contain phosphorus or arsenic ligands and in a series of [M(L-

24

L)₃L] complexes of the rare-earth metals. Up to four carbonyl groups can be mutually *cis* thereby avoiding competition for the metal dπ electrons. The capped octahedral geometry is generally not suited to multidentate ligands because no three adjacent sites are coplanar to the metal. As a result there are no tri- tetra-, penta- or hexadentate ligands in a capped octahedron structure.
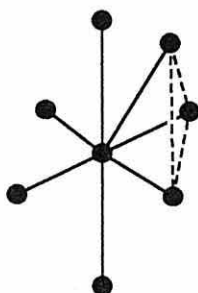
Figure 1.9 : Capped Octahedron

1.6.3 Capped Trigonal Prism

The capped trigonal prismatic structure is shown in Figure 1.10. The capped trigonal prism geometry is not usually found for monomers especially those with mostly monodentate ligands.
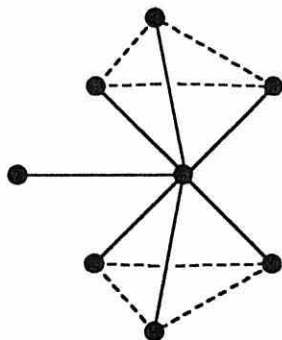
Figure 1.10 : Capped Trigonal Prism

25

1.6.4 The 'Piano Stool' Geometry or 4:3 Geometry

This structure comprises of a plane of four donor atoms parallel to a plane of three donor atoms. There are two extremes as seen in Figure 1.11 [83] and examples of these can be found in the literature [84, 85]. The two extremes of the 4:3 geometry are closely related to the capped octahedron (cf. **a**), eg. ZrO_2, and the capped trigonal prism respectively (cf. **b**), eg. $YbCl_3$. It is found often that the 4:3 structure is rarely referred to as a separate geometry except in the case of complexes such as $[ML_4L'_3]$ or for polymers such as ZrO_2 where the 4:3 nomenclature emphasises their layer nature.

a   **b**
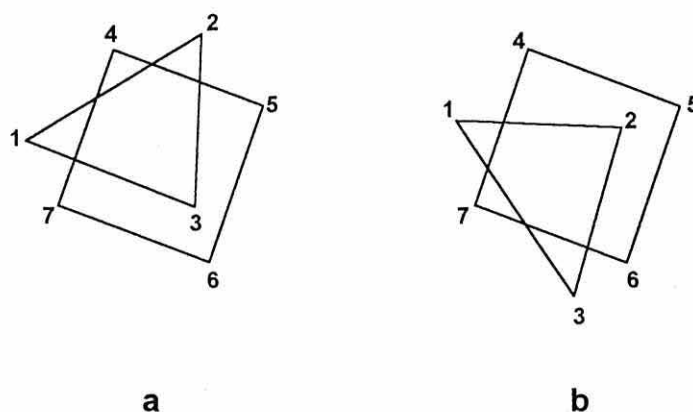
Figure 1.11 : The 4:3 Geometry

1.6.5 Isomers of the Seven Co-ordinate Structures

An in depth discussion on isomerism will not be given as a part of this introduction to seven co-ordinate structures. Suffice to say there are three types of isomer :

- polytopal isomers - these have different geometries
- stereoisomers - these have the same geometries but a different arrangement of the ligands
- permutational isomers - these have the same geometries and identical stereochemistry.

26

1.7   THE AIMS OF THIS THESIS

The primary objective of this work was to bridge the two areas of chemistry defined so far in the introduction. The synthesis of three distinct types of compound were attempted

- molybdenum and tungsten complexes attached to fluorescent nitrile compounds - to examine the effect of the transition metal on the fluorescence of the nitrile compound.
- dithiolene complexes of molybdenum and tungsten - to study any unusual properties that may arise from the combination of the two systems.
- thiophene complexes of molybdenum and tungsten - to investigate the effect of the oxidation state of the transition metal upon the thiophene in its polymeric state.

There was also an overall aim to investigate any interesting materials properties that maybe associated with these novel complexes. The results of this work are presented in this thesis.

Chapter Two

Complexes of Molybdenum

and Tungsten containing

Fluorescent Ligands

2.1   INTRODUCTION TO FLUORESCENCE

Under normal conditions at room temperature, the electrons in a molecule will reside in the ground state. This ground state is usually a singlet state (S_0) with all the electrons paired. When the molecule absorbs a photon of UV energy, an electron is promoted from the ground state to an excited energy level where it possesses the same spin as in the ground state. The excited electron has one of three possible fates at this stage :

    i.   to lose energy *via* collision processes and relax to the ground state

    ii.   to degenerate to a triplet state, where the spin is altered, and then emit energy to relax back to the ground state

    iii.   to emit energy and relax back to the ground state.

The first case is the most common. The majority of electrons when promoted to a higher energy level will lose their extra energy by collision processes. However, in a few situations the second or third processes can also occur. The longer lived process, phosphorescence, will occur when an electron degenerates to a triplet state, with an opposite spin before relaxing to the ground state and emitting the excess energy. The third case is fluorescence when the excited electron relaxes to the ground state without changing its spin.
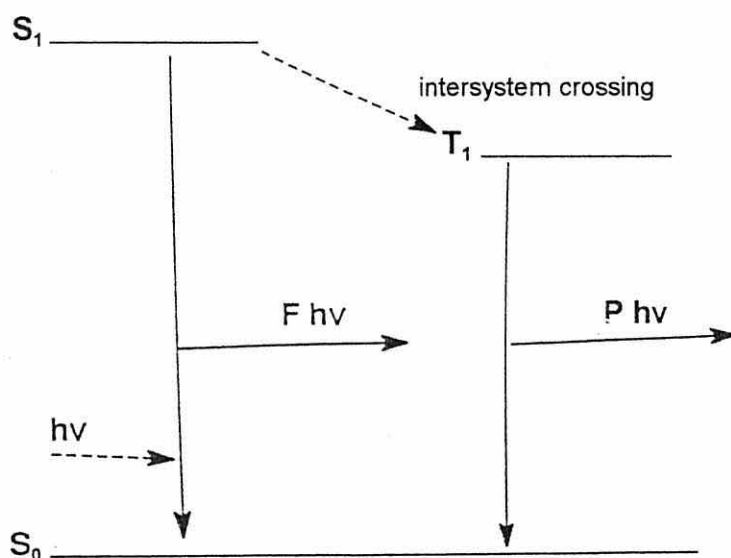
Scheme 2.1 : The Excitation and Relaxation Processes in a Molecule

2.1.1 Chemical Structure and Fluorescence

In general the greater the absorption of ultraviolet light by a molecule, the greater its fluorescence. Compounds with multiple conjugated double bonds are favourable to fluorescence, since they can absorb a large amount of ultraviolet energy. Electron donating groups such as -OH or -NH$_2$ will enhance fluorescence. Electron withdrawing groups such as -NO$_2$, -COOH, or halides tend to inhibit fluorescence. The nature of other substituents may also alter the degree of fluorescence. As well as the fluorescence being affected by the structure of a compound, in some cases it can also be greatly pH dependent with only the ionised or the un-ionised form being fluorescent. For example phenol, C$_6$H$_5$OH, is fluorescent but its anion, C$_6$H$_5$O$^-$, is not.

2.1.2 Concentration and Fluorescence

In solutions where the concentration of the fluorescent complex is low, the fluorescent intensity is directly proportional to the concentration of the complex and to the intensity of the incidence radiation. At higher concentrations the fluorescent intensity may decrease with increasing concentration, however, unlike absorption, it is still dependent upon the intensity of the source of irradiation. Fluorescent intensity is given by the equation :

$$I_F = \phi_F I_o(1 - 10^{-A})$$

I_F = Fluorescent intensity

ϕ_F = Fluorescent Quantum Yield

A = Absorbance = (extinction coefficient) x (concentration) x

(path length) (Beer-Lambert Law)

The fluorescent quantum yield is the ratio of photons emitted to photons absorbed. That is the fraction of the photons absorbed that are converted to fluorescent photons.

30

$$\Phi_F = \frac{I_F}{I_A}$$

Φ_F = Fluorescent Quantum Yield
I_F = Fluorescent Intensity
I_A = absorbed intensity

The development, over the last decade, of molecules that exhibit controllable fluorescence has opened up a large area of new possibilities in the area of materials research, and in particular chemical sensors. For example, it has been found that the fluorescence quantum yield of some benzo-crown ether derivatives are enhanced by the presence of alkali metal ions, and this property has been exploited by incorporating these materials into alkali-cation sensors [86 - 88]. The fluorescence is also affected by the solvent system used as may be demonstrated by the enhanced fluorescence of some molecules in 2-propanol compared with methanol. For example, the enhancement of the fluorescence by binding of a potassium ion to a molecule based on an anthracene group attached to a crown ether rises from a factor of 3 in methanol to 45 in 2-propanol [87].

Similar molecules have also displayed a propensity towards proton selection, with the detection of pH being an obvious progression from this feature. The molecule in Figure 2.1 shows certain structural differences that affect the pH switching ability.
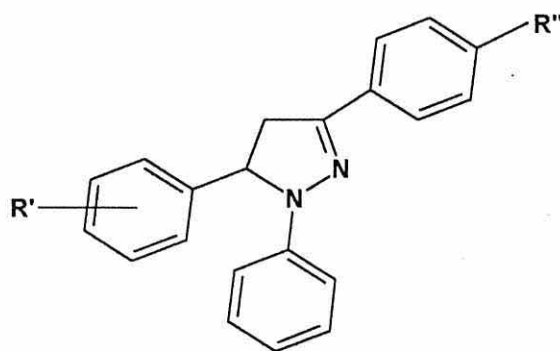
R' =   4-COOH / COO⁻ or 2-COOH / COO⁻
R" =   OCH₃   ✓
       H   ✓   pH switching
       Ph   ✓   ability
       CN   ✗

Figure 2.1 : A Fluorescent pH Indicator

31

The absorption and emission spectra are independent and remain unaffected by changes in pH, however the fluorescent quantum yield (ϕ_F) is directly related to pH [86]. The parameters of fluorescent indicators can be predicted from the appropriate data from the constituent units of the molecule. The ionic binding constants of fluorescent molecules can be predicted and this leads to the estimation of the fluorescent quantum yield (ϕ_F). The maximum fluorescence quantum yield can not be determined accurately, however it can be predicted to an order of magnitude. Since these factors can be calculated with a fair amount of precision, it is theoretically possible to tune the optical properties of molecules whilst maintaining the pH indicating properties [89].

Molecular systems that perform logic operations may have important applications in molecular information processing and computation. The fluorescence of the molecule 9,10-bis {(1-aza-4,7,10,13,16-pentaoxacyclooctadecyl)methyl} anthracene, see Figure 2.2, is 'switched on' only when both of the nitrogen lone pairs of electrons are blocked. This can be achieved by the binding of ethyl ammonium $(CH_3CH_2NH_3)^+$ or alkane diammonium $(H_3N(CH_2)_nNH_3)^{2+}$ ions. The fluorescence is 'switched on' more effectively by the latter since the second electron pair can be blocked by an pseudo-intramolecular cyclisation [90].
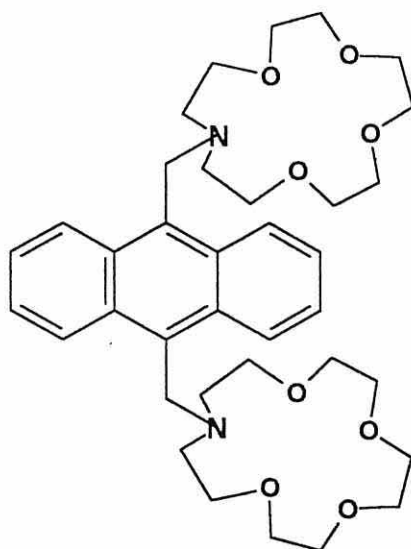
Figure 2.2 : The Fluorescent Molecule, 9,10-bis {(1-aza-4,7,10,13,16-pentaoxacyclooctadecyl)methyl} anthracene

Since such molecules have been developed that selectively recognise changes in conditions, for example pH or cation concentrations, the controllability of the fluorescence towards a particular function by the alteration of physical factors has become more realistic. Receptor molecules that can be considered to perform simple logic operations by coupling ionic bonding, or more complex molecular recognition processes, with fluorescent signals resulting in a change in fluorescent intensity from the receptor, have been developed [88, 89, 91, 92], See Figure 2.3.
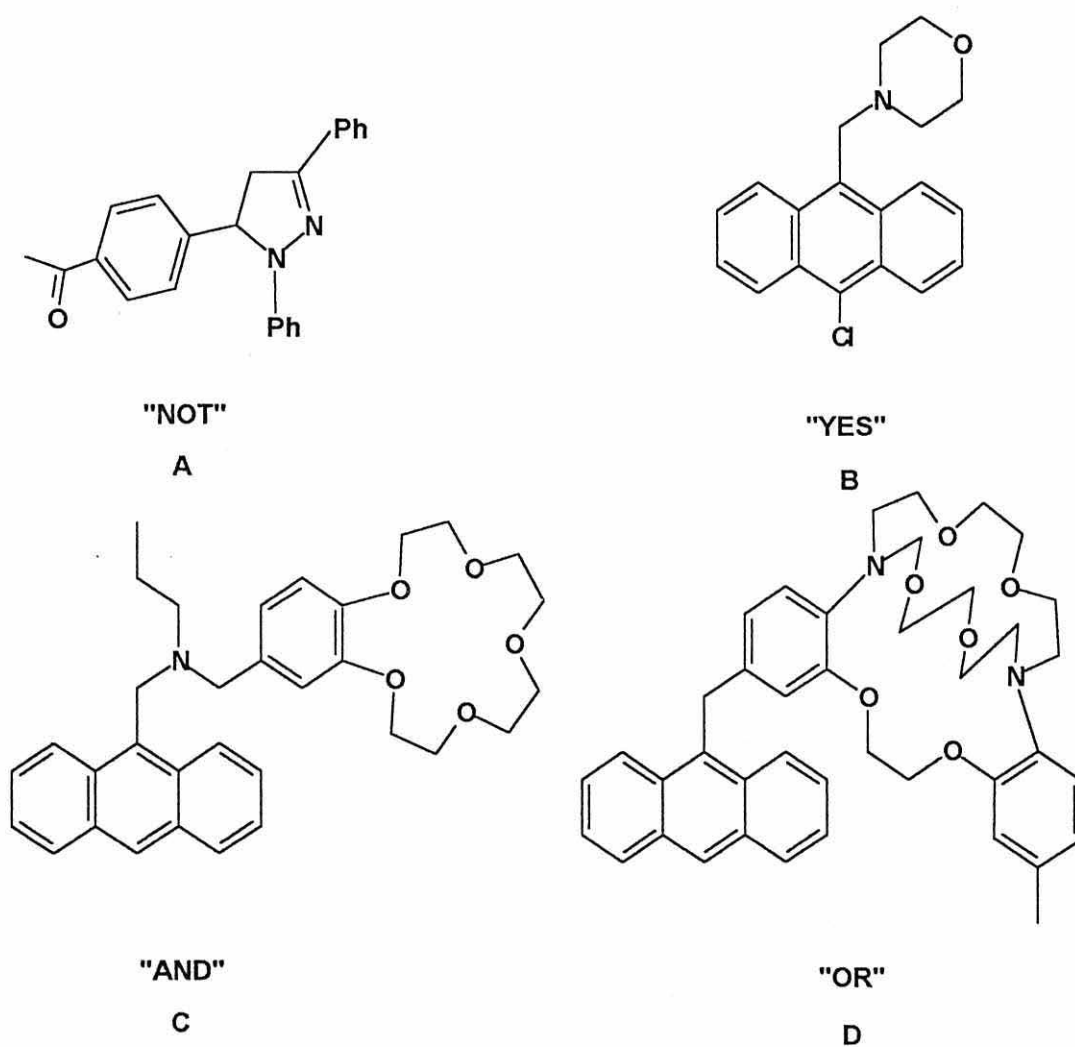
Figure 2.3 : Simple Logic Gates based on Fluorescent Molecules

The molecules shown in Figure 2.3 have been developed by de Silva and co-workers [88, 89, 91, 92] to perform simple logic functions when in a solution of aqueous methanol. When the concentration of protons is high, the fluorescence of molecule (A) decreases to nearly zero, and therefore this molecule may be regarded as a "NOT" gate [89]. Conversely, the fluorescence of molecule (B) rises when the proton concentration is high and so molecule (B) is a "YES" gate [91]. The nitrogen atom in molecule (C) will accept protons and the crown ether will receive sodium ions. The fluorescence of molecule (C) is increased when the concentration of both of the ions are high, and therefore functions as an "AND" gate [92]. The fluorescence of molecule (D) is enhanced when the crown ether moiety accepts either rubidium or potassium ions, thereby making it an "OR" gate [86].

Transition-metal complexes, containing molybdenum or tungsten in either the zero-valent state or in an oxidation state of +2, provide versatile centres for the design and synthesis of novel compounds. The ligands surrounding the metal centre can be displaced with varying ease, depending upon the initial ligand and the introduced species. The complexes $[MI_2(CO)_3(NCMe)_2]$ {M = Mo or W} contain acetonitrile groups that can be replaced with relative ease by other nitrile functional groups. The zero-valent complexes of molybdenum and tungsten can also be functionalised in a similar manner, by replacing the existing ligands around the metal with other neutral ligands. The properties of the complex can be changed by introducing other ligands, and the properties of the introduced ligand can also be altered by changing the nature of the metal centre, for example by electrochemical methods. In the systems synthesised in this chapter, it was hoped to prepare a molecular system that would reflect different fluorescent properties under changing conditions, such as the controlled electrochemical oxidation or reduction of the molybdenum or tungsten complex.

2.2   PREPARATION OF THE FLUORESCENT LIGAND

There are obviously many fluorescent molecules that could be used in an investigation of this type. The requirements for the chosen molecule were firstly that it must be able to bind to a molybdenum or tungsten complex and, secondly, that other sites on the molecule would not interfere with neighbouring molecules. The ligand chosen was a hydrazine-based molecule containing a nitrile group so that it could be easily incorporated into the metal complex *via* nitrile exchange. The molecule also possesses a carboxylic acid functionalisation, however this has no effect on the transition-metal centre. The synthesis of the cyclic hydrazone-based ligand is shown in Scheme 2.2 [93]. The product was isolated as a bright yellow powder.
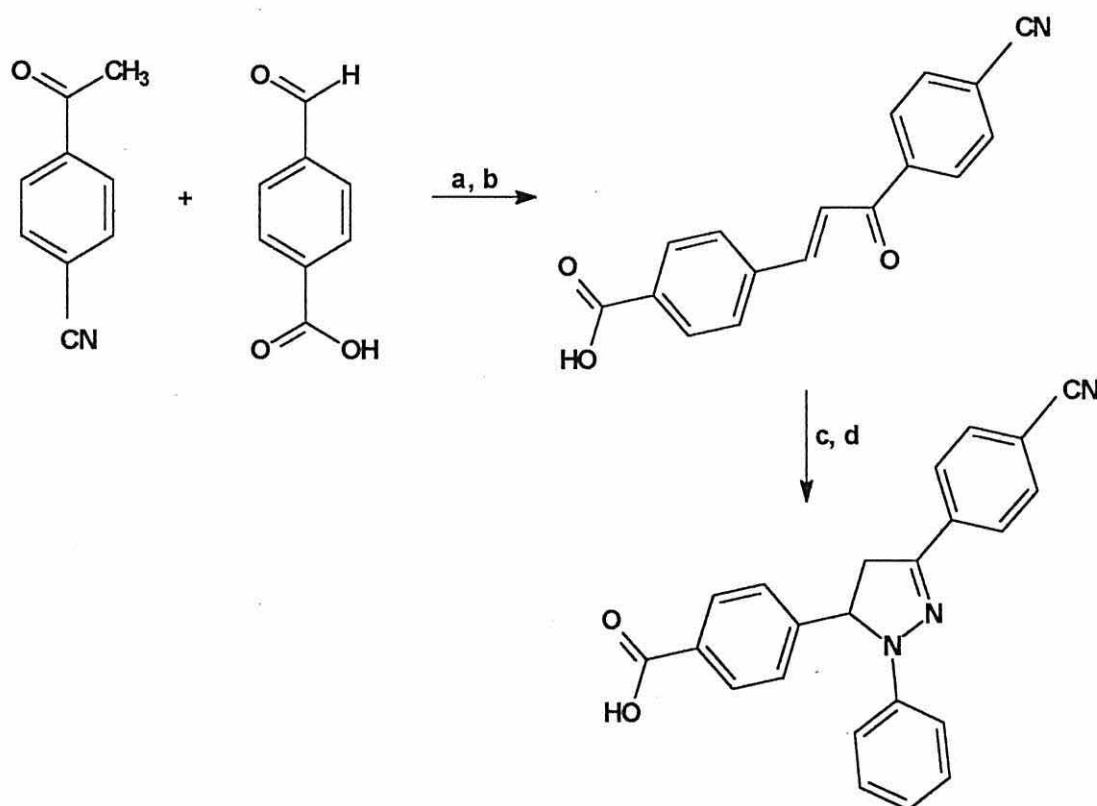
Reagents and Conditions
a.   Sodium hydroxide / ethanol / RT 3 hrs
b.   5M HCl acid
c.   Phenyl hydrazine / glacial acetic acid / 118 °C 3 hrs
d.   Ethanol / 0 °C

Scheme 2.2 : Preparation of the Fluorescent Ligand, $C_{23}H_{17}N_3O_2$

35

2.3 PREPARATION OF THE MOLYBDENUM AND TUNGSTEN COMPOUNDS

The preparation of molybdenum and tungsten complexes containing the fluorescent ligand, $C_{23}H_{17}N_3O_2$, was attempted in two ways according to the oxidation state of the metal. It was envisaged that the cyano- functional group on the ligand was the most likely site for attachment to the metal centre.

2.3.1 Reaction of Zero-Valent Complexes of Molybdenum and Tungsten with the Fluorescent Ligand, $C_{23}H_{17}N_3O_2$

Extensive studies on the reactivity of the zero-valent metal centres [39] have shown that it is possible to attach ligands by refluxing the metal hexacarbonyl in an inert solvent, such as toluene or xylene, with the ligand. Using this as a guideline, equimolar quantities of molybdenum hexacarbonyl and the fluorescent ligand, $C_{23}H_{17}N_3O_2$, were heated in toluene. A yellowish brown powder was obtained. The powder was characterised by elemental analysis (Table 2.1) and infrared spectroscopy (Table 2.2) and the composition was determined to be $[Mo(CO)_5(C_{23}H_{17}N_3O_2)]$. A similar reaction of the tungsten hexacarbonyl with the fluorescent ligand yielded a mixture of inseparable products, and failed to give the required product, $[W(CO)_5(C_{23}H_{17}N_3O_2)]$.

The infrared spectrum for the zero-valent molybdenum complex, $[Mo(CO)_5(C_{23}H_{17}N_3O_2)]$, shows only one carbonyl stretch at 1983.1 cm^{-1}. This suggests that the complex is a six co-ordinate complex, very similar to $[Mo(CO)_6]$, possibly possessing the same octahedral structure.

2.3.2 Reaction of Molybdenum(II) and Tungsten(II) Complexes with the Fluorescent Ligand, $C_{23}H_{17}N_3O_2$

It is known from previous studies that the acetonitrile groups on the complex $[MI_2(CO)_3(NCMe)_2]$ are very labile and readily undergo substitution by other nitrile ligands [66]. The compounds $[MI_2(CO)_3(NCMe)_2]$ {M = Mo or W} were prepared by

36

controlled oxidation of $[M(CO)_3(NCMe)_3]$ using iodine [62]. Stirring a solution of the bisacetonitrile complex in CH_2Cl_2 with two equivalents of the fluorescent ligand gave the seven co-ordinate complexes $[MI_2(CO)_3(C_{23}H_{17}N_3O_2)_2]$ {M = Mo or W} in high yield, see Table 2.1. Both complexes were brown and were found to be soluble in chlorinated solvents, acetonitrile and acetone, but insoluble in diethyl ether and hexane. The complexes were fairly air-stable but oxidised after prolonged exposure to the atmosphere, especially when in solution.

2.3.3 Characterisation of $[MI_2(CO)_3(C_{23}H_{17}N_3O_2)_2]$ {M = Mo or W}

The elemental analyses for the complexes $[MI_2(CO)_3(C_{23}H_{17}N_3O_2)_2]$ {M = Mo or W} compared favourably with their proposed stoichiometry. The infrared spectra of the complexes $[MI_2(CO)_3(C_{23}H_{17}N_3O_2)_2]$ were investigated, see Table 2.2. The absorption frequencies in bold type can be attributed to the fluorescent ligand. Carbonyl complexes exhibit sharp $C \equiv O$ absorption bands and these bands can often provide much information about the structure of the complex. Both the molybdenum and the tungsten complexes show three carbonyl stretching bands in the region 2100 to 1944 cm^{-1}. These are comparable to the bis(acetonitrile) products $[MI_2(CO)_3(NCMe)_2]$ which have three carbonyl bands at 2038 cm^{-1}, 1968 cm^{-1} and 1940 cm^{-1} when M = Mo and 2040 cm^{-1}, 1985 cm^{-1} and 1948 cm^{-1} when M = W. This suggests that the complexes may have a similar structure to $[WI_2(CO)_3(NCR)_2]$ (R = Me or Et), which is a capped octahedron, as revealed by X-ray crystallography studies, see Figure 1.6 [63].

**Table 2.1 : Analytical Data for Molybdenum and Tungsten Complexes
Containing the Fluorescent Ligand, $C_{23}H_{17}N_3O_2$**

COMPLEX	COLOUR	Yield %	C	H	N
$[WI_2(CO)_3(C_{23}H_{17}N_3O_2)_2]$	yellow brown	60 - 70	35.8 (36.1)	2.5 (2.2)	5.4 (6.0)
$[MoI_2(CO)_3(C_{23}H_{17}N_3O_2)_2]$	pale brown	65 - 70	48.7 (50.3)	3.2 (2.9)	7.7 (7.2)
$[Mo(CO)_5(C_{23}H_{17}N_3O_2)]$	pale brown	50 - 60	55.3 (55.7)	2.5 (2.8)	6.6 (6.9)

Calculated values in parentheses

**Table 2.2 : Infrared Data for Molybdenum and Tungsten Complexes
Containing the Fluorescent Ligand, $(C_{23}H_{17}N_3O_2)$**

COMPOUND[a]	υ (cm^{-1})	BOND
$[WI_2(CO)_3(C_{23}H_{17}N_3O_2)_2]$	**3019.4**	**C-H$_{AR}$**
	2399.9	C-N
	2224.0	**C-N**
	2075.7	CO
	2007.4	CO
	1944.1	CO
	1692.1	**CO**
$[MoI_2(CO)_3(C_{23}H_{17}N_3O_2)_2]$	**3019.3**	**C-H$_{AR}$**
	2399.9	C-N
	2227.4	**C-N**
	2100.3	CO
	2033.7	CO
	1962.9	CO
	1694.1	**CO**
$[Mo(CO)_5(C_{23}H_{17}N_3O_2)]$	**3019.0**	**C-H$_{AR}$**
	2400.2	C-N
	2217.1	**C-N**
	1983.1	CO
	1688.3	**CO**

[a] measured as a thin film between NaCl plates.

2.4   FLUORESCENCE STUDIES

Theoretically, the excitation spectrum of a molecule will usually correspond closely in shape to the absorption spectrum. The longest wavelength of the absorption band and the shortest wavelength of the fluorescence band are often the same. However, in practice, this is not always the case due to the difference in the latent heat of solvation in the excited molecule and in the ground state molecule.

As an initial approximation, and ignoring the contribution of the heats of solvation, the absorption spectrum is measured as a method of estimating the excitation wavelength, λ_A. The emission wavelength, λ_{EM}, can be accurately determined by recording an emission spectrum at the estimated wavelength, λ_A. It is then possible to accurately measure the excitation wavelength (λ_{EX}) by rerunning the spectrum at λ_{EM}.
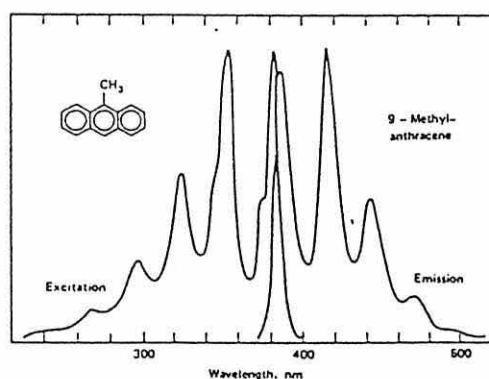
Figure 2.4 : Excitation and Emission Spectra of a Fluorescent Molecule
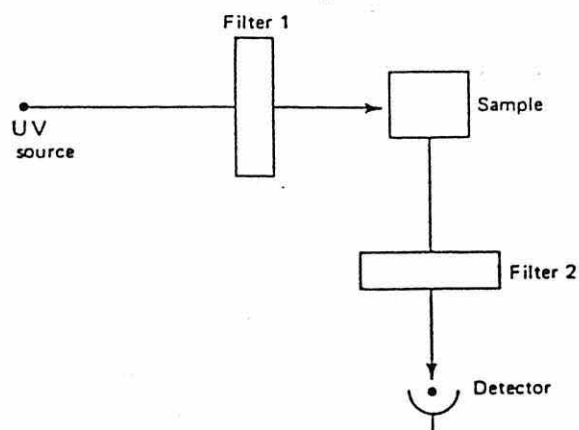
Figure 2.5 : A Simple Fluorometer

39

The fluorescence spectra of the complexes were measured in a mixed solvent system of water and acetone, and the results are presented in Table 2.3. The fluorescence spectra were measured in a mixture of water and acetone, since the signal from the solution would be too strong otherwise. The spectra clearly indicate that there is no significant variation in emission wavelengthwhen the fluorescent ligand is attached to a metal centre. The figures in bold type indicate the emission and excitation due to the solvent.

Table 2.3 : Emission and Excitation Spectral Data of Molybdenum and Tungsten Complexes Containing the Fluorescent Ligand, $C_{23}H_{17}N_3O_2$

COMPOUND	EMISSION (nm)	EXCITATION (nm)
$C_{23}H_{17}N_3O_2$	545	331
	770	**481**
$WI_2(CO)_3(C_{23}H_{17}N_3O_2)_2$	541	400
	770	**475**
$MoI_2(CO)_3(C_{23}H_{17}N_3O_2)_2$	533	367
	769	**403**
$Mo(CO)_5(C_{23}H_{17}N_3O_2)$	539	419
	767	**481**

2.5   ELECTROCHEMICAL STUDIES

Electrochemical studies on the fluorescent transition metal complexes were undertaken in order to investigate the effect of change of oxidation state on the fluorescence of the complex.

2.5.1 Cyclic Voltammetry

Cyclic voltammetric studies of the metal(II) complexes $[MI_2(CO)_3(C_{23}H_{17}N_3O_2)_2]$ {M = Mo or W} were carried out. The cyclic voltammograms of the complexes were measured in acetonitrile with $[^nBu_4N][PF_6]$ as a supporting electrolyte using a Ag/AgCl reference electrode. Three irreversible oxidations at 0.5 V, 0.8 V and 1.0 V were observed for both $[WI_2(CO)_3(C_{23}H_{17}N_3O_2)_2]$ and $[MoI_2(CO)_3(C_{23}H_{17}N_3O_2)_2]$. When the scans were repeated at -35 °C, the irreversible nature of the oxidations had not changed. A reduction peak at -1.8 V in the cyclic voltammogram of the tungsten complex was observed at room temperature. This was also observed to occur at -1.9 V in the cyclic voltammogram of the molybdenum complex. This peak in each of the systems became more reversible at lower temperatures. The increase in the reversible nature of the reduction peaks can be interpreted as being attributable to the reduction products becoming more stable at lower temperatures.

2.5.2 Coulometry

Coulometry allows the complete conversion of starting material to product. It involves holding the electrodes at a constant potential difference and measuring the current. Thus, if after a potential of E volts has been applied to the solution, and peak A is the product, then peak B will not be present in the CV after the experiment has been completed. However, if A is a by-product, or B is the product, B will be observed.
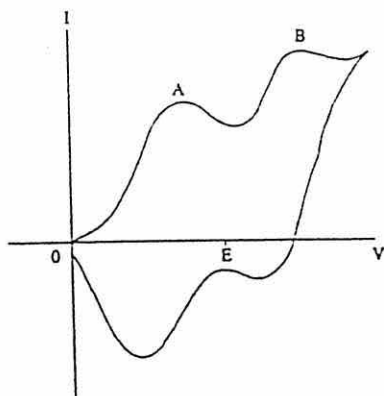
Figure 2.3 : A Typical Cyclic Voltammogram Showing Coulometry Potentials

The number of electrons involved in the electrochemical process can be determined from the equation

$$Q = nFm$$

Q = charge passed (calculated from the current : 1 A = 1 C s^{-1})
n = number of electrons
F = Faraday's constant = 96, 484 C mole^{-1}
m = number of moles of the complex

Coulometry was performed on the molybdenum(II) complex, $[MoI_2(CO)_3(C_{23}H_{17}N_3O_2)_2]$. The cyclic voltammogram of the complex is shown in Figure 2.4, and the coulometry potentials E_1 and E_2 are indicated.

The potential E_1 was held constant at 0.58 V. There was no colour change and there was no difference between the CV spectrum before and after the coulometry. However, when the potential was held at 1.2 V the solution changed in colour from bright yellow to deep blue. The oxidation peak at 1.0 V and the reversible reduction at -1.8 V are not present in the cyclic voltammogram after the coulometry.

These observations suggest that the peaks at 1.0 V and at -1.8 V are connected and are both ligand based processes. This is supported by evidence of peaks around 1 V and -2 V in the cyclic voltammogram of the ligand. The peaks at 0.4 V and 0.8 V are due to the iodide being lost by the complex. Iodide ions have their own electrochemistry. The reason for there being no change after the coulometry at 0.58 V, is that the first peak is a "pre"-peak before the actual peak at 0.8 V.
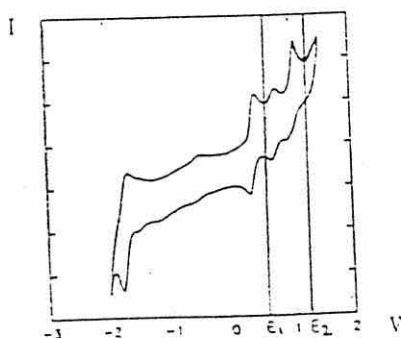
Figure 2.4 : Cyclic Voltammogram of $[MoI_2(CO)_3(C_{23}H_{17}N_3O_2)_2]$

The complexes, although showing oxidation and reduction, are not suitable for spectro-electrochemistry due to the irreversible nature of the electrochemical processes.

2.6 INTRODUCTION TO THIRD ORDER OPTICAL NONLINEARITY

A brief introduction to nonlinear optical (NLO) effects and materials was given in Chapter 1, see Section 1.1.4. The second order effects were discussed along with the structural requirements for such materials. A short introduction to third-order effects will be included here.

One of the more widely studied $\chi^{(3)}$ effects is that of third harmonic generation (THG). This phenomenon is analogous to process described in the introduction, SHG. THG involves a laser of frequency ω interacting with a third-order material and light of frequency 3ω being subsequently produced. Whereas SHG is an example of three-wave mixing, THG is an example of four-wave mixing. The third harmonic that is produced is often near an absorption band of the material and hence the measured γ value may not be a true value.

The symmetry requirements for third-order NLO materials are not as rigid as those for corresponding second-order compounds, however there are certain structural features which can help to maximise the nonlinear effects. The presence of polarisable electrons within a material, for example a conjugated system, will assist in enhancing third-order effects. Another important prerequisite is that the material is optically transparent to laser light at the fundamental wavelength.

An important third-order effect is optical phase conjugation [94]. This is a further example of four-wave mixing, but different beams geometries are used to those in THG. Three laser beams interact with a third-order NLO material and produce a fourth beam at the same frequency, proportional to the input beams. The generated beam is reflected along the path of the probe beam.

43
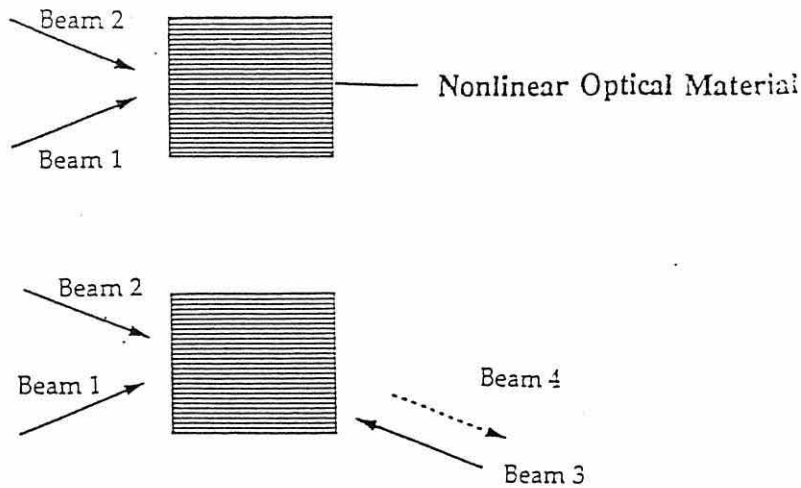
Figure 2.5 : Optical Phase Conjugation

A simplified explanation of optical phase conjugation is that the two coherent counter-propagating pump beams form an optical grating in the material, causing a change in the refractive index because of the variation in light intensity. The change in refractive index is known as the optical Kerr effect and is comparable to the second-order Pockel's effect except that the index change is induced by light rather than an applied electric field. The generated fourth beam is called the phase conjugate signal and the optical grating is known as a phase conjugate mirror.

The phenomenon of the phase conjugate signal being reflected back along the path of the probe beam is peculiar to the phase conjugate mirror. A diverging beam reflecting from a conventional mirror will continue to diverge. Whereas a diverging beam reflected from a phase conjugate mirror will be reflected back through the source, see Figure 2.6.

CONVENTIONAL MIRROR   **PHASE CONJUGATE MIRROR**
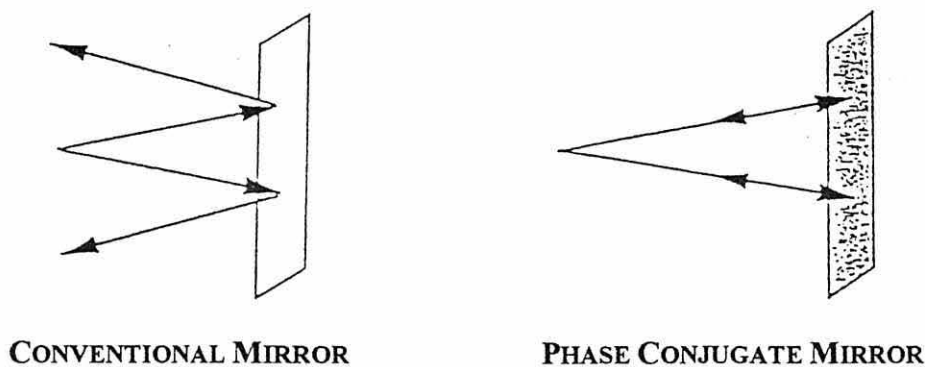
Figure 2.6 : A Diverging Beam reflected from
a Conventional Mirror and a Phase Conjugate Mirror

44

2.6.1 Third-Order Measurements

There are many techniques for measuring the third-order NLO effects in a material. The most common experimental setups are those of degenerate four-wave mixing (DFWM), Z-scan and THG.

2.6.1.1 Degenerate Four-Wave Mixing (DFWM)

Optical phase conjugation can be used as a means of determining the magnitude of the $\chi^{(3)}$ coefficient in nonlinear optical materials by using the ratio of the conjugate signal to the incident probe beam. The technique of ascertaining this ratio is known as degenerate four-wave mixing (DFWM) [95]. An important experimental consideration is that short laser pulses (<100 ps) are required to measure a purely electrical nonlinearity. Slower processes such as thermal, vibrational and orientational effects, can result from longer pulses. These contribute to the observed signal and complicate the interpretation of experimental results when attempting to evaluate structure and property relationships within a material based on electronic nonlinearities.

The relative polarisations of the four beams in the DFWM experiment define the four tensorial components that constitute $\chi^{(3)}$. If all four beams are polarised in the plane of the experimental setup, then the grating formed by the pump beams is described as scalar and both thermal and electronic effects contribute to the tensorial component ($\chi^{(3)}_{1111}$) that is measured and hence, the nonlinearity. However if the probe beam is polarised orthogonal to one of the pump beams, a different tensorial component ($\chi^{(3)}_{1221}$) is measured. The grating is now described as a tensor grating and purely electronic effects contribute to the observed nonlinear response.

2.6.1.2 Z Scan [96]

This technique utilises the 'self-action effects' derived from the intensity dependent refractive index properties of $\chi^{(3)}$ nonlinear optical materials. This relies on the generation

45

of a NLO response in a material at the same frequency as the incident beam, of which there is only one as in contrast to DFWM where there are two. The polarisation response produced in the material affects the propagation characteristics of the transient light and is thus termed a self-action effect. There are two main examples of such an effect : self-focussing and self-defocussing. Self-focussing occurs in materials with a positive value of the nonlinear refractive index, n_2, and results in a spatial variation of the intensity of the incident laser pulse. Consequentially, the magnitude of n_2 is greater at the centre of the pulse and the material acts as a positive lens and focuses the beam. Self-defocussing arises from a negative value of n_2 and a negative lens is created, causing self-defocussing of the laser beam. The Z-scan technique can be used to measure the sign and the magnitude of the third-order nonlinearity in materials.

2.6.1.3 The Maker Fringe Technique

The Maker fringe technique was used to measure the third-order NLO response of the complexes $[MI_2(CO)_3(C_{23}H_{17}N_3O_2)_2]$ {M = Mo or W} and $[Mo(CO)_5(C_{23}H_{17}N_3O_2)]$. One of the difficulties with THG measurements of the $\chi^{(3)}$ coefficient of a material is that the measured third harmonic of 355 nm often lies in the optical absorption band of most NLO active molecules, enhancing the THG response. The enhancement is caused by resonance effects and non-electronic effects, however, these processes occur much slower than the purely electronic effects measured by the Maker fringe technique.

A simplified description of the Maker fringe technique is that a laser beam of frequency 1064 nm is directed through the material, deposited as a thin film on a silica slide, and the beam of light emitted at the third harmonic frequency of 355 nm is measured. The experimental set up for the THG measurements is shown in the Figure 2.7. The slide was mounted on a rotational stage in a vacuum chamber. This was rotated through from -30° to +30° and the third harmonic generation intensity recorded. When the measurements on the film were complete, the film was wiped off the glass without movement of the slide, and the laser passed through exactly the same site on the glass as it did through the film and the glass. The full set of parameters required to calculate the nonlinear response

is given in Table 2.4. The thickness (t), extinction coefficient (ϵ) and percentage weighting in the polymer (%) were all calculated and the absorbance at λmax, 1064 nm and 355 nm can be measured. When the THG intensity is plotted against the angle of incidence (-30° to +30°) for the substrate and for the substrate and film, it is obvious whether the film has shown any nonlinear response by comparison of the plots of the film on the substrate and the substrate alone, see Figure 2.8.

For nonlinear optical studies to be carried out on a compound, thin films of the material have to be deposited on a substrate. The THG properties of the complexes $[MI_2(CO)_3(C_{23}H_{17}N_3O_2)_2]$ {M = Mo or W} and $[Mo(CO)_5(C_{23}H_{17}N_3O_2)]$ were investigated using thin films which were made by dip coating a solution of the complex onto a glass slide. A host polymer of polymethylmethacrylate (PMMA) was used since this gives a high host-guest weighting and is also transparent to the laser beam. The thickness of the film was calculated using the formula :

$$\textbf{Thickness (t)} = \frac{\textbf{(A x MW) x 10}^3}{\textbf{(}\rho \textbf{ x } \epsilon \textbf{ x \%)}}$$

A	=	absorbance of the film at λ_{max}
MW	=	molecular weight of the sample
ρ	=	density of guest and host (g cm^{-1}) = 1.3
ϵ	=	Molar Extinction Coefficient of the sample
%	=	weight % of the sample in host polymer

2.6.2   Calculation of the $\chi^{(3)}$ Coefficient

The relative magnitude of the susceptibility, $\chi^{(3)}_f$, with respect to that of the substrate can be determined from the equation :

$$|\chi^{(3)}_f (-3\omega:\omega.\omega.\omega)| = (2/\pi)\, \chi^{(3)}_s \left[\frac{I_{c,s}}{I_f} \frac{I_{3\omega,s}}{I_{3\omega,f}} \right]^{½} F$$

ω = 3rd order NLO susceptibility of the substrate

$I_{c,s}$ = coherence length of the substrate (glass)

I_f = thickness of the film (t)

$I_{3\omega.f}$ = 3rd harmonic intensity of the film, taking into account a correction for the substrate

$I_{3\omega.s}$ = 3rd harmonic intensity of the substrate without the film

F   = attenuation factor

At the fundamental wavelength (λ = 1064 nm), the coherence length of the glass ($I_{c,s}$) = 6.823 m and $\chi^{(3)}_s$ = 434 pm^2 V^{-2} = 3.11 x 10^{-14} cm^4 sC^{-2}. (1sC = 1 statcoulomb). The third harmonic intensities, $I_{3\omega.f}$ and $I_{3\omega.s}$, are obtained from the envelope function (indicated in Figure 2.11) at normal incidence. The attenuation factor, F, is only needed when the film under investigation absorbs at 1064 nm. This equation does not give an absolutely accurate value of the $\chi^{(3)}$ value, since it assumes certain factors, however, it is a good approximation of the magnitude of the $\chi^{(3)}$ coefficient.

Table 2.4 : Complete Parameters Required for the Determination of the $\chi^{(3)}$ Coefficient

FILM	t (nm)	λ (nm)	ϵ	w % wt	MW	$A_{\lambda max}$	A_{1064}	A_{355}
Sample	~200	x	x	~10	x	x	~0	x

The shape of the plot of THG intensity against the angle of incidence is that of a sine curve and is known as a Maker fringe pattern. Only one half of the plot is considered when calculating $\chi^{(3)}$.
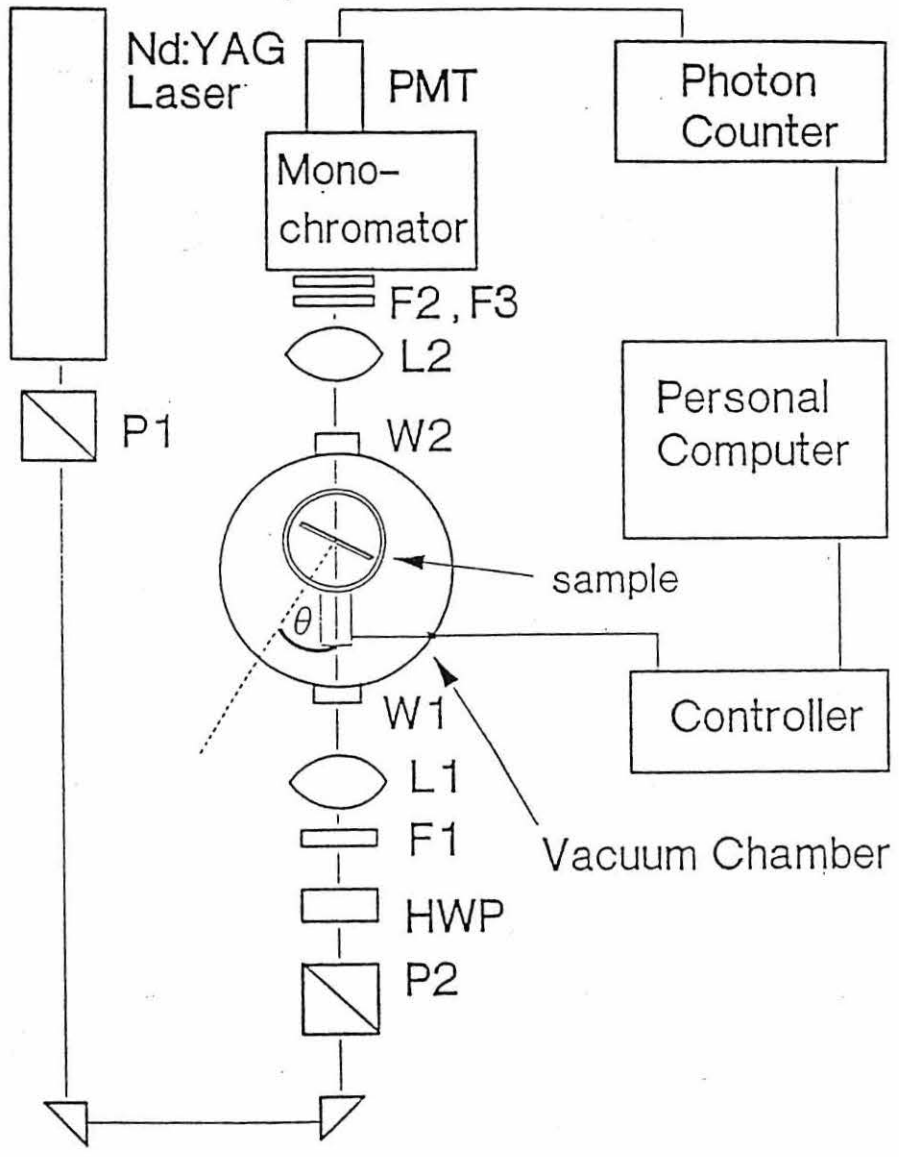
Figure 2.7 : Experimental Setup for THG
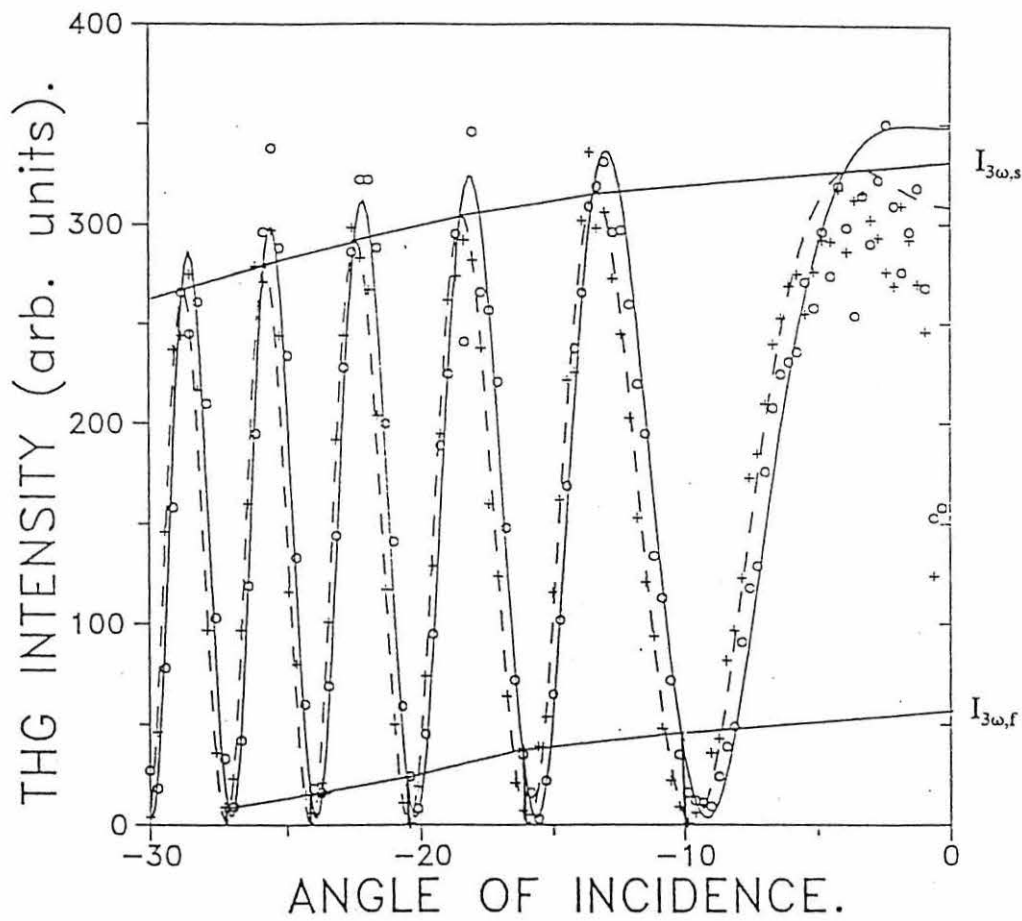
Figure 2.8 : Maker Fringe Pattern Showing the Envelope Function

50

2.6.3 THG Studies on Molybdenum(0) and Molybdenum(II) Complexes Containing the Fluorescent Ligand $C_{23}H_{17}N_3O_2$

The nonlinear optical properties of the complexes $[Mo(CO)_5(C_{23}H_{17}N_3O_2)]$ and $[MoI_2(CO)_3(C_{23}H_{17}N_3O_2)_2]$ were investigated. The fluorescent ligand, $C_{23}H_{17}N_3O_2$, contains both an electron donor (CN) and an electron acceptor (COOH) and, as a result, would be expected to have a dipole moment. This, linked with the seven co-ordinate structure of the molybdenum(II) complex, $[MoI_2(CO)_3(C_{23}H_{17}N_3O_2)_2]$, and the bulky nature of the ligand, $C_{23}H_{17}N_3O_2$, suggests that it may crystallise in a non-centrosymmetric space group, thereby maintaining a net dipole moment over the bulk material. The zero-valent molybdenum complex, $[Mo(CO)_5(C_{23}H_{17}N_3O_2)]$ is six co-ordinate, however by incorporating only one fluorescent ligand the complex becomes unsymmetrical and the probability of the molecule crystallising in a non-centrosymmetric space group is increased. As mentioned in Section 1.1.4, a non-centrosymmetric space group and the presence of a dipole moment are favourable for the material exhibiting second-order effects. However, the materials $[Mo(CO)_5(C_{23}H_{17}N_3O_2)]$ and $[MoI_2(CO)_3(C_{23}H_{17}N_3O_2)_2]$ were not found to possess any observable second-order properties.

The third-order NLO properties of the complexes $[Mo(CO)_5(C_{23}H_{17}N_3O_2)]$ and $[MoI_2(CO)_3(C_{23}H_{17}N_3O_2)_2]$ were then assessed. The plot of the THG response of the complex $[Mo(CO)_5(C_{23}H_{17}N_3O_2)]$ is shown in Figure 2.10 and the THG plot of the fluorescent ligand, $C_{23}H_{17}N_3O_2$ is shown in Figure 2.9. It can be seen from the plot of $[Mo(CO)_5(C_{23}H_{17}N_3O_2)]$ that there is an observable third-order response. The $\chi^{(3)}$ value was calculated to be 3.3×10^{-13} esu. Comparison of the $\chi^{(3)}$ values of the complex and the ligand show that the complexation of the molybdenum(0) with the ligand actually lowers the $\chi^{(3)}$ value by an order of 0.1 esu. The $\chi^{(3)}$ value of the fluorescent ligand was determined to be 1.3×10^{-12} esu. This value can be compared to the $\chi^{(3)}$ values obtained for other well studied systems, such as metal dithiolenes. In 1992, Winter *et al* [97] published the results of a comprehensive investigation into the third-order nonlinearities of a variety of metal dithiolenes. A range of $\chi^{(3)}$ values for substituted nickel dithiolenes were calculated (DFWM technique at 1064 nm in dichloromethane) however, it is difficult

$C_{23}H_{17}N_3O_2$

Film Thickness = 71 nm
Fundamental Wavelength = 1064 nm
Fused Silica Substrate
$\chi^{(3)} = 1.3 \times 10^{-12}$ esu
$\gamma = 1.5 \times 10^{-33}$ esu
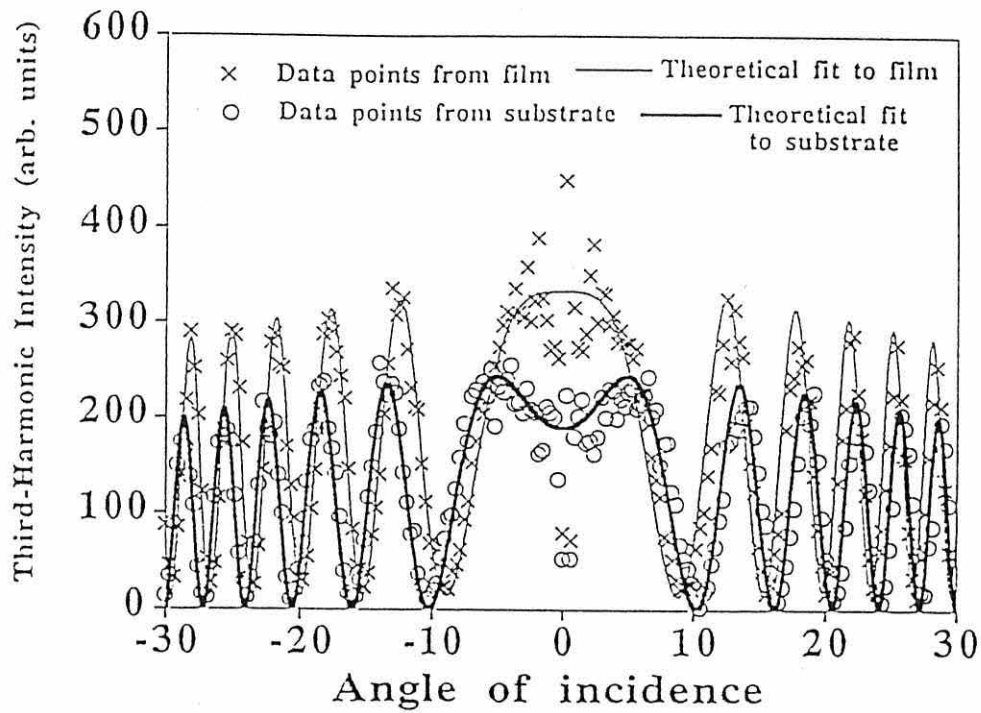
Figure 2.9 : Maker Fringe Pattern for $C_{23}H_{17}N_3O_2$

Mo(CO)$_5$(C$_{23}$H$_{17}$N$_3$O$_2$)

Film Thickness = 240 nm
Fundamental Wavelength = 1064 nm
Fused Silica Substrate
$\chi^{(3)}$ = 3.3 x 10^{-13} esu
γ = 7.9 x 10^{-34} esu
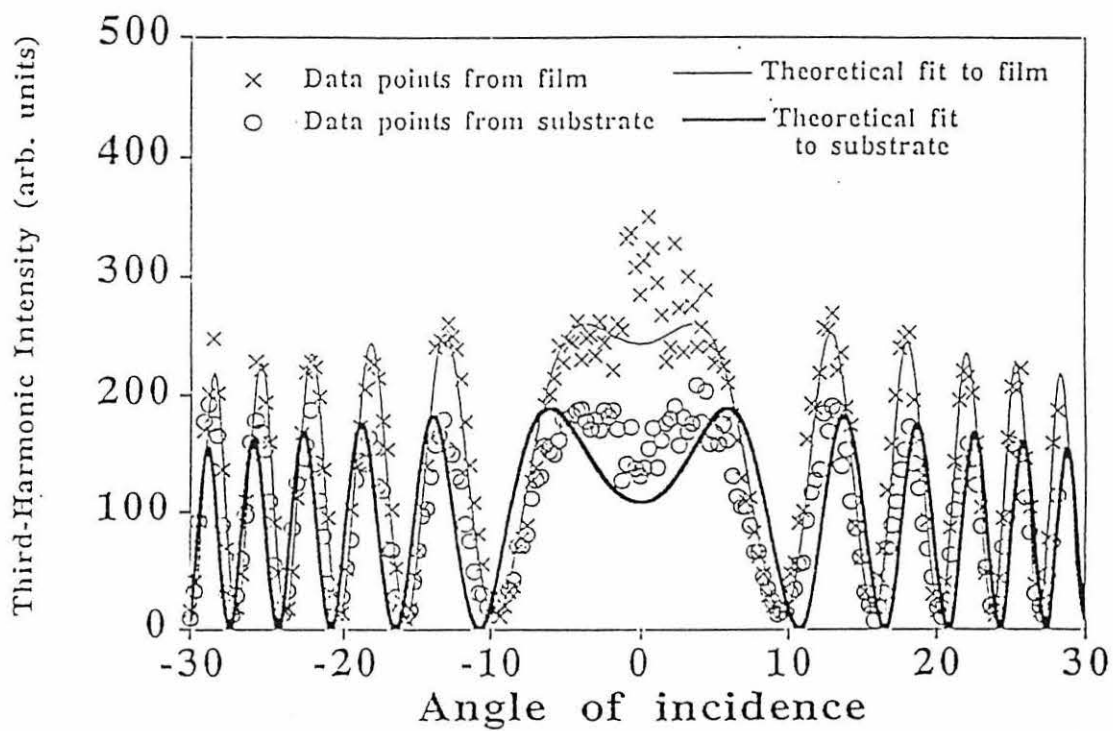
Figure 2.10 : Maker Fringe Pattern for Mo(CO)$_5$(C$_{23}$H$_{17}$N$_3$O$_2$)

to compare the results with the values of $\chi^{(3)}$ for the fluorescent ligand, $C_{23}H_{17}N_3O_2$, and the molybdenum complexes since different techniques and solvents were used. It is interesting to note that, although dithiolenes have shown $\chi^{(3)}$ values when measured using DFWM techniques, very low values were reported when the Maker fringe technique was used [98].

More comparable are the ruthenium cyclopentadienyl complexes such as [Ru(η^5-C_5H_5)((+)-DIOP)(p-NCC$_6$H$_4$NO$_2$)][PF$_6$], see Figure 2.11, which has a $\chi^{(3)}$ value of 2.4 x 10^{-13} esu [12]. This complex has also been found to possess second-order properties [99].
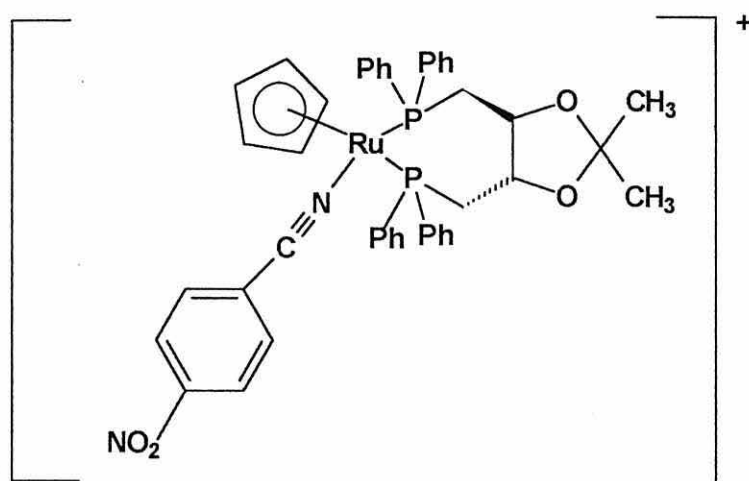
Figure 2.11 : [Ru(η^5-C$_5$H$_5$)((+)-DIOP)(p-NCC$_6$H$_4$NO$_2$)]$^+$

The complex [MoI$_2$(CO)$_3$(C$_{23}$H$_{17}$N$_3$O$_2$)$_2$] was found to possess third-order properties, however discrepancies arose over the reproducibility of the $\chi^{(3)}$ values and investigations into this compound are continuing.

The tungsten complex, [WI$_2$(CO)$_3$(C$_{23}$H$_{17}$N$_3$O$_2$)$_2$] did not give a measurable third-order response. It may be expected that since the complex is analogous with [MoI$_2$(CO)$_3$(C$_{23}$H$_{17}$N$_3$O$_2$)$_2$], it would show a third-order response. The effect of the bonding in the molybdenum complex compared with the tungsten complex may be directly related to this.

2.7 CONCLUSIONS

The work described in this chapter has described the preparation of three metal complexes containing a fluorescent ligand and the subsequent investigations of their physical properties. The results are summarised below.

- It is feasible to prepare the fluorescent ligand, $C_{23}H_{17}N_3O_2$, and to attach it to the metal centres Mo(0), Mo(II) and W(II) *via* the pendant nitrile group.

- The fluorescence spectra of these complexes, when compared to the fluorescence spectrum of the ligand, do not show any significant changes. This implies that there is no noticeable perturbation of the electron flow through the ligand by the metal centre in each of the complexes.

- There are no observable SHG effects shown by the complexes. There could be many reasons for this, one of which could be that there is no induced dipole moment. One might expect the ligand to have a dipole moment by virtue of the fact that there is a nitrile group (donor) and a carboxylic acid group (acceptor) at opposite ends of the ligand, $C_{23}H_{17}N_3O_2$. However, the presence of the phenyl group and the extra nitrogen atoms in the ligand will probably alter the dipole, so the situation is not so straightforward.

- The tungsten complex, $[WI_2(CO)_3(C_{23}H_{17}N_3O_2)_2]$, did not show any observable third-order effects.

- The complexes $[Mo(CO)_5(C_{23}H_{17}N_3O_2)]$ and $[MoI_2(CO)_3(C_{23}H_{17}N_3O_2)_2]$ both showed a sizeable THG response, comparable to other systems. The co-ordination of the ligand to the metal centre causes a small quenching of the THG response and the $\chi^{(3)}$ value is diminished by ca. 0.1 esu.

Chapter Three

Synthesis, Characterisation

and Further Investigation of

Tungsten-1,2-Dithiolenes

3.1 INTRODUCTION

The work presented in this chapter describes the reactions between $[WI_2(CO)_3(L)]$ {L = $(PPh_3)_2$, $(PEt_3)_2$ or (dppe)} and dithiolene-type sulphur ligands, mnt, dmit or bdt, and the characterisation of the resulting six co-ordinate complexes. Both tungsten complexes and metal complexes of 1,2-dithiolenes have been extensively studied and characterised over the last decade and therefore there is an interest in research into compounds which combine these two molecular systems. The electrochemistry of molecules possessing both redox-active centres was also of interest.

In recent years the growing interest in delocalised sulphur donor chelating ligands has promoted a surge in the development of new complexes containing such ligands. The areas of interest are diverse. The ability of compounds containing sulphur donor groups to conduct electrical currents and to show unusual magnetic properties has led to investigation of their use in molecular electronics as conductors [1] and superconductors [5]. Molybdenum-sulphur complexes have received much attention due to their use in modelling biological systems such as xanthine oxidase and nitrogenase [100].

The dithiolene ligands may be divided into two general categories. The 1,1-dithiolates form four-membered rings on complexation to a metal centre. They consist of two sulphur atoms separated by a single carbon atom.

R = Functional group

Figure 3.1 : 1,1-Dithiolato Ligands

57

The 1,2-dithiolates form five-membered rings on complexation to a metal.
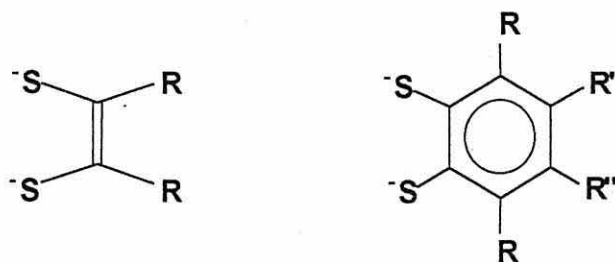
ETHENE-**1,2**-DITHIOLENES   BENZENE-**1,2**-DITHIOLENES

R = Functional group
R' and R" can be different or the same as R

Figure 3.2 : 1,2-Dithiolato Ligands

3.1.1   1,1 - Dithiolenes

The general formula of this group of sulphur donor ligands is $[S_2CY]^{x-}$ (x = 2 or 1), and includes dithiocarbamates $(S_2CNR_2)^-$, dithiocarboxylates $(S_2CR)^{2-}$, xanthates $(S_2COR)^-$, thioxanthates $(S_2CSR)^-$, dithiocarbonates $(S_2CO)^{2-}$, trithiocarbonates $(S_2CS)^{2-}$ and dithiophosphinates $(S_2CPR_2)^-$. The electron density on the sulphur atoms can be controlled by varying the substituent R. If R is an electron withdrawing group such as a halide or hydroxide then the negative electron density on the sulphur atoms will be decreased and thus the co-ordinate bond with the metal will be weaker. Similarly, if the substituent R is an electron donating group such as a nitrile then the metal-sulphur bond will be stronger since the electron density will flow towards the sulphur. These ligands can co-ordinate to the metal centre in either a monodentate [101] or, more commonly, a bidentate manner. Six and seven co-ordinate dithiocarbamate complexes of molybdenum(II) and tungsten(II), such as $[M(CO)_n(S_2CNR_2)_2]$ {M = W or Mo; n = 2 or 3; R = Me, Et or Pr^i}, have been studied extensively [102, 103]. When acting as a bidentate ligand the 1,1-dithiolates are found to stabilise the metal centre in unusually high oxidation states. As well as behaving as mono- or bidentate ligands the 1,1-dithiolato anions can also act as bridging ligands [104].

3.1.2 1,2-Dithiolenes

3.1.2.1 Background

The first studies on the metal-1,2-dithiolenes were made sixty years ago based on the reactions of toluene-3,4-dithiol and 1-chlorobenzene-3,4-dithiol with metal halides [105, 106]. Compounds of the type [M(dithiol)$_2$] {M = metal, particularly tin} were isolated.

R = Me or Cl
X = Halide
M = Metal
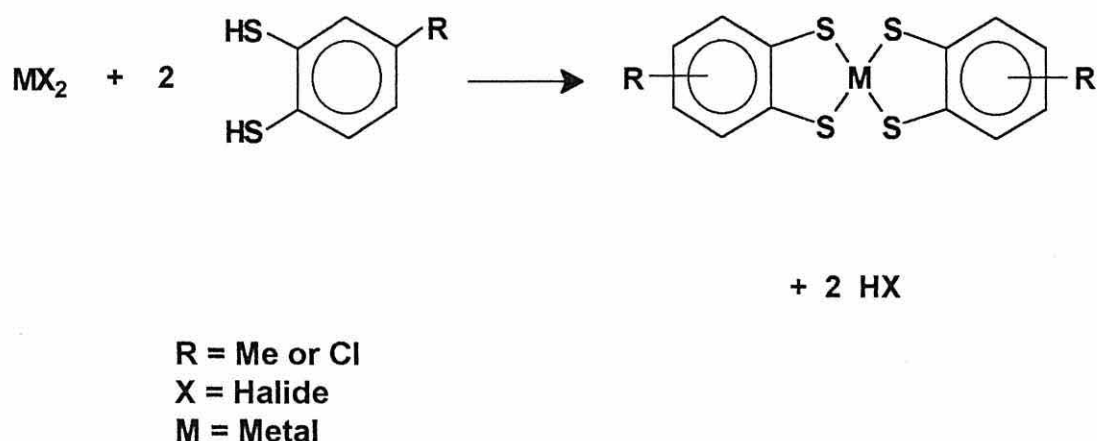
Figure 3.3 : Reaction of Metal Halides with either
Toluene-3,4-Dithiol or 1-Chlorobenzene-3,4-Dithiol

However it was not until almost thirty years later that interest in the unsaturated 1,2-dithiols was reawakened. In 1957, Bähr and Schleitzer synthesised the salt disodium maleonitrile-1,2-dithiolate [Na$_2$S$_2$C$_2$(CN)$_2$] [107]. The discovery that this salt readily formed complexes with palladium prompted a surge in thiolate chemistry over the next few years. Various bis-dithiolene systems were reported such as [M(mnt)$_2$]$^{2-}$ {M = Cu, Ni, Pd or Co; mnt = (S$_2$C$_2$(CN)$_2$)} and nickel bis-diphenyldithiolate [Ni(S$_2$C$_2$Ph$_2$)$_2$] [108]. In 1960, Gilbert and Sandell isolated and characterised the diamagnetic molybdenum tris-toluene-3,4-dithiolate complex [Mo(S$_2$C$_6$H$_3$Me)$_3$] [109]. This was the first reported tris-substituted dithiolene complex.

3.1.2.2 Properties of the Metal-1,2-Bisdithiolenes

The general formula of the 1,2-dithiolates is $[(S_2C_2R_2)^{2-}]$ as shown in Figure 3.2. As with the 1,1-dithiolenes, the properties of the sulphur ligand and hence the properties of the complex can be modified by the nature of the functional group R. The more electronegative the R group, the more the electron density will move away from the sulphur atoms, and therefore the weaker the metal-sulphur interaction. Conversely, if R is an electropositive group then the metal-sulphur interaction will be strengthened.

The d^8 metal complexes of the 1,2-dithiolenes are effectively analogues of the planar organic donor molecule tetrathiafulvalene (TTF).

Figure 3.4 : Tetrathiafulvalene and the Bis-Dithiolene Metal Complex
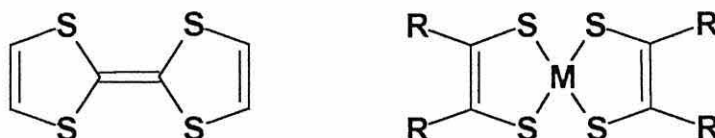
The metal complexes stack in a similar manner to TTF in the solid state and the close proximity of the molecules enables strong inter- and intra-stack interactions, see Figure 3.5. Short S··S distances between adjacent molecules give rise to the material properties that are associated with these complexes.

Altering the nature of the sulphur atoms will affect the attributes of the ligands, and therefore the complex. Changing the functional group R will affect electron density throughout the ligand thereby affecting the electron density on the sulphur atoms. Changing the central metal, M, will influence the metal-sulphur interactions and as a result, the nature of the sulphur atoms. Modifications to the metal and the functional groups of the metal-1,2-bisdithiolene will affect the properties of the individual molecules

60

as well as the bulk co-operative properties of the material. Amendments to the size and charge of the counter cation will change the way the molecules interact in the bulk material, and so changing the properties associated with the material.
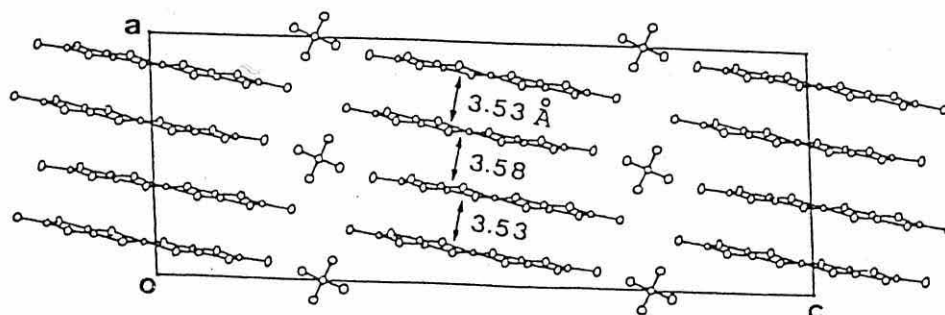
Figure 3.5 : Crystal Structure of [Me₄N][Ni(dmit)₂]₂
Showing the Inter-Molecular Spacing [110]

It is possible to effect the redox cycle between the dianionic species and the neutral species *via* the intermediate monoanionic species. The three species are easily interchangeable and the metal complexes can typically be isolated in each of the three forms.
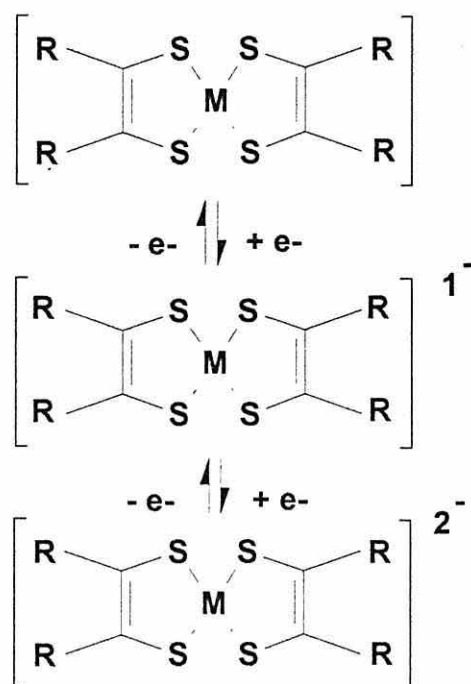
Figure 3.6 : The Redox Cycle between the Dianion,
the Monoanion and the Neutral Species of the 1,2-Bisdithiolenes

3.1.2.3 Organometallic Complexes of the 1,2-Dithiolenes

Many π-cyclopentadienyl metal complexes containing 1,2-dithiolene ligands were synthesised and characterised at the end of the 1960's by King [111] and McCleverty *et al* [112, 113]. Two basic synthetic routes were followed, depending upon the oxidation state of the dithiolene. If the dithiolene used was of the neutral form then the reacting metal complex was a π-cyclopentadienyl metal carbonyl. However if the sulphur donor ligand was employed in its dianionic form, the π-cyclopentadienyl metal halide was used in the synthesis. The complexes $[(Cp)Co(S_2C_2R_2)]$ {R= CF_3 or CN}, have been fully characterised, however their structural identification has proved controversial.

An infrared study of $[(Cp)Co\{S_2C_2(CF_3)_2\}]$ in 1963 [111] led King to propose a nominally six co-ordinate sandwich type structure of cobalt(III) as shown in Figure 3.7 with the co-ordination through the C=C bond to the metal in addition to the two sulphur bonds. The structure was based on the observed diamagnetism, the decrease in the C=C infrared stretching frequency of the dithiolene moiety and the 18-electron rule. The structure proposed by King was disproved by Baird and White [114] three years later by X-ray crystallography. They found the sulphur donor ligands to be co-ordinated to the metal through the S atoms in the same way as was observed for the monomeric bis-dithiolenes. From the bond distances, Baird and White concluded that the complex should be considered a five co-ordinate complex of cobalt(I) and not, as originally thought, a six co-ordinate complex of cobalt(III). The structure of $[(Cp)_2Mo(S_2C_6H_3(CH_3))]$ [115] was elucidated around the same time and this agreed with the structural implications put forward by Baird and White. R. Eisenberg in a comprehensive review of 1,1- and 1,2-dithiolato chelates [116], proposed that in view of the structures of the cobalt and molybdenum π-cyclopentadienyl complexes containing 1,2-dithiolene ligands, they can be regarded as derivatives of bis- or tris- dithiolene systems with one or more of the ligands replaced by the cyclopentadienyl ligand in a plane normal to the axis of the $[MS_2C_2]$ chelate ring.
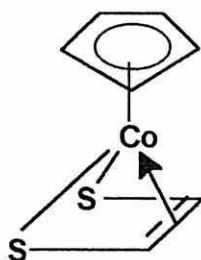
Figure 3.7 : Proposed Structure for $[(Cp)Co(S_2C_2(CF_3)_2)]$

This chapter describes the synthesis and full characterisation of a series of novel tungsten-1,2-dithiolenes of the type $[W(X)(CO)_2(L)]$ {X = 1,2-dithiolene = dmit, mnt or bdt; L = phosphine = $(PPh_3)_2$, $(PEt_3)_2$ or dppe}.

3.2   RESULTS AND DISCUSSION

3.2.1   Preparation of the 1,2-Dithiolenes

The alkali metal salts of the dithiolene ligands used are shown in Figure 3.8. The dmit salt, Na_2(dmit) {dmit = S_5C_3}, was prepared *in situ* by stirring the ester-protected dmit in an ethanolic solution of sodium ethoxide (Scheme 3.1). The $(TTFS_4)^+$ salt is prepared in a similar manner by stirring the ethyl nitrile-protected compound in a solution of caesium hydroxide in thf to give Cs_4(TTFS$_4$) (Scheme 3.2). The disodium salt of maleonitrile-1,2-dithiol is prepared and stored in this fairly stable form (Scheme 3.3). Attempts to prepare and use the caesium and the sodium salts of the benzene dithiol were not wholly satisfactory, however the untreated H_2(bdt) reacted quickly and cleanly with the tungsten-phosphine complexes in an acetonitrile medium.
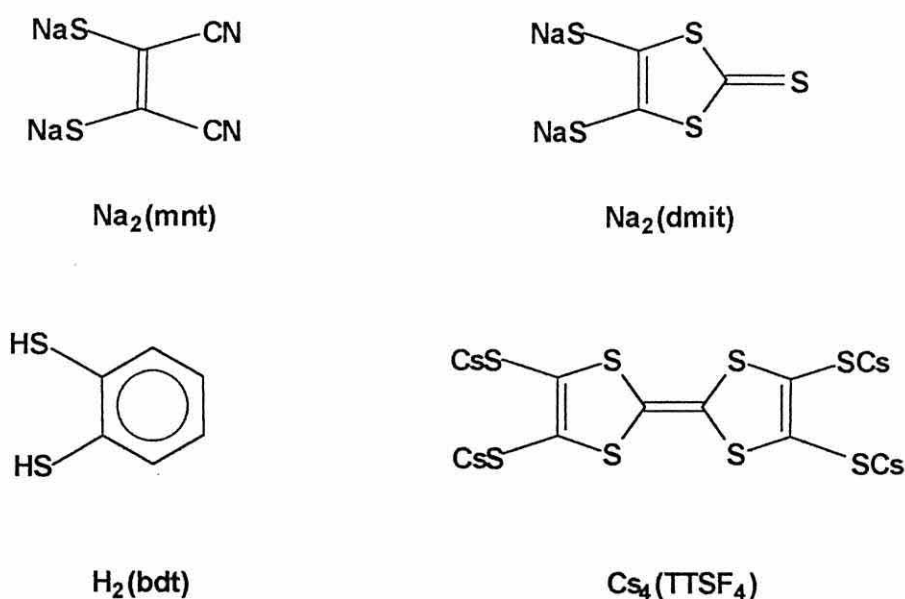
Figure 3.8 : The Dithiolene Ligands in their Reactive Forms

4 CS$_2$ + 4 Na

dmf

a, b, c

[NEt$_4$]

d

e
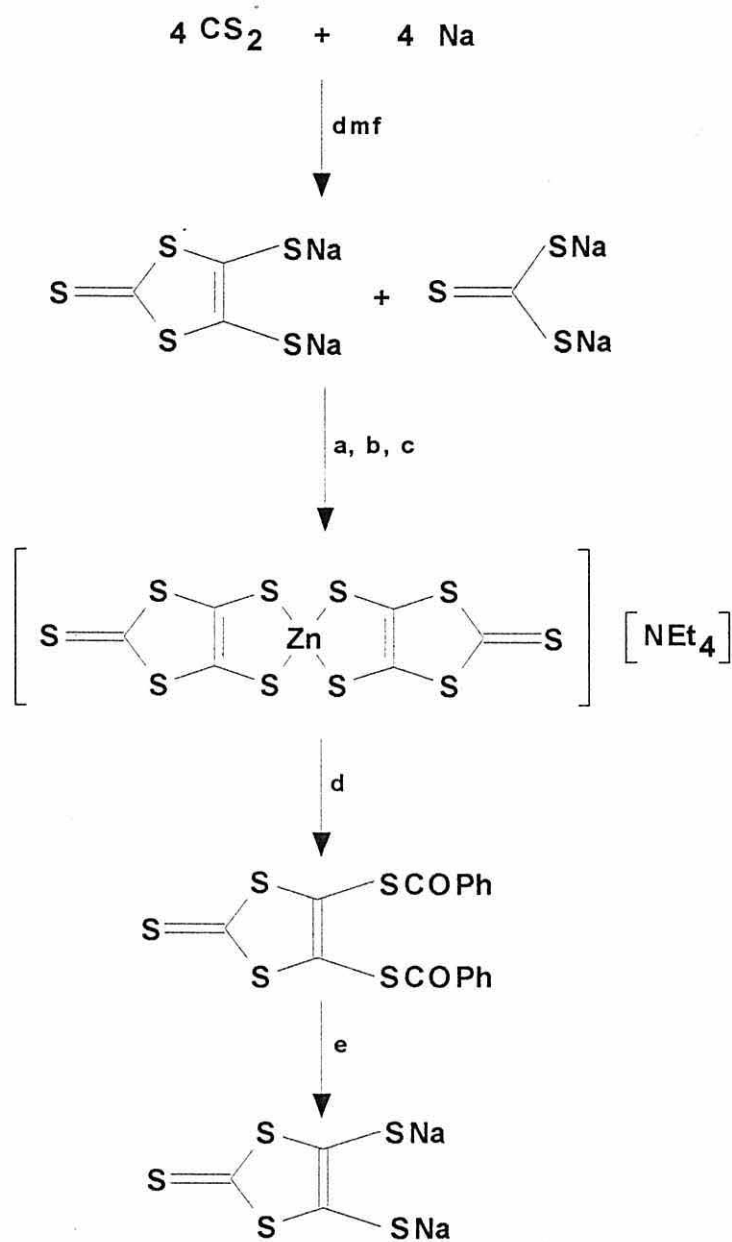
a : MeOH / H$_2$O
b : ZnCl$_2$ / NH$_3$ / MeOH
c : NEt$_4$Br / H$_2$O
d : PhCOCl / acetone
e : NaOEt / EtOH

Scheme 3.1 : Preparation of Na$_2$(dmit)

65
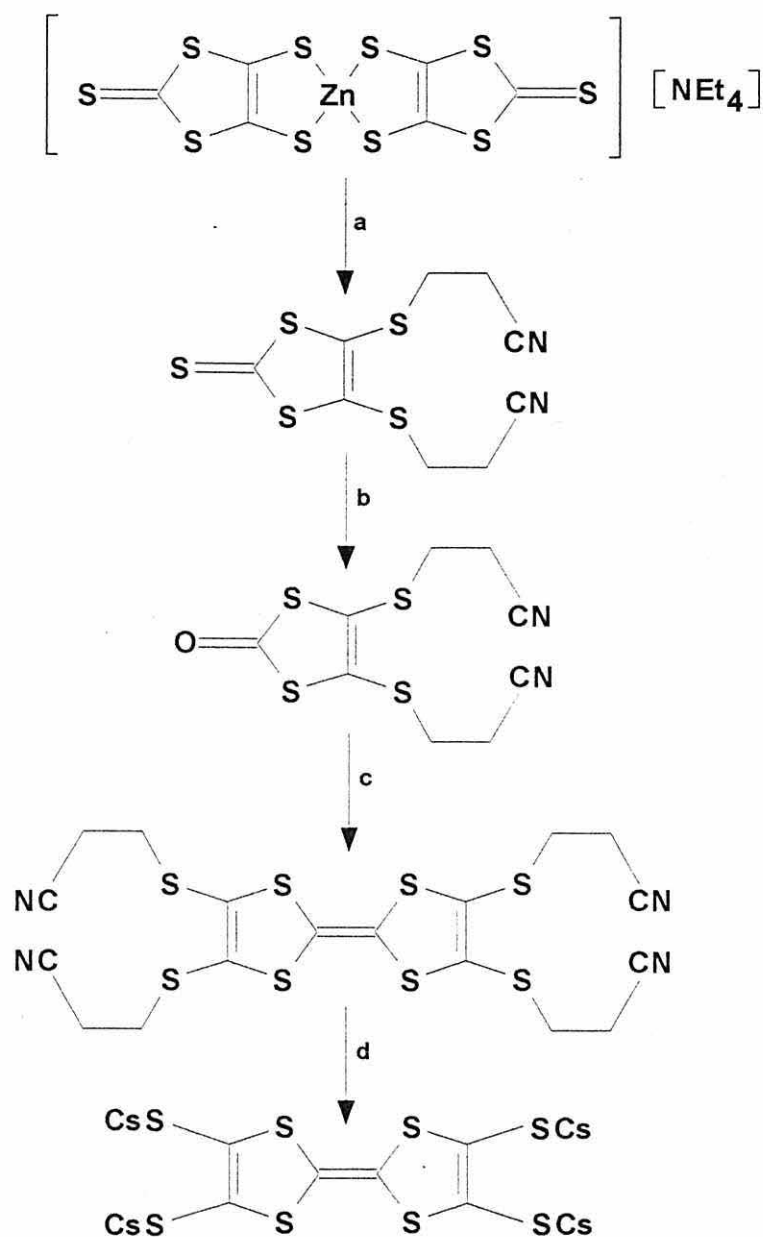
a : 4 BrEtCN / MeCN / reflux 1 hour
b : Hg(OAc)$_2$ / CHCl$_3$ / AcOH / 16 hours
c : P(OEt)$_3$ / toluene / 110 °C 30 minutes
d : CsOH.H$_2$O / thf / 1 hour

Scheme 3.2 : Preparation of Cs$_4$(TTFS$_4$)

$$NaCN \quad + \quad CS_2$$

$$\Big| \, dmf$$

$$\blacktriangledown$$

$$NC - C \overset{\displaystyle \diagup S}{\underset{\displaystyle \diagdown S\,Na}{}}$$

$$-S_8 \, \Big| \, H_2O$$

$$\blacktriangledown$$

$$\overset{\displaystyle NC}{\underset{\displaystyle NC}{}} \!\!\! \diagdown \!\!\! \overset{\displaystyle S\,Na}{\underset{\displaystyle S\,Na}{}} \!\!\! \diagup$$
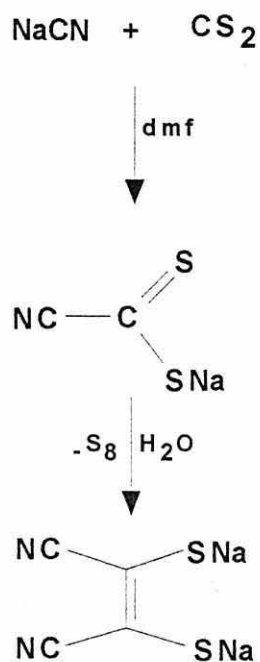
Scheme 3.3 : Preparation of Na$_2$(mnt)

3.2.2 Preparation of the Tungsten-1,2-Dithiolene Complexes

In general, the alkali metal salts of the dithiolene ligands in dry ethanol were added dropwise to a stirred solution of the metal complex in dry acetonitrile. The solution was stirred for 4 - 6 hours under a constant stream of dinitrogen and the product was isolated by resolvating it in dichloromethane and filtering the solution to remove the sodium or caesium halide. The products of the reaction between $[WI_2(CO)_3(L)]$ and the dithiolenes were all dark brown powders. See Scheme 3.4.

3.2.2.1 Reaction of $[WI_2(CO)_3(NCMe)_2]$ with Na$_2$(dmit)

The acetonitrile ligands on the transition metal complex $[WI_2(CO)_3(NCMe)_2]$ are readily substituted and it was thought that the lability of this group may influence the substitution of the iodide ligands by the dithiolene. Trial reactions between $[WI_2(CO)_3(NCMe)_2]$ and Na$_2$(dmit) did not yield the expected complex $[W(dmit)(CO)_2(NCMe)_2]$. An ethanolic

solution of the sodium salt of dmit was added to a solution of the complex [WI$_2$(CO)$_3$(NCMe)$_2$] and stirred for six hours. The solution was filtered and the solvent removed. The resulting brown oil was resolvated in CH$_2$Cl$_2$, filtered and the solvent removed, this was repeated several times to ensure removal of sodium iodide before the oil was finally recrystallised in CH$_2$Cl$_2$ and hexane. The dark brown powder isolated does not analyse to be [W(dmit)(CO)$_2$(NCMe)$_2$], see Table 3.1. There is the possibility of side-reactions and the formation of by-products because of the lability of the acetonitrile ligands. By substituting the acetonitrile ligand by a phosphine ligand, which will be more bulky and less labile, the stability of any products should be greater and there should be less chance of any side reactions taking place. It would also be advantageous to look at how the properties of the product change by varying the phosphine ligand.
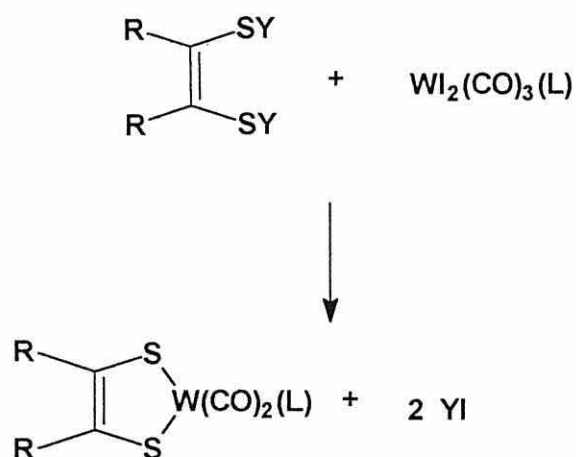
R = Functional Group
Y = Protecting Group
L = (dppe)
    (PPh$_3$)$_2$
    (PEt$_3$)$_2$

Scheme 3.4 : Preparation of the Tungsten-1,2-Dithiolene Complexes

68

3.2.3 Reaction of [WI$_2$(CO)$_3$(NCMe)$_2$] with Phosphine Ligands

Due to the lack of success of the reactions of [WI$_2$(CO)$_3$(NCMe)$_2$] with 1,2-dithiolenes the acetonitrile groups were replaced with more bulky, less labile phosphine ligands. The ligands used were triphenylphosphine (PPh$_3$), triethylphosphine (PEt$_3$) and bis(diphenlyphosphinoethane) (dppe). It was found that these groups did, considerably, improve the stability of the complexes. The synthesis of [WI$_2$(CO)$_3$(L)] was carried out by reaction of [WI$_2$(CO)$_3$(NCMe)$_2$] with two equivalents of L {L = PPh$_3$ or PEt$_3$} or one equivalent of dppe in dichloromethane at room temperature, see Scheme 3.5.

$$[\text{WI}_2(\text{CO})_3(\text{NCMe})_2] \xrightarrow{\text{L}} [\text{WI}_2(\text{CO})_3(\text{L})]$$

L = 2 PPh$_3$, 2 PEt$_3$ or dppe
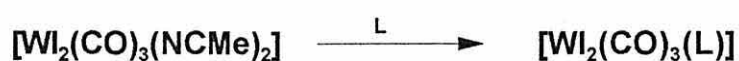
Scheme 3.5 : Preparation of the Tungsten Complex

3.2.4 Reaction of [WI$_2$(CO)$_3$(L)] with the 1,2-Dithiolenes

Reaction of [WI$_2$(CO)$_3$(L)] with one equivalent of [Y$_2$X] {Y$_2$X = Na$_2$(dmit), Na$_2$(mnt) or H$_2$(bdt)} in a mixture of acetonitrile and ethanol, gave the complexes [W(X)(CO)$_2$(L)] {X = dmit, mnt or bdt; L = (PPh$_3$)$_2$, (PEt$_3$)$_2$ or dppe} in high yield.

The elemental analysis data for the complexes prepared is given in Table 3.2, along with selected FAB mass spectroscopic data. The analytical data in the majority of cases was in close agreement with the calculated values.

The complexes [W(X)(CO)$_2$(L)] {X = dmit, mnt or bdt; L = (PPh$_3$)$_2$, (PEt$_3$)$_2$ or dppe} are all brown powders. They are soluble in chlorinated solvents such as dichloromethane, and acetonitrile. They are insoluble in hexane, but show some solubility in diethyl ether. They are relatively stable in air, however after prolonged exposure to the atmosphere they show signs of decomposition.

69

3.2.5 Reaction of Other Tungsten Compounds with the 1,2-Dithiolenes

As well as investigating complexes of the type [W(X)(CO)$_2$(L)] where L is a phosphine ligand, preliminary studies have also been made on other types of tungsten complexes and on the molybdenum analogue of the triphenylphosphine tungsten complex, [MoI$_2$(CO)$_3$(PPh$_3$)$_2$].

The complex [WI$_2$(CO)$_3$(dppm)] {dppm = bis(diphenylphosphino)methane} was reacted with Na$_2$(dmit) under the same conditions as the dppe derivative. A dark brown product was obtained. The analysis did not correspond with that of the expected complex [W(dmit)(CO)$_2$(dppm)], see Table 3.1.

Tungsten(II) complexes containing bulky, less labile phosphine ligands rather than smaller ligands like acetonitrile ligands were used because the more bulky phosphine groups would be expected to enhance the stability of the molecule, thereby making the reactions with the alkali salts of the 1,2-dithiolenes more feasible. On this premise, the next progression was to investigate these reactions using the arsine derivatives of the complex [WI$_2$(CO)$_3$(NCMe)$_2$]. The complex [WI$_2$(CO)$_3$(AsPh$_3$)$_2$] was reacted with one equivalent of Na$_2$(dmit) in CH$_2$Cl$_2$ at room temperature to yield a brown / black powder which was recrystallised from CH$_2$Cl$_2$. However, the elemental analysis data did not compare well with the expected product of [W(dmit)(CO)$_2$(AsPh$_3$)$_2$], see Table 3.1. This was repeated several times, however the C, H and S content were always lower than expected. It was not possible to assign a stoichiometry which fits with the analytical data.

Complexes of tungsten(II) that contain acetylene groups are well documented in the literature. The complex [WI$_2$(CO)(NCMe)(η^2-PhC$_2$Ph)$_2$] was prepared and reacted with one equivalent of Na$_2$(dmit) in dichloromethane at room temperature. The elemental analysis from the initial product, [W(dmit)(CO)(NCMe)(η^2-PhC$_2$Ph)$_2$], was reasonable, see Table 3.1, however, upon recrystallisation of the product from CH$_2$Cl$_2$, an intractable oil was yielded. It is possible that if a phosphine group were to replace the acetonitrile group the stability of the product may be increased. However, due to constraints of time,

the reactions were not investigated.

It had been established that in order to produce tungsten-1,2-dithiolenes, it was necessary to replace the acetonitrile ligands of the initial starting material, $[WI_2(CO)_3(NCMe)_2]$ by phosphine groups. The next logical step was the attempted preparation of the analogous molybdenum product, $[Mo(X)(CO)_2(L)]$. The complex $[MoI_2(CO)_3(PPh_3)_2]$ was stirred with an equimolar amount of $Na_2(dmit)$ and the resulting brown oil recrystallised from CH_2Cl_2 and hexane. The analysis of the resulting brown powder did not correspond to the expected product $[Mo(dmit)(CO)_2(PPh_3)_2]$, see Table 3.1. Molybdenum complexes are usually less stable than the corresponding tungsten complexes and it could be that this is the case for this complex.

3.2.6 Reaction of $[WI_2(CO)_3(L)]$ with Other 1,2-Dithiolenes

This study on the tungsten(II) complexes of 1,2-dithiolenes has concentrated on the three ligands, dmit, mnt and bdt. These are all bidentate ligands and they illustrate different types of dithiolenes. As well as investigating these ligands in depth, initial studies were carried out on the ligands $(TTFS_4)^{4-}$, see Figure 3.8, and tdas, see Figure 3.9.
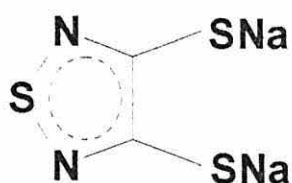
Figure 3.9 : $Na_2(tdas)$

The preparation of $Cs_4(TTFS_4)$ has been described in Scheme 3.2. The disodium salt of tdas is prepared from sodium sulphide and 3,4-dichloro-1,2,5-thiadiazole, see Section 5.4.16.

71

The tungsten complexes of tdas proved to be difficult to prepare as the preparation and use of tdas is in an aqueous environment and tungsten(II) complexes are not stable in water.

Initially the preparation of the bimetallic complex [{W(CO)$_2$(PPh$_3$)$_2$}$_2$(TTFS$_4$)] proved to be more difficult than expected. However, refinements of experimental techniques eventually yielded the product as a dark brown powder. Further studies on this compound were limited as the complex prepared often did not analyse as the expected product [{W(CO)$_2$(PPh$_3$)$_2$}$_2$(TTFS$_4$)], although occasionally the analysis was extremely good, see Table 3.2.

Table 3.1 : Physical and Analytical Data for Other Tungsten-1,2-Dithiolenes

COMPLEX	COLOUR	C	H	S	N
[W(dmit)(CO)$_2$(NCMe)$_2$]	brown	37.8 (20.9)	2.3 (1.2)	17.8 (30.9)	
[Mo(dmit)(CO)$_2$(PPh$_3$)$_2$]	dark brown	4.0 (56.4)	0.3 (3.4)	0.7 (0.2)	0.1 (0.0)
[W(dmit)(CO)$_2$(dppm)]	dark brown	21.7 (42.9)	1.5 (2.7)	4.2 (19.5)	
[W(dmit)(CO)$_2$(AsPh$_3$)$_2$]	brown/ black	7.4 (20.9)	2.3 (1.2)	12.6 (30.9)	
[W(dmit)(CO)(NCMe)(η^2-PhC$_2$Ph)]	brown	59.2 (50.7)	3.2 (2.9)	10.9 (19.9)	0.0 (1.7)
[W(tdas)(CO)$_2$(PPh$_3$)$_2$]	pale brown	68.0 (52.6)	0.0 (3.3)	5.7 (10.5)	5.2 (3.1)

Calculated values in parentheses

Table 3.2 : Physical and Analytical Data for the Tungsten-1,2-Dithiolenes

COMPLEX	COLOUR	%	C	H	S	N
[W(dmit)(CO)$_2$(PPh$_3$)$_2$]	dark brown	60-80	50.0 (51.3)	3.4 (3.8)	15.8 (16.6)	
[W(dmit)(CO)$_2$(PEt$_3$)$_2$]*	brown/ black	60-80	30.4 (30.4)	4.6 (4.5)	23.7 (23.8)	
[W(dmit)(CO)$_2$(dppe)]*	dark brown	40-50	43.6 (44.6)	3.3 (2.9)	19.0 (23.0)	
[W(bdt)(CO)$_2$(PPh$_3$)$_2$]	dark brown	30-50	54.0 (58.4)	1.3 (3.7)	11.5 (7.1)	
[W(bdt)(CO)$_2$(PEt$_3$)$_2$]	brown	30-50	38.8 (39.0)	5.6 (5.5)	10.4 (10.4)	
[W(bdt)(CO)$_2$(dppe)]	dark brown	30-50	53.3 (52.4)	3.9 (3.6)	4.8 (8.2)	
[W(mnt)(CO)$_2$(PPh$_3$)$_2$]	brown	60-70	55.5 (55.8)	3.7 (3.3)	3.9 (7.0)	2.2 (3.1)
[W(mnt)(CO)$_2$(PEt$_3$)$_2$]	brown/ black	60-70	34.9 (35.1)	5.0 (4.9)	8.9 (10.4)	4.3 (4.5)
[W(mnt)(CO)$_2$(dppe)]	brown	60-70	49.2 (49.4)	3.0 (3.1)	9.1 (8.2)	3.4 (3.6)
[(TTFS$_4$){W(CO)$_2$(PPh$_3$)$_2$}$_2$]	brown/ black	<20	53.0 (53.0)	4.5 (3.2)	12.2 (13.8)	

* FAB mass spectroscopic data obtained (see 3.8.2)
  Calculated values in parentheses

3.3   MOLECULAR STRUCTURES

3.3.1. [WI$_2$(CO)$_3$(PEt$_3$)$_2$]

The complex [WI$_2$(CO)$_3$(PEt$_3$)$_2$] was synthesised by reacting [WI$_2$(CO)$_3$(NCMe)$_2$] with two equivalents of triethyl phosphine in a mixture of dichloromethane and diethyl ether at room temperature, see Section 5.4.2. Single crystals were grown in dichloromethane

and hexane at 0 °C.

The crystal structure of the complex [WI$_2$(CO)$_3$(PEt$_3$)$_2$] is depicted in Figure 3.10. The complex is seven co-ordinate, possessing a distorted capped octahedral structure with the phosphine ligands *trans* to each other. If this structure is compared with the crystal structure of [WI$_2$(CO)$_3$(NCMe)$_2$], see Figure 1.6, it is clear that the relative positions of the iodine atoms within the two structures are very different. The iodine atoms in the acetonitrile complex are *trans* to one another whereas in the phosphine complex they occupy the *cis* positions. In both structures two of the carbonyls are *cis* to one another, with the third carbonyl in a capping position.

In the complex [WI$_2$(CO)$_3$(PEt$_3$)$_2$] the phosphine groups are bent towards the iodine atoms. The P2 phosphorus in the PEt$_3$ group is on the same face as the capping carbonyl. The P1-W1-I1 and the P1-W1-I2 angles are 86° and 92° whereas the P2-W1-I1 and P2-W1-I2 are 83° and 78° respectively. Thus the corresponding angles involving P2 are significantly smaller than those involving P1 due to the presence of the capping carbonyl on the same side as P2.

3.3.2 [W(dmit)(CO)$_2$(PEt$_3$)$_2$]

The complex [W(dmit)(CO)$_2$(PEt$_3$)$_2$] was synthesised by the reaction of [WI$_2$(CO)$_2$(PEt$_3$)$_2$] with Na$_2$(dmit) in a mixture of acetonitrile and ethanol at room temperature. Single crystals grown from dichloromethane and diethyl ether at 0 °C, see Section 5.4.8.

The crystal structure for [W(dmit)(CO)$_2$(PEt$_3$)$_2$] is shown in Figure 3.11. Compared with [WI$_2$(CO)$_3$(PEt$_3$)$_2$], the dithiolene ligand has replaced the *cis* iodine ligands and the capping carbonyl has been lost. Most significantly the phosphine groups now bend towards the remaining two carbonyl groups as opposed to towards the iodine atoms as in the seven co-ordinate complex [WI$_2$(CO)$_3$(PEt$_3$)$_2$]. The geometry around the tungsten is a distorted octahedral structure.

74

The angle between the phosphine groups has decreased by ca. 23° from 165° to 142° in the [W(dmit)(CO)$_2$(PEt$_3$)$_2$]. The angle between the two carbonyl groups has decreased slightly from the seven co-ordinate starting material to the six co-ordinate product by 3° from 110° to 107°. The most notable feature is that the phosphine-carbonyl angles have changed dramatically. The angle between the phosphine, P2, that was on the same face as the capping carbonyl and the two remaining *cis* carbonyls decreases from 110° and 113° when the third carbonyl was present, to 78° and 79° in the product when the third carbonyl is no longer present. However, the angles between the other phosphine, P1, and the carbonyls have only changed slightly. See Table 3.4.

3.3.3 [W(bdt)(CO)$_2$(PEt$_3$)$_2$] - Comparison with [W(dmit)(CO)$_2$(PEt$_3$)$_2$]

The structure of this complex as seen in Figure 3.12, is a distorted octahedron and is very similar to [W(dmit)(CO)$_2$(PEt$_3$)$_2$]. The phosphine groups are *trans* to one another, inclining towards the carbonyl groups as in the structure of [W(dmit)(CO)$_2$(PEt$_3$)$_2$].

It is clear from the data presented in Tables 3.3 and 3.4, that the complexes [W(dmit)(CO)$_2$(PEt$_3$)$_2$] and [W(bdt)(CO)$_2$(PEt$_3$)$_2$] are very similar, with the bond angles differing by less than 2°. There is a significant reduction in the metal-ligand atom bond lengths in [W(bdt)(CO)$_2$(PEt$_3$)$_2$] compared with [W(dmit)(CO)$_2$(PEt$_3$)$_2$]. In particular the tungsten-sulphur distances which are slightly shorter in the bdt complex than in the corresponding dmit complex.

The structures of [W(dmit)(CO)$_2$(PEt$_3$)$_2$] and [W(bdt)(CO)$_2$(PEt$_3$)$_2$] are very similar, but there is a significant difference in the metal-ligand bond distances possibly arising from steric effects or from differences in the strength of the metal-ligand bond. The metal-ligand bond may have both a σ- and a π-components and it is sometimes possible to get an insight into the relative importance of these two effects by considering additional data. The σ-bonding ability of a ligand can be assessed by considering the bonding of the ligand to H$^+$ when there can be no π-component. The ease with which the H$^+$ can be removed, and hence the ease of breaking the hydrogen-ligand bond, is given by the pK$_a$ value of the

protonated ligand. When the ligand is bound to a metal, the strength of the metal-ligand bond will be dependent in part on the pK_a value of the ligand. If a protonated ligand has a low pK_a value (i.e. it is acidic and loses protons easily) then the metal-ligand bond will be weaker, and therefore longer, than if the pK_a value is high. When the metal is tungsten, π-bonding also has to be considered. This will also influence the strength of the metal-ligand bond and, consequently, the length. In a series of compounds, the length of the metal-ligand bonds may follow the same trend as the pK_a values of the ligands. If this is the case then either the π-component of the bond has no influence on the bond strength, or the π-component does affect the strength of the bond but to the same degree in all of the series. Conversely, if the bond lengths of the series of compounds do not follow the trend of the pK_a values of the series, then the π-component is obviously exerting a significant influence.

The pK_a value of benzene thiol is 6.6 and the first pK_a value of benzene dithiol is 6.8, see Figure 3.14.

BENZENE THIOL

$pK_a = 6.6$

BENZENE-1,2-DITHIOL

$pK_{a,1} = 6.8$

$pK_{a,2} = 12.4$
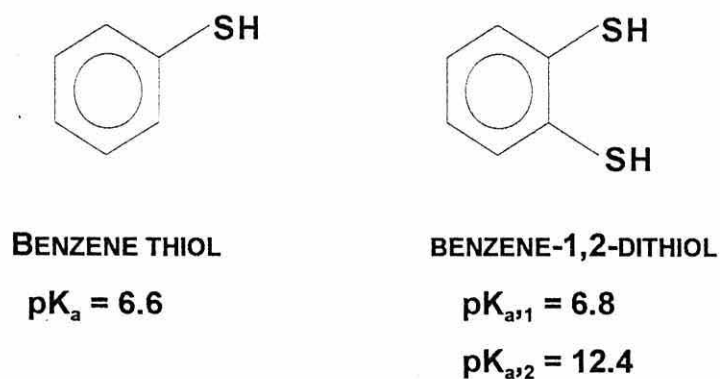
Figure 3.14 : pK_a Values of Benzene Thiol and Benzene-1,2-Dithiol

The more electron-withdrawing nature a functionalised thiol possesses, then the lower the pK_a value will be. Employing this principle, it is reasonable to assume that by replacing the phenyl constituent by a sulphur-rich moiety which is electron-withdrawing, the acidity of the molecule would be increased. This suggests that the bdt ligand will probably be less acidic than a dmit ligand.

The conclusions reached about the pK_a of the bdt and dmit ligands suggests that if the tungsten-sulphur bond is mostly σ in nature, or the π-component influences the nature of the bond to the same degree for both ligands, then the tungsten-sulphur bond in the bdt complex should be stronger and therefore shorter than in the dmit complex. This is found to be the case with the tungsten-sulphur bond length in the complex $[W(bdt)(CO)_2(PEt_3)_2]$ being ca. 2.30 Å and in the complex $[W(dmit)(CO)_2(PEt_3)_2]$ being ca. 2.39 Å.

The angle between the phosphine groups L1-W1-L2 has decreased by ca. 25° from 165° to 140° from the seven co-ordinate complex to the six co-ordinate complex $[W(bdt)(CO)_2(PEt_3)_2]$. This is 3° more than in the complex $[W(dmit)(CO)_2(PEt_3)_2]$. The angles L1-W1-C1 and L1-W1-C2, increase by ca. 4° when the complex goes from seven co-ordinate to the six co-ordinate $[W(bdt)(CO)_2(PEt_3)_2]$. This compliments the decrease in the angles L2-W1-C1 and L2-W1-C2 by ca. 34° under the same circumstances. This can be presumed to occur because the capping carbonyl is removed, therefore the phosphines that were being forced away from the carbonyls, and the *cis* carbonyls that were constrained by the capping carbonyl, shift in position to make the structure less strained.
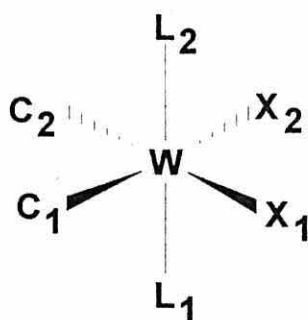
L = Phosphorus of the phosphine ligand
X = Iodine or Sulphur of the 1,2-dithiolene ligand
C = Carbon of the carbonyl group

Figure 3.15 : Pictorial Representation of the Complexes,
$[WI_2(CO)_3(PEt_3)_2]$ and $[W(X)(CO)_2(PEt_3)_2]$

Table 3.3 : Bond Length Data for the Complexes

$[WI_2(CO)_3(PEt_3)_2]$ and $[W(X)(CO)_2(PEt_3)_2]$

BONDS	$[WI_2(CO)_3(PEt_3)_2]$	X = (dmit)	X = (bdt)
W1-C1	1.985(13) Å	1.95(2) Å	1.88(3) Å
W1-C2	1.999(13) Å	1.98(2) Å	1.91(4) Å
W1-L1	2.581(3) Å	2.464(5) Å	2.387(8) Å
W1-L2	2.568(3) Å	2.462(5) Å	2.393(8) Å
W1-X1	2.847(61) Å	2.400(4) Å	2.306(9) Å
W1-X2	2.864(31) Å	2.384(3) Å	2.296(7) Å

Table 3.4 : Bond Angle Data for the Complexes

$[WI_2(CO)_3(PEt_3)_2]$ and $[W(X)(CO)_2(PEt_3)_2]$

ANGLES	$[WI_2(CO)_3(PEt_3)_2]$	X = (dmit)	X = (bdt)
L1-W1-L2	164.85(10) °	142.42(12) °	140.8(3) °
C1-W1-C2	110.3(5) °	107.8(8) °	108.0(2) °
X1-W1-X2	90.34(4) °	83.78(12) °	82.8(3) °
C1-W1-L1	75.3(3) °	78.5(8) °	79.7(12) °
C2-W1-L1	77.1(4) °	79.9(6) °	79.5(9) °
C1-W1-L2	112.6(4) °	78.5(8) °	77.4(9) °
C2-W1-L2	110.4(4) °	78.9(7) °	78.2(13) °
C1-W1-X1	78.0(4) °	90 °	89.6(8) °
C2-W1-X1	158.0(4) °	155 °	153.1(13) °
C1-W1-X2	162.8(3) °	156 °	150.7(9) °
C2-W1-X2	76.5(4) °	87 °	89.9(12) °

3.3.4 The Structure of the Complex, [W(bdt)(CO)₂(dppe)]

The structure shown in Figure 3.13 and represented pictorially in Figure 3.16 of [W(bdt)(CO)₂(dppe)], is clearly different from those observed for the other tungsten-1,2-dithiolenes. The phosphine ligand is a bidentate ligand and therefore the phosphorus atoms have to occupy *cis* positions unlike the other complexes.

The structure can no longer be considered as a distorted octahedron. The ligands appear to be arranged on three sides of the molecule. The angles L1-W1-L2 and C1-W1-C2 are equal to 76° and 77° respectively, and the angle X1-W1-X2 is 83°. The latter angle is the bite angle of the dithiolene and is as expected with regard to the previous structures. The angle between the carbonyl ligands and the bite angle of the phosphorus ligand are very alike and are ca. 6° more acute than the angle of the dithiolene. Therefore, it is expected that the arrangement of the ligands will be a triangular arrangement when observing the molecule from above, as in Figure 3.17.
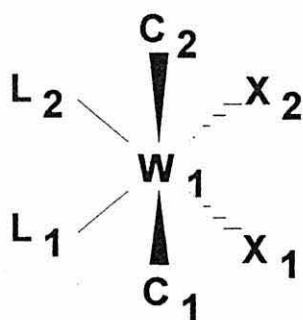
L = Phosphorus of the phosphine ligand
X = I or Sulphur of the 1,2-dithiolene ligand
C = Carbon of the carbonyl group

Figure 3.16 : Pictorial Representation of [W(bdt)(CO)₂(dppe)]

The angle between the phosphine groups is larger by 64° when the ligand, L, is the monodentate phosphine ligand, PEt₃. This is because the bidentate ligand obviously can not have an obtuse chelating angle with the tungsten. The tungsten-carbon angle is also

smaller in the complex [W(bdt)(CO)$_2$(dppe)] than in the complex [W(bdt)(CO)$_2$(PEt$_3$)$_2$] by 31°.
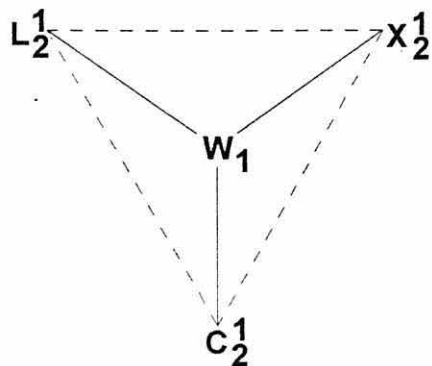
L = Phosphorus of the phosphine ligand, dppe
X = Sulphur of the 1,2-dithiolene ligand, bdt
C = Carbon of the carbonyl group

Figure 3.17 : Pictorial Representation of the View Looking down on the Molecule.

The bond lengths in the complex [W(bdt)(CO)$_2$(dppe)] are comparable to those in the other tungsten-1,2-dithiolene complexes and in [WI$_2$(CO)$_3$(PEt$_3$)$_2$]. The tungsten-carbon bonds are ca. 2.50 Å in the bidentate phosphine complex [W(bdt)(CO)$_2$(dppe)] and are slightly longer than the corresponding bonds in [W(bdt)(CO)$_2$(PEt$_3$)$_2$] ca. 2.40 Å. The bond lengths between the phosphorus and the tungsten in the complex [W(bdt)(CO)$_2$(dppe)] are longer by ca. 0.5 Å, at ca. 1.97 Å, as opposed to 1.90 Å in [W(bdt)(CO)$_2$(PEt$_3$)$_2$].

Table 3.5 : Bond Angle Data in the Complexes [W(bdt)(CO)$_2$(L)]

ANGLES	L = (PEt$_3$)$_2$	L = dppe
L1-W1-L2	140.8(3) °	76.26(14) °
C1-W1-C2	108.0(2) °	76.6(7) °
X1-W1-X2	82.8(3) °	82.84(14) °
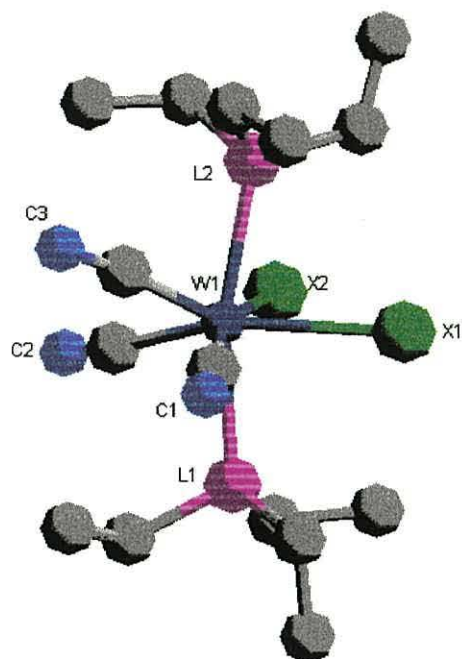
Figure 3.10 : The Crystal Structure of [WI$_2$(CO)$_3$(PEt$_3$)$_2$]
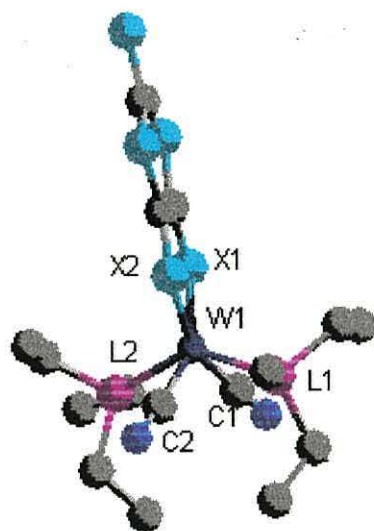
Figure 3.11 : **The Crystal Structure of [W(dmit)(CO)₂(PEt₃)₂]**
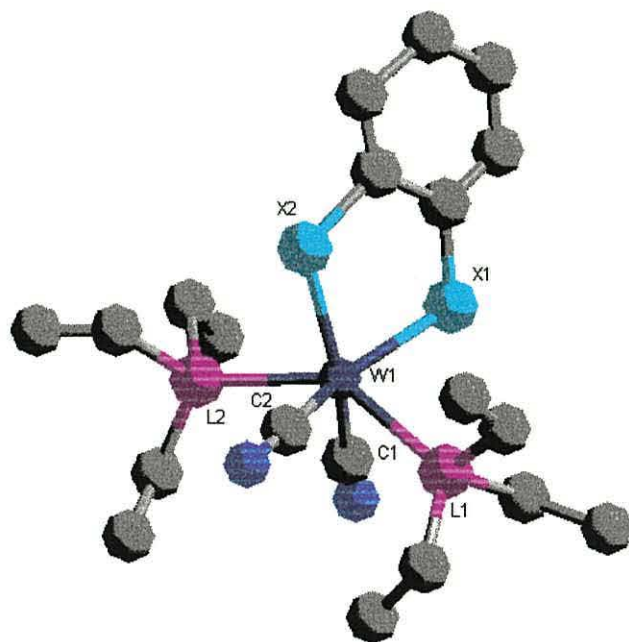
Figure 3.12 : The Crystal Structure of [W(bdt)(CO)₂(PEt₃)₂]
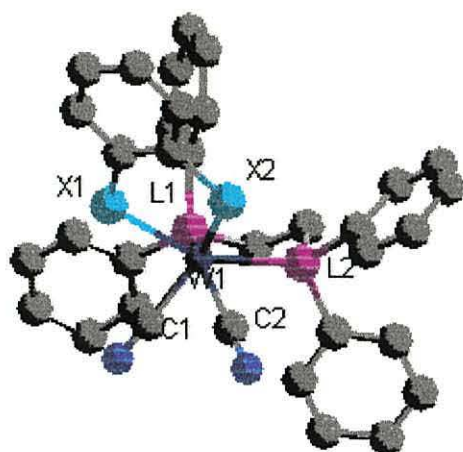
Figure 3.13 : The Crystal Structure of [W(bdt)(CO)₂(dppe)]

Table 3.6 : Bond Length Data in the Complexes [W(X)(CO)₂(L)]

BONDS	L = (PEt₃)₂ X = bdt	L = dppe X = bdt
W1-L1	2.387(8) Å	2.472(4) Å
W1-L2	2.393(8) Å	2.505(4) Å
W1-C1	1.88(3) Å	1.99(2) Å
W1-C2	1.91(4) Å	1.95(2) Å
W1-X1	2.306(9) Å	2.368(4) Å
W1-X2	2.296(7) Å	2.394(4) Å

3.4   INFRARED SPECTRAL STUDIES

The infrared spectra of the complexes were measured in dichloromethane solution as thin films between sodium chloride plates. The frequencies of the main absorption bands are shown in Table 3.8. The frequencies believed to originate solely from the dithiolate ligand are shown in bold face.

3.4.1   Infrared Studies of [WI₂(CO)₃(L)] {L = (PPh₃)₂, (PEt₃)₂ or (dppe)}

The seven co-ordinate complexes [WI₂(CO)₃(L)] {L = (PPh₃)₂, (PEt₃)₂ or (dppe)}, display certain characteristic absorption bands in their infrared spectra. The most distinctive of these are those attributed to the carbonyl groups, for example at 2040 cm⁻¹, 1950 cm⁻¹ and 1943 cm⁻¹ for the complex [WI₂(CO)₃(PPh₃)₂]. These may be tentatively assigned to the capping carbonyl and the two *cis* carbonyls respectively.

The absorption bands associated with the phosphine groups occur in the region 3200 - 3000 cm⁻¹, corresponding to the aromatic carbon-hydrogen bonds and 3000 - 2800 cm⁻¹ corresponding to the aliphatic carbon-hydrogen bonds.

85

3.4.2 Infrared Studies of the 1,2-Dithiolenes

Previous studies [116] on the infrared spectra of the dithiolenes have shown that they all possess three characteristic absorption bands : one $\upsilon_{(C=C)}$ at ca. 1400 cm^{-1}; and two $\upsilon_{(C-S)}$ bands at ca. 1110 cm^{-1} and ca. 860 cm^{-1}. These frequencies are dependent upon the substituents on the dithiolene ligand. The dithiolene ligands that have been studied have, in addition, some very characteristic absorption bands. The dmit ligand has an absorption band at ca. 1065 cm^{-1} corresponding to the terminal C=S bond. The mnt ligand shows an absorption band due to the C≡N group at ca. 2200 cm^{-1}. The bdt ligand exhibits absorption bands arising from the aromatic C-H bond at ca. 3000 cm^{-1}, however these bands are often indistinguishable from bands arising from the C=C-H bonds in the other substituents in a complex.

3.4.3 Infrared Studies of the Complexes [W(X)(CO)$_2$(L)]
{X = (dmit), (mnt) or (bdt); L = (PPh$_3$)$_2$, (PEt$_3$)$_2$ or (dppe)}

From the stretching frequencies reported in Table 3.8, it is apparent that there are two absorption bands in the regions 1937 - 1961 cm^{-1} and 1863 - 1889 cm^{-1}. These correspond to the two *cis* carbonyl groups attached to the tungsten centre. The capping carbonyl observed in the infrared spectrum of the tungsten complexes, [WI$_2$(CO)$_3$(L)] {L = (PPh$_3$)$_2$, (PEt$_3$)$_2$ or dppe}, at ca. 2000 cm^{-1} are no longer present. This is supported by the crystal structures (see Figure 3.11 - 3.13) which show only the two *cis* carbonyls to be present in the product, [W(X)(CO)$_2$(L)] {X = (dmit), (mnt) or (bdt); L = (PPh$_3$)$_2$, (PEt$_3$)$_2$ or (dppe)}, the capping carbonyl having been lost. The characteristic absorption bands for the dithiolene ligands, that is the bands arising from the C=C and the C-S bonds are present in the infrared spectra. Comparison of the absorption bands of the metal bound dithiolene and the free dithiolene in Table 3.7 shows there to be only a slight change in frequency. The stretching frequency of the C-S bond in the ligated dithiolene is slightly lower than in the free ligand, as would be expected when bound in a bidentate manner to a metal complex. It has been observed that the absorption bands in the infrared spectra of the neutral 1,2-dithiolenes are weaker than those of the charged species [112].

Table 3.7 : Comparison of the Absorption bands in the

Infrared Spectra for the Metal-bound Dithiolene

and Free Dithiolene

	$\upsilon_{(C=C)}$ (cm^{-1})		$\upsilon_{(C-S)}$ (cm^{-1})				$\upsilon_{(C=N)}$ (cm^{-1})	
dmit	**1422**	1435[a] 1426[b] 1424[c]			**1066**[x]	1062[a] 1059[b] 1057[c]		
bdt		[y]	**1112**	1115[a] 1119[b] 1128[c]	**1039**	1031[a] 1028[b] 1027[c]		
mnt	**1445**	1436[a] 1423[b] 1436[c]	**1117**	1120[a] 1113[b] 1154[c]	**1058**	1091[a] 1035[b] 1024[c]	**2195**	2209[a] 2210[b] 2202[c]

[a] $L = (PPh_3)_2$

[b] $L = (PEt_3)_2$

[c] $L = (dppe)$

[x] $\upsilon_{C=S}$

[y] bdt has a benzene ring and therefore the aromatic υ_{CH} is indistinguishable

from the other benzene carbon bonds

Frequencies in **boldface** denote free dithiolene ligand

All spectra were measured in solution as thin films between NaCl plates

Table 3.8 : Infrared Absorption Frequencies of the Complexes [W(X)(CO)$_2$(L)]

COMPOUND	υ (cm^{-1})^a	BOND
W(dmit)(CO)$_2$(PPh$_3$)$_2$	1943 1863 **1435** **1062**	C≡O C=C C=S
W(dmit)(CO)$_2$(PEt$_3$)$_2$	1950 1879 **1426** **1059**	C≡O C=C C=S
W(dmit)(CO)$_2$(dppe)	1961 1885 **1424** **1057**	C≡O C=C C=S
W(bdt)(CO)$_2$(PPh$_3$)$_2$	1955 1886 **1031 1115**	C≡O C-S
W(bdt)(CO)$_2$(PEt$_3$)$_2$	1941 1884 **1028 1119**	C≡O C-S
W(bdt)(CO)$_2$(dppe)	1946 1873 **1027 1128**	C≡O C-S
W(mnt)(CO)$_2$(PPh$_3$)$_2$	1955 1886 **2209** **1436** **1091 1120**	C≡O C≡N C=C C-S
W(mnt)(CO)$_2$(PEt$_3$)$_2$	1937 1855 **2210** **1423** **1035 1113**	C≡O C≡N C=C C-S
W(mnt)(CO)$_2$(dppe)	1962 1889 **2202** **1436** **1024 1154**	C≡O C≡N C=C C-S

^{a} measured in solution as a thin film between NaCl plates
Figures in **boldface** denote absorptions due to dithiolene ligand

3.5   NUCLEAR MAGNETIC RESONANCE SPECTRA

3.5.1 ^{13}C NMR Spectrum of the Complex [WI$_2$(CO)$_3$(PEt$_3$)$_2$] at -30 °C

At room temperature, the ^{13}C NMR of the complex [WI$_2$(CO)$_3$(PEt$_3$)$_2$] shows one single peak corresponding to the carbonyls groups. As the temperature is lowered, the fluxionality of the carbonyl groups is slowed down, and a carbonyl resonance at 234 ppm is observed, which is typical of a carbonyl in a face-capping position of an octahedron [117]. The signal is split into a doublet of doublets and this is consistent with the crystal structure, see Figure 3.10, one of the phosphines being on the capped face of the octahedron. A more intense resonance at 212 ppm can be attributed to the axial carbonyl groups. This again is split into a doublet of doublets by the phosphine in the capped face and the other phosphine.

3.5.2 ^{1}H NMR Spectrum of the Complex [WI$_2$(CO)$_3$(PEt$_3$)$_2$] at Room Temperature

The structure of [WI$_2$(CO)$_3$(PEt$_3$)$_2$], see Figure 3.10, as determined by X-ray crystallography at room temperature, shows that the PEt$_3$ ligands are not in equivalent positions. Therefore it could be expected that there would be two separate methyl signals and two methylene signals.

The spectrum of the complex, [WI$_2$(CO)$_3$(PEt$_3$)$_2$], in solution shows a signal at 1.3 ppm arising from the proton in the methyl group and at 2.6 ppm corresponding to the protons in the CH$_2$ group. The methyl protons give rise to the signal at 1.3 ppm which is a doublet of triplets due to the splitting of the triplet by the phosphorus (spin = ½) and has identical intensity ratios to those observed in the free ligand.

The signal at 2.6 ppm (quintet; integration 2H) corresponds to the protons of the CH$_2$ group. The quartet observed in the free [PEt$_3$], is now split by the phosphorus nucleus into a quintet as in Figure 3.18. The phosphorus would be expected to split the proton signal into eight lines, but only five peaks are observed because the coupling constant J$_{P-H}$

89

is approximately the same as the coupling constant J_{H-H}.

Thus the spectra observed at room temperature can be interpreted in terms of two identical PEt$_3$ components, implying that the ethyl groups of the triethylphosphine ligands are all equivalent at room temperature on the NMR timescale and that the nuclei are fluxional.

Proton signal split by methyl protons

1 3 3 1

Signal split by phosphorus nucleus

1 13 33 31 1

Quintet observed in ^{1}H NMR

1 4 6 4 1
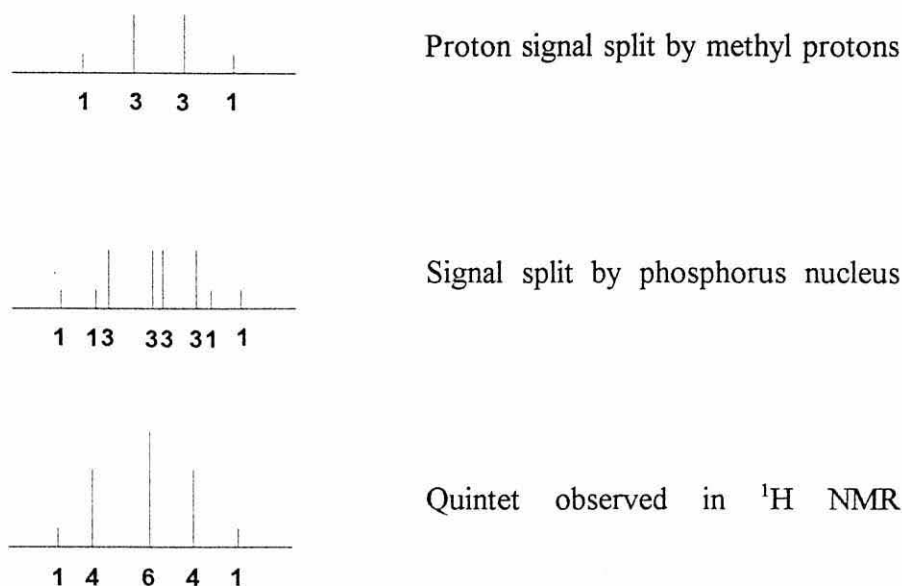
Figure 3.18 : Splitting of the Proton Signal of the CH$_2$

by the Phosphorus Nucleus, Assuming $J_{P-H} = J_{H-H}$

3.5.3 ^{1}H NMR Spectrum of the Complex [WI$_2$(CO)$_3$(PEt$_3$)$_2$] at -40 °C

The complex [WI$_2$(CO)$_3$(PEt$_3$)$_2$] was cooled to -40 °C and the ^{1}H NMR spectrum recorded. The fluxional processes in the seven co-ordinate complex slow down as the temperature is lowered, and the triethyl phosphine groups now should become inequivalent.

The same pattern from the methyl protons is seen at 1.1 ppm (doublet of triplets; integration 3H) as for the methyl protons in the free ligand, except that all the peaks appear to be split by long range ^5J (^{1}H ^{31}P) coupling.

The CH$_2$ proton signal at 2.4 ppm (integration 2H) now consists of a sextet instead of the quintet, see Figure 3.19. This suggests that the PEt$_3$ groups are now no longer in identical environments thus each is giving rise to a slightly different signal resulting in an increased number of bands.

Quintet observed in ^{1}H NMR at room temperature

14641

Splitting of the quintet when the complex is cooled to -40 °C

1 5 10 10 5 1
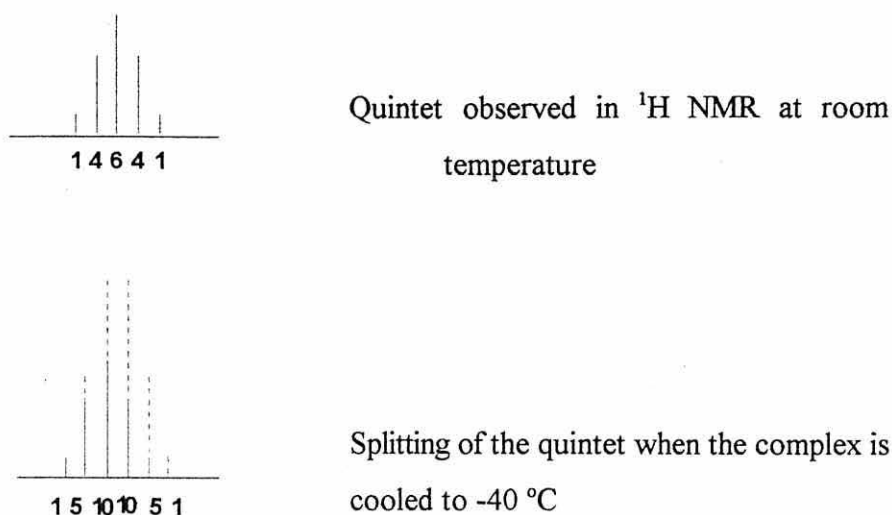
Figure 3.19 : Splitting of the Proton Signal of the CH$_2$ at -40 °C

3.5.4 ^{1}H NMR Spectroscopic Studies of the Complexes [W(X)(CO)$_2$(L)$_2$] {X = dmit, mnt or bdt; L = (PPh$_3$)$_2$, (PEt$_3$)$_2$ or dppe}

The ^{1}H NMR spectra of the complexes [W(X)(CO)$_2$(L)] {L = dmit, mnt or bdt; X = (PPh$_3$)$_2$, (PEt$_3$)$_2$ or (dppe)} are not affected greatly by the three dithiolene ligand groups as there are no protons present on these groups, except in the case of bdt. Therefore, it is more meaningful to categorise and discuss the complexes according to the phosphine ligands.

The complexes [W(X)(CO)$_2$(PPh$_3$)$_2$] {X = dmit, mnt or bdt} only have protons on the phenyl rings, consequently the only signal that would be expected to be observed would be a multiplet at ca. 7.5 ppm. This was found and the signals do not vary greatly with changing dithiolene ligand.

91

The ^{1}H NMR spectra of the complexes [W(X)(CO)$_2$(dppe)] {X = dmit, mnt or bdt} show the phenyl protons and the CH$_2$ protons clearly as signals ca. 7.4 ppm and 2.5 ppm respectively. The chemical shifts of the signals are not affected considerably by the different dithiolene ligands, however in the case of bdt another multiplet is observed at 7.7 ppm.

3.5.5 Comparison of the Chemical Shifts of the Complexes [W(X)(CO)$_2$(L)] {X = dmit, mnt or bdt; L = (PEt$_3$)$_2$, (PPh$_3$)$_2$ or dppe}

By comparing the ^{1}H NMR spectral data of the complexes [W(X)(CO)$_2$(PEt$_3$)$_2$] {X = dmit, mnt or bdt} when X = bdt or mnt, it has been observed that the chemical shifts are very similar to each other. The nature of the dithiolene groups clearly affect the proton signals from the triethylphosphine ligands much more than in the triphenylphosphine and the dppe containing complexes. The effect of the nature of the dithiolene ligands on the proton signals will be dissipated more over the phenyl protons than the ethyl protons because of the delocalised character of the aromatic rings. Hence the effect of the dithiolene ligand is hardly noticeable in the proton NMR of the triphenylphosphine and dppe containing complexes, although it is very apparent in the complexes [W(X)(CO)$_2$(PEt$_3$)$_2$]. Also, the protons on the phenyl containing phosphine groups are further away from the dithiolene ligands (ca. 4 - 6 bonds) than the protons on the PEt$_3$ (ca. 3 - 4 bonds), and so will experience the effect of the sulphur containing ligands to a lesser degree.

Table 3.9 : Comparison of the Chemical Shifts in the ^{1}H NMR Spectra of the Complexes [W(X)(CO)$_2$(PEt$_3$)$_2$]

X	Chemical Shift δ
dmit	1.1 (CH$_3$) 1.8 (CH$_2$)
mnt	1.3 (CH$_3$) 2.5 (CH$_2$)
bdt	1.4 (CH$_3$) 2.4 (CH$_2$)

92

3.5.6 ^{31}P NMR Spectra of the Tungsten-1,2-Dithiolenes

The complexes [W(X)(CO)(L)] {X = dmit or mnt; L = (PPh$_3$)$_2$, (PEt$_3$)$_2$ or dppe} show a singlet resonance with tungsten satellites in the ^{31}P NMR spectrum. The tungsten satellites arise due to one tungsten nuclide (^{183}W) having a natural abundance of about 14% and a I = ½; other nuclides of tungsten do not possess a nuclear spin and therefore will not affect the magnetic field experienced by the phosphorus nuclei. The ^{31}P NMR spectra are proton decoupled so that there is no splitting of the phosphorus signal by the protons in the molecule. In the ^{31}P NMR spectrum of the free PEt$_3$ ligand, a singlet is observed at -19.2 ppm. In the complexes [W(X)(CO)$_2$(L)] {X = dmit or mnt; L = (PPh$_3$)$_2$, (PEt$_3$)$_2$ or dppe}, the ^{31}P signal is shifted downfield as would be expected for bound phosphines, see Table 3.10. This is upheld by the ^{31}P NMR spectrum of [WI$_2$(CO)$_3$(PPh$_3$)$_2$] which shows a singlet at 23.0 ppm.

Table 3.10 : ^{31}P NMR Spectral Data for the Complexes [W(X)(CO)$_2$(L)] Measured in CDCl$_3$

COMPLEX	^{31}P δ(ppm) J$_{W-P}$ (Hz)
[W(dmit)(CO)$_2$(PEt$_3$)$_2$]	23.0 (s, 174)
[W(dmit)(CO)$_2$(dppe)]	32.3 (s, 116)
[W(mnt)(CO)$_2$(PEt$_3$)$_2$]	28.6 (s, 174)
[W(mnt)(CO)$_2$(PPh$_3$)$_2$]	29.0 (s)

Table 3.11 : ^{1}H NMR Spectral Data for the Complexes [W(X)(CO)$_2$(L)] Measured in (CD$_3$)$_2$CO at 25 °C

COMPLEX	^{1}H δ(ppm) J(Hz)
[W(dmit)(CO)$_2$(PEt$_3$)$_2$]	1.1 (dt, 3H, J$_{P-H}$ 15.4, J$_{H-H}$ 7.7, CH$_3$) 1.8 (q, 2H, J$_{P-H}$=J$_{H-H}$ 7.0, CH$_2$)
[W(dmit)(CO)$_2$(PPh$_3$)$_2$]	7.5 (m, 3H, *m-* ,*p*-Ph) 7.8 (m, 2H, *o*-Ph)
[W(dmit)(CO)$_2$(dppe)]	2.5 (bm, 2H, CH$_2$) 2.7 (bm, 2H, CH$_2$) 7.4 (m, 12H, *m-, p*-Ph) 7.8 (m,8H, *o*-Ph)
[W(mnt)(CO)$_2$(PEt$_3$)$_2$]	1.3 (dt, 3H, J$_{P-H}$ 11.6, J$_{H-H}$ 5.8, CH$_3$) 2.5 (q, 2H, J$_{P-H}$=J$_{H-H}$ 7.1, CH$_2$)
[W(mnt)(CO)$_2$(PPh$_3$)$_2$]	7.5 (m, 3H, *m-* ,*p*-Ph) 7.7 (m, 2H, *o*-Ph)
[W(mnt)(CO)$_2$(dppe)]	2.4 (bm, 2H, CH$_2$) 2.5 (bm, 2H, CH$_2$) 7.4 (m, 20H, Ph)
[W(bdt)(CO)$_2$(PEt$_3$)$_2$]	1.4 (dt, 3H, J$_{P-H}$ 11.4, J$_{P-H}$ 5.6, CH$_3$) 2.4 (q, 2H, J$_{P-H}$=J$_{H-H}$ 7.1, CH$_2$) 7.7 (m, 4H, Ph)
[W(bdt)(CO)$_2$(PPh$_3$)$_2$]	7.4 (m, 5H, Ph) 7.7 (m, 4H, Ph bdt)
[W(bdt)(CO)$_2$(dppe)]	2.5 (bm, 4H, CH$_2$) 7.3 (m, 20H, Ph) 7.7 (m, 4H, Ph bdt)

dd = doublet of doublets   q = quintet
dt = doublet of triplets   m = multiplet

3.6   CYCLIC VOLTAMMETRIC STUDIES

All of the complexes studied were measured as a solution in acteonitrile with a supporting electrolyte of [TBAPF$_6$] (0.1 M) against a standard calomel electrode (SCE). The potential was cycled between 0.0 V and 0.9 V unless stated otherwise with a scan rate of 0.1 VS^{-1}.

3.6.1   Cyclic Voltammetric Studies of [WI$_2$(CO)$_3$(PPh$_3$)$_2$]

Cyclic voltammetric studies of the complex [WI$_2$(CO)$_3$(PPh$_3$)$_2$] show there to be an

irreversible oxidation at 0.39 V and a quasi-reversible oxidation at 0.63 V. The oxidation at 0.63 V has a reduction peak at 0.57 V associated with it. For an electrode process to be reversible, the difference between the oxidation potential and the reduction potential, ΔE, should be less than 0.059 V, so that although the second oxidation peak is reversible in that the difference between the oxidation and reduction potentials is 0.06 V it is at the limit before it can be considered irreversible.

3.6.2 Cyclic Voltammetric Studies of [W(dmit)(CO)$_2$(PPh$_3$)$_2$]

The cyclic voltammogram of [W(dmit)(CO)$_2$(PPh$_3$)$_2$] has two oxidation peaks at 0.39 V and 0.78 V. Neither oxidation is reversible although, there is a reduction peak at 0.58 V associated with the peak at 0.78 V. There is a small reduction peak that increases with increasing number of cycles at 0.24 V. The peaks decrease with increasing number of cycles, due to a build up of some side product on the electrode surface. The oxidation peak at 0.39 V can be attributed to traces of unreacted [WI$_2$(CO)$_2$(PPh$_3$)$_2$] contaminating the complex [W(dmit)(CO)$_2$(PPh$_3$)$_2$]. There is some evidence of oxidation and reduction processes occurring in the complex, [W(dmit)(CO)$_2$(PPh$_3$)$_2$], however, it is difficult to determine which are due to impurities, and which are due to the actual complex.

3.6.3 Cyclic Voltammetric Studies of [W(mnt)(CO)$_2$(PPh$_3$)$_2$]

The cyclic voltammogram for the complex [W(mnt)(CO)$_2$(PPh$_3$)$_2$] when the potential is cycled between 0.0 V and 1.5 V shows no evidence of any oxidation or reduction processes.

3.6.4 Cyclic Voltammetric Studies of [{W(CO)$_2$(PPh$_3$)$_2$}$_2$][TTFS$_4$]

The complex [{W(CO)$_2$(PPh$_3$)$_2$}$_2$][TTFS$_4$], see Figure 3.21, has two redox active sites, the TTF based moiety and the tungsten centres. It might be expected that the redox process would be delocalised over the molecule and the cyclic voltammogram observed would be expected to be different to the cyclic voltammograms of [WI$_2$(CO)$_3$(PPh$_3$)$_2$] and

E (V)

0

I (A)

1.0 V

――――― $[\{W(CO)_2)(PPh_3)\}_2(TTFS_4)]$

················· TTF

- - - - - - - $[WI_2(CO)_3(PPh_3)_2]$

1 M TBAPF$_6$ / MeCN
Scan Rate = 0.1 VS^{-1}
vs. SCE
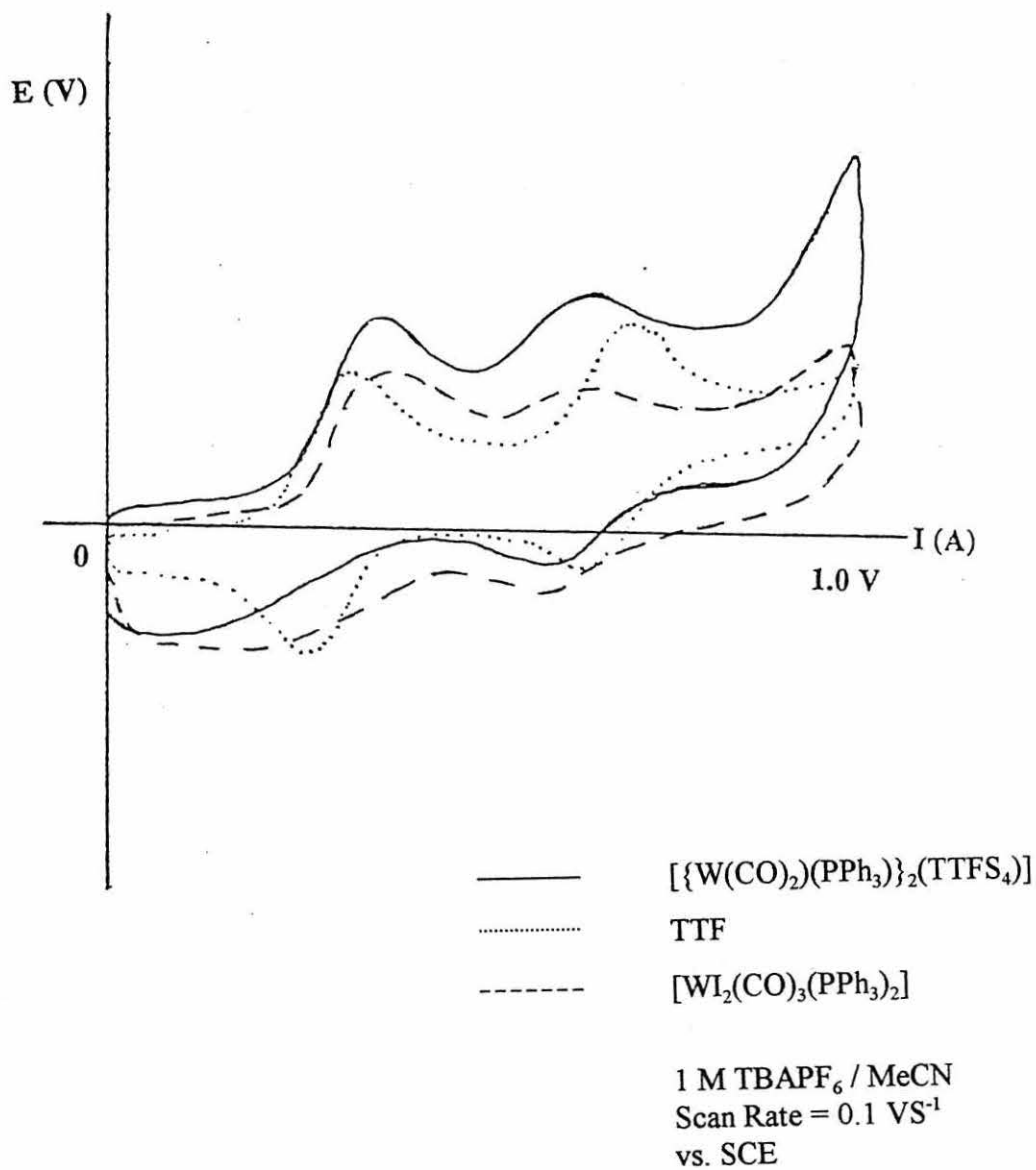
Figure 3.20 : Comparison of the Cyclic Voltammograms of
$[\{W(CO)_2)(PPh_3)\}_2(TTFS_4)]$, TTF and $[WI_2(CO)_3(PPh_3)_2]$

96

TTF. However, this is not the case. The cyclic voltammogram of the complex [{W(CO)$_2$(PPh$_3$)$_2$}$_2$][TTFS$_4$] has an irreversible oxidation at 0.36 V. A reversible oxidation at 0.65 V is seen with an associated reduction peak at 0.58 V. The cyclic voltammogram of the complex, [WI$_2$(CO)$_3$(PPh$_3$)$_2$] shows an irreversible oxidation at 0.39 V. There is a quasi-reversible oxidation at 0.62 V with an associated reduction peak at 0.57 V. TTF shows two reversible oxidation peaks at 0.32 V and 0.69 V. If the cyclic voltammogram of [{W(CO)$_2$(PPh$_3$)$_2$}$_2$][TTFS$_4$] is compared with the cyclic voltammograms of the starting complexes, see Figure 3.20, it can be seen that the redox processes in this complex appear to be associated with the tungsten centre, rather than the TTF centre. Therefore, the two redox centres are acting independently of each other.

3.6.5 Comparison of the Cyclic Voltammograms of the Complexes Containing Triphenyl Phosphine

The monometallic complexes [W(dmit)(CO)$_2$(PPh$_3$)$_2$] and [W(mnt)(CO)$_2$(PPh$_3$)$_2$] show no evidence of any redox processes in their cyclic voltammograms. However, the cyclic voltammogram of the bimetallic complex [{W(CO)$_2$(PPh$_3$)$_2$}$_2$][TTFS$_4$] shows evidence of oxidation processes that can be attributed to the tungsten centre, by comparison with the cyclic voltammograms of both [WI$_2$(CO)$_3$(PPh$_3$)$_2$] and TTF. This suggests that maybe when two redox active tungsten centres are joined by a redox active, delocalised sulphur containing ligand such as [TTFS$_4$]$^{4-}$, the two metal centres communicate through the central moiety and combine to produce a redox effect. When there is only one tungsten centre and a dithiolene ligand, it is possible that they combine to produce the apparent effect of no redox activity although both centres are active.
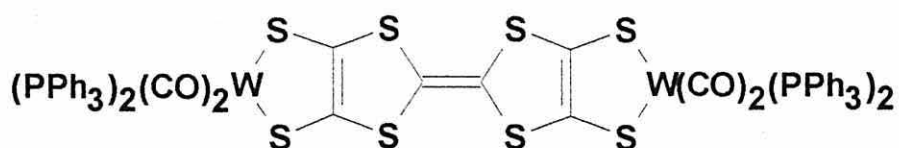
Figure 3.21 : [{W(CO)$_2$(PPh$_3$)$_2$}$_2$][TTFS$_4$]

97

3.7 ABSORPTION STUDIES OF THE COMPLEXES [W(X)(CO)$_2$(L)]

3.7.1 UV / Visible Spectroscopic Studies of the Complexes [W(X)(CO)$_2$(L)]
{ X = dmit or mnt; L = (PPh$_3$)$_2$ or dppe}

The absorption spectra in the ultraviolet / visible region (200 - 700 nm) of the complex in dichloromethane were recorded and the results are tabulated in Table 3.12. The complexes [W(X)(CO)$_2$(L)] {X = dmit or mnt; L = (PPh$_3$)$_2$ or (dppe)} all have a maximum absorption at ca. 230 nm and molar extinction coefficients within the range 0.04 - 0.06. All of the complexes show a small shoulder at 264 nm which can be attributed to another peak underneath the absorption peak at 230 nm.

The complex [W(dmit)(CO)$_2$(dppe)] shows a broad absorption at 368 nm, this is also seen in the corresponding triphenylphosphine complex occurring at 414 nm with a shoulder at 380 nm. The complex [W(mnt)(CO)$_2$(PPh$_3$)$_2$] has an absorption at 410 nm, however this is a very broad shoulder, more like a plateau in appearance than a peak.

The occurence of a band at ca. 375 nm in the complexes [W(dmit)(CO)$_2$(dppe)]and [W(dmit)(CO)$_2$(PPh$_3$)$_2$], but not in the complex [W(mnt)(CO)$_2$(PPh$_3$)$_2$] suggests that the absorption may be due to the dmit ligand. The peak at ca. 400 nm is observed in the two complexes containing the triphenylphosphine but not in the complex [W(dmit)(CO)$_2$(dppe)] implying that the absorption may be due to the triphenylphosphine ligand, and the likely reason that both absorptions are observed in [W(dmit)(CO)$_2$(PPh$_3$)$_2$] is that both ligands occur in the complex.

3.7.2 Near Infrared Absorption Studies of the Complexes [W(dmit)(CO)$_2$(L)]
{L = (PPh$_3$)$_2$ or dppe}

The absorption spectra of the complexes [W(dmit)(CO)$_2$(L)] {L = (PPh$_3$)$_2$ or dppe} were measured in dichloromethane in the near infrared region (800 - 2500 nm) of the spectrum. The spectrum of the complex [W(dmit)(CO)$_2$(PPh$_3$)$_2$] has an absorption band at ca. 2325

nm and a broad band at 900 - 700 nm. An absorption band at ca. 900 nm is usually seen in dmit complexes. The NIR spectrum of [W(dmit)(CO)$_2$(dppe)] shows no such band, only a band at ca. 2310 nm.

Table 3.12 : Data derived from the UV/Visible Absorption Spectra of the Complexes [W(X)(CO)$_2$(L)]

[W(X)(CO)$_2$(L)]	MW	Molarity (molesL^{-1})	λ_{max} (nm)	Absorption A	Molar Extinction Coefficient ϵ
X = dmit L = dppe	834	3.197 x 10^{-5}	229.8	0.95	29, 773.8
X = dmit L = (PPh$_3$)$_2$	960	3.194 x 10^{-5}	230.4	1.24	38, 854.1
X = mnt L = (PPh$_3$)$_2$	904	3.097 x 10^{-5}	229.7	1.54	49, 590.9

Table 3.13 : The Second Peak Observed in the UV/Visible Absorption Spectra of the Complexes [W(X)(CO)$_2$(L)]

[W(X)(CO)$_2$(L)]	λ (nm)	Absorption A	Molar Extinction Coefficient ϵ
X = dmit L = dppe	264 (s) 368 (b)	0.31 0.45	9, 696.6 14, 075.7
X = dmit L = (PPh$_3$)$_2$	264 (s) 380 (s) 414 (b)	0.49 0.19 0.27	15, 326.9 5, 943.1 8, 445.4
X = mnt L = (PPh$_3$)$_2$	264 (s) 271 410 (bs)	1.15 1.17 0.08	37, 132.7 37, 778.5 2, 583.1

(s) = shoulder
(bs) = broad shoulder
(b) = broad

3.8   OTHER CHARACTERISATION OF THE COMPLEXES [W(X)(CO)$_2$(L)]

3.8.1   Magnetic Susceptibility

Tungsten(II) complexes are almost always diamagnetic. Magnetic susceptibility measurements have shown that the complexes [W(X)(CO)$_2$(L)] are diamagnetic. This is borne out by the observation of a proton NMR spectrum, if the complexes were paramagnetic, then there would be no obvious NMR response.

3.8.2   FAB Mass Spectrometry

This has been carried out for the complexes [WI$_2$(CO)$_3$(PEt$_3$)$_2$], [W(dmit)(CO)$_2$(PEt$_3$)$_2$] and [W(dmit)(CO)$_2$(dppe)] and the data is presented in Table 3.14. The mass spectra of the complexes [W(dmit)(CO)$_2$(PEt$_3$)$_2$] and [W(dmit)(CO)$_2$(dppe)] show their molecular ion and the mass spectrum of seven co-ordinate complex [WI$_2$(CO)$_3$(PEt$_3$)$_2$] only shows the molecular ion peak with loss of the carbon monoxide fragments. The complex [W(dmit)(CO)$_2$(dppe)] has fragmentation of the two phosphine groups.

Table 3.14 : FAB Mass Spectrometry Peaks
for the Complexes [W(X)(CO)$_2$(L)]

COMPLEX	Mass Peak
[WI$_2$(CO)$_3$(PEt$_3$)$_2$]	730 M$^+$ - CO
	702 M$^+$ - 2CO
	673 M$^+$ - 3CO
[W(dmit)(CO)$_2$(PEt$_3$)$_2$]	672 M$^+$
	673 M$^+$ + H
	695 M$^+$ + Na
[W(dmit)(CO)$_2$(dppe)]	834 M$^+$

3.9 INFRARED STUDIES OF THE REACTION OF [W(dmit)(CO)$_2$(PPh$_3$)$_2$] WITH CARBON MONOXIDE

It is evident from the X-ray crystal structures of the complexes, [W(X)(CO)$_2$(L)] {X = 1,2-dithiolene; L = (PPh$_3$)$_2$, (PEt$_3$)$_2$ or (dppe)} (Figures 3.11, 3.12, 3.13), that there are only two carbonyls in the structures. The tungsten complex [WI$_2$(CO)$_3$(PEt$_3$)$_2$] (Figure 3.10) is seven co-ordinate, therefore it may be possible to re-attach a third carbonyl group to the complexes [W(X)(CO)$_2$(L)] by saturating a solution of the complex in dichloromethane with carbon monoxide.

The infrared spectrum of [W(dmit)(CO)$_2$(PPh$_3$)$_2$] shows two carbonyl bands at $\nu_{(C \equiv O)}$ = 1928 cm^{-1} and $\nu_{(C \equiv O)}$ = 1844 cm^{-1} corresponding to the two *cis* carbonyls. The capping carbonyl at ca. 2050 cm^{-1}, as observed in the infrared spectrum of [WI$_2$(CO)$_3$(PPh$_3$)$_2$], is not present in the spectrum of the product. It was anticipated that as the experiment proceeded a peak might be observed in this region.

The complex [W(dmit)(CO)$_2$(PPh$_3$)$_2$] was dissolved in CH$_2$Cl$_2$ and carbon monoxide bubbled through the solution. The carbon monoxide was produced *in situ* by the oxidation of formic acid by sulphuric acid. The experiment was monitored by measuring the infrared spectrum of the solution as a thin film between NaCl plates at regular intervals.

As the experiment proceeded a peak was observed at 1720 cm^{-1}. This absorption band is too low for it to be assigned to a capping carbonyl, these typically occur at around 2000 cm^{-1}. Carbon-oxygen double bonds typically show absorption bands between 1600 and 1800 cm^{-1}, with a ketonic carbonyl absorbing at ca. 1700cm^{-1}. Bridging carbonyl groups also show peaks in the region around 1700 cm^{-1}, which is reasonable as they are more double than triple bond in character, see Figure 3.22. The absorption band at ca. 1720 cm^{-1} may be a bridging carbonyl. The infrared spectrum was taken again 24 hours after carbon monoxide had ceased to bubble through the solution, only the two original carbonyl bands at 1928 and 1844 cm^{-1} were present. This suggests that the species

formed was not stable and decomposed when allowed to stand.

| Triple Bond | Bridging | Double Bond |
| Carbonyl | Carbonyl | Ketone |
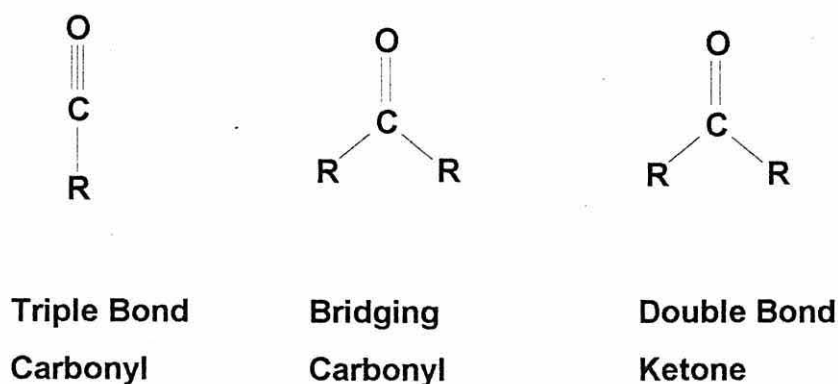
Figure 3.22 : Simplified Types of Bonding in Carbonyl Ligands

When the experiment was repeated, the initial infrared spectrum showed three carbonyl bands at 1928, 1844 and 1714 cm^{-1}. The only difference in the conditions between the two experiments was the age of the samples used. The older sample, ca. 14 days old, shows two carbon-oxygen absorption bands whilst the fresh sample, ca. 3 hours old, shows three carbonyl bands.

Assuming the peak observed at 1720 cm^{-1} to be a bridging carbonyl, then the reaction scheme would appear to be as in Scheme 3.6. The tungsten(II) complex reacts with the alkali metal salt of the 1,2-dithiolene to form the carbonyl-bridged dimer. The unstable dimer loses the bridging carbonyl and splits into two equivalents of the six co-ordinate complex. This is in contrast to the observations made when the dithiolene ligand is ethane-1,2-dithiolene [SCH$_2$CH$_2$S]$^{2-}$. When the complex [W(SCH$_2$CH$_2$S)(CO)$_2$(PPh$_3$)$_2$] is dissolved in CH$_2$Cl$_2$ and carbon monoxide is bubbled through the solution, a peak at ca. 2000 cm^{-1} corresponding to a capping carbonyl, is observed to develop. This suggests that the functional groups on the dithiolene influence whether the carbonyl will attach in a capping position or as a bridging group. The functional groups will affect the bite angle of the dithiolene ligand and, hence, the geometry of the resulting tungsten complex. The geometry will evidently influence the way in which the carbonyl can attach to the complex.

102
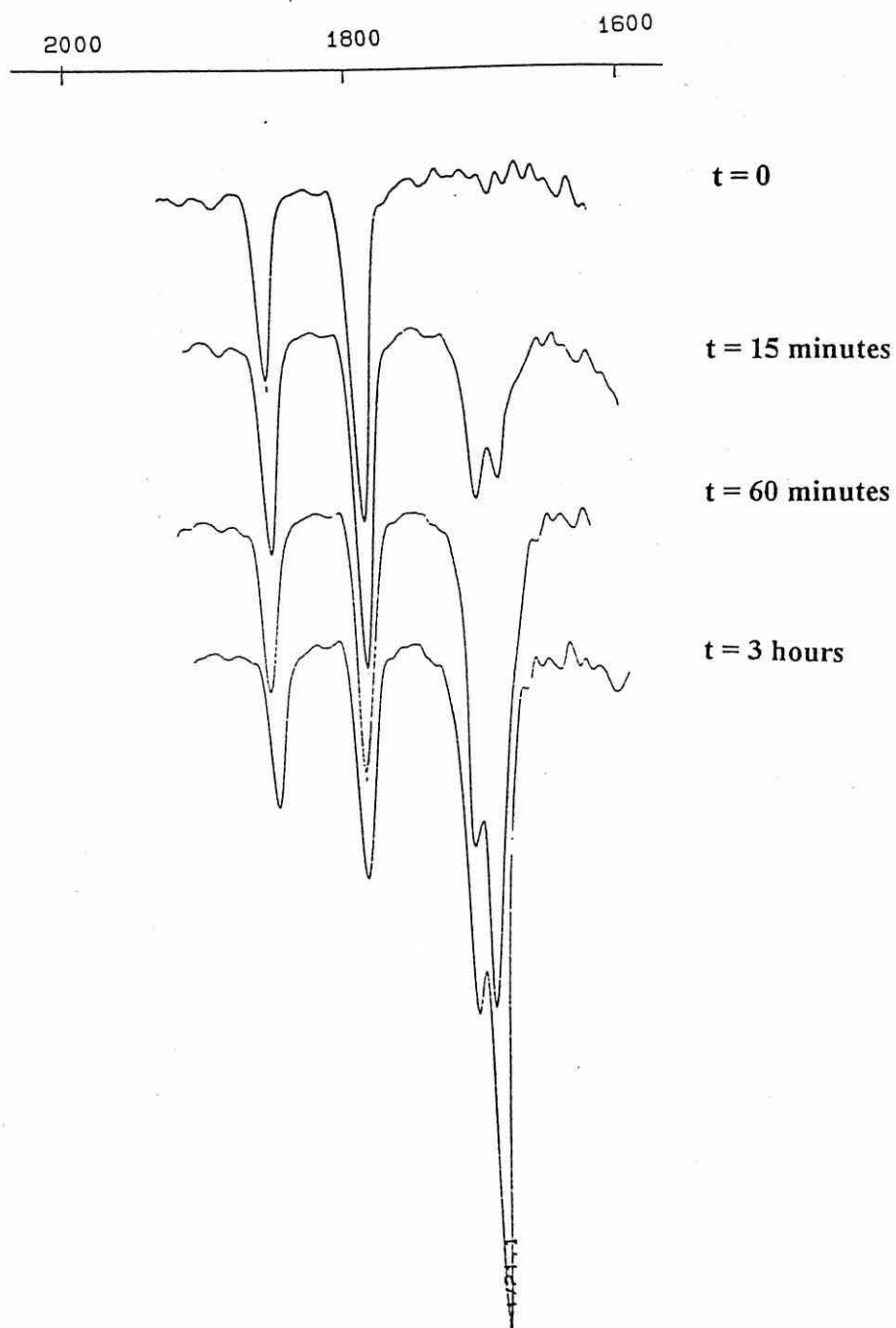
Figure 3.23 : Infrared Spectra of the Complex, [W(dmit)(CO)₂(PPh₃)₂]
during the Experiment taken at Time = t

$$WI_2(CO)_3(PPh_3)_2 \quad + \quad Na_2(dmit)$$

$$(PPh_3)_2(CO)_2(dmit)W — (CO) — W(dmit)(CO)_2(PPh_3)_2$$

CO bubbled through   **Allowed to stand**

$$W(dmit)(CO)_2(PPh_3)_2 \quad + \quad CO \quad + \quad 2\ NaI$$
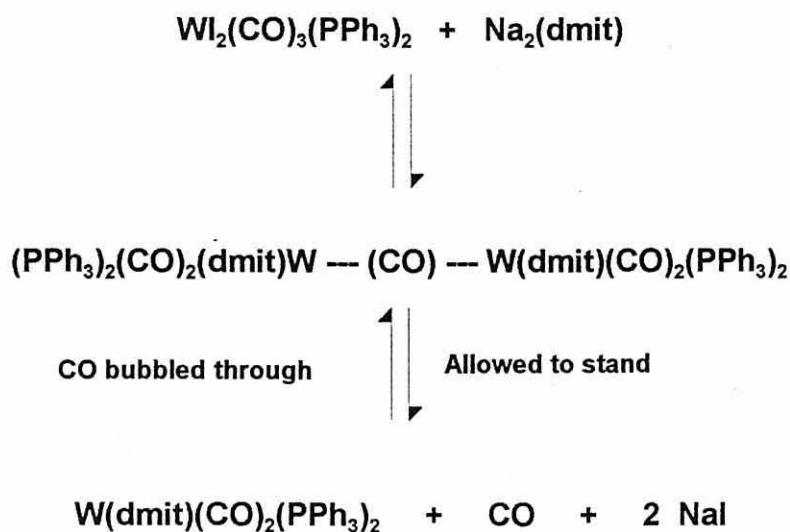
Scheme 3.7 : Proposed Reaction Scheme between the Tungsten(II) Complex and the 1,2-Dithiolene

3.10   CONCLUSIONS

This chapter has described the reaction between multisulphur donors and seven co-ordinate phosphine complexes of tungsten. The main points can be summarised as :

- Seven co-ordinate phosphine complexes of tungsten of the type $[WI_2(CO)_3(L)]$ where L is a phosphine ligand and can be monodentate such as $\{(PEt_3)_2\}$ or $\{(PPh_3)_2\}$ or bidentate such as (dppe) were reacted with the multisulphur ligand precursors, Y_2X. The complexes Y_2X were dithiolene-type systems with Y being either Na or H and X the dithiolene.

- The products of these reactions were six co-ordinate complexes of the type $[W(X)(CO)_2(L)]$. The crystal structures of three of the complexes can be seen in Figures 3.11, 3.12 and 3.13.

- The X-ray crystal structure and low temperature NMR studies of the seven co-ordinate complex, $[WI_2(CO)_3(PEt_3)_2]$ have been described.

104

- The reaction of the six co-ordinate complexes [W(X)(CO)$_2$(L)] {X = dmit, mnt or bdt; L = (PPh$_3$)$_2$, (PEt$_3$)$_2$ or dppe} with carbon moonoxide was followed by infrared spectroscopy. It was found that when carbon monoxide gas was bubbled through a solution of the complex, [W(dmit)(CO)$_2$(PPh$_3$)$_2$], a carbonyl peak reappeared in the infrared spectrum of the solution. However, this carbonyl appears to be bridging in nature and not capping, as seen in the original tungsten complex before reaction with the dithiolene.

- The theory that the reaction between seven co-ordinate tungsten complexes and dithiolenes may take place *via* the formation of some type of carbonyl-bridged dimer can be illustrated to a certain extent by the results of the infrared studies discussed in Section 3.9.

Chapter Four

Complexes of Molybdenum

and Tungsten containing

Thiophene Moieties

4.1 INTRODUCTION

4.1.1 Conducting Polymers

In 1974, Shirakowa *et al* synthesised polyacetylene [120]. It is difficult to synthesise a polymeric chain with a regular stereochemistry and in the case of polyacetylene, a chain of both *cis-* and *trans-* isomers is formed. The *cis*-polyacetylene is the less stable form and spontaneously isomerises to the *trans-* form. The polymer chain contains solitons. A soliton is an uncharged defect having associated with it an unpaired electron which is free to travel along the chain. Towards the end of the 1970's Heeger and MacDiarmid discovered that polyacetylene $[(CH)_x]$ underwent an increase in conductivity of up to 12 orders of magnitude upon oxidation [121]. When the polymer is oxidised, or p-doped, an electron is removed and thus the soliton becomes positively charged. Likewise, the polymer may be reduced, or n-doped, and the soliton becomes negatively charged. The soliton moves along the polymer chain carrying the charge with it.

4.1.2 Polyheterocycles

Polyheterocycles can be regarded as analogous to *cis*-polyacetylene in which the heteroatom stabilises the structure, see Figure 4.1.

The heterocycles differ in three aspects from $[(CH)_x]$

- They can exist in a quinoidal and an aromatic state which are non-equivalent in energy
- They have higher stability due to the heteroatoms
- They are structurally more versatile

107

POLYHETEROCYCLE   **CIS-POLYACETYLENE**
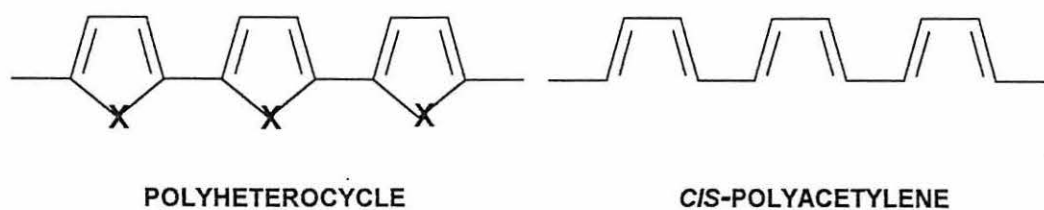
X = NH = Polypyrrole

S = Polythiophene

Figure 4.1 : Comparison Between Polyheterocycles and *cis*-Polyacetylene

Out of the area of electrogenerated heterocycles, polythiophene has emerged as the theoretical model for the study of charge transport in conducting polymers with a non-degenerate ground state. Its high stability has prompted developments towards applications as a conductor, semiconductor or an electrode material [122].

Polythiophenes can be synthesised by either a chemical [123 - 130] or an electrochemical [131 - 134] route. A common preparation of polythiophene is by the Grignard coupling of 2,5-dihalothiophenes in the presence of transition-metal complexes, for example, the polycondensation of 2,5-dibromothiophene using 2, 2'-bipyridinenickel dichloride [128] or nickel acetylacetonate [129]. Whilst the chemical synthesis of polythiophenes produces the most controlled oligomers, the most extensively conjugated and therefore the most conductive polythiophenes have been prepared by electropolymerisation techniques. The mechanism of the electropolymerisation of thiophene is based on the supposition that it will follow a similar mechanism to that of polypyrrole [135], see Scheme 4.1.

4.1.3   Conjugation and Conductivity

The extent of the conjugation is the limiting factor that controls the energy gap, conductivity and electroactivity of conducting polymers [136]. The conductivity of polythiophene has been shown to be correlated to the mean conjugation length of the

polymer [137]. The rigidity of the conjugated, unsubstitued structure tends to make polythiophene and other conducting polymers very insoluble.

X = HETEROATOM
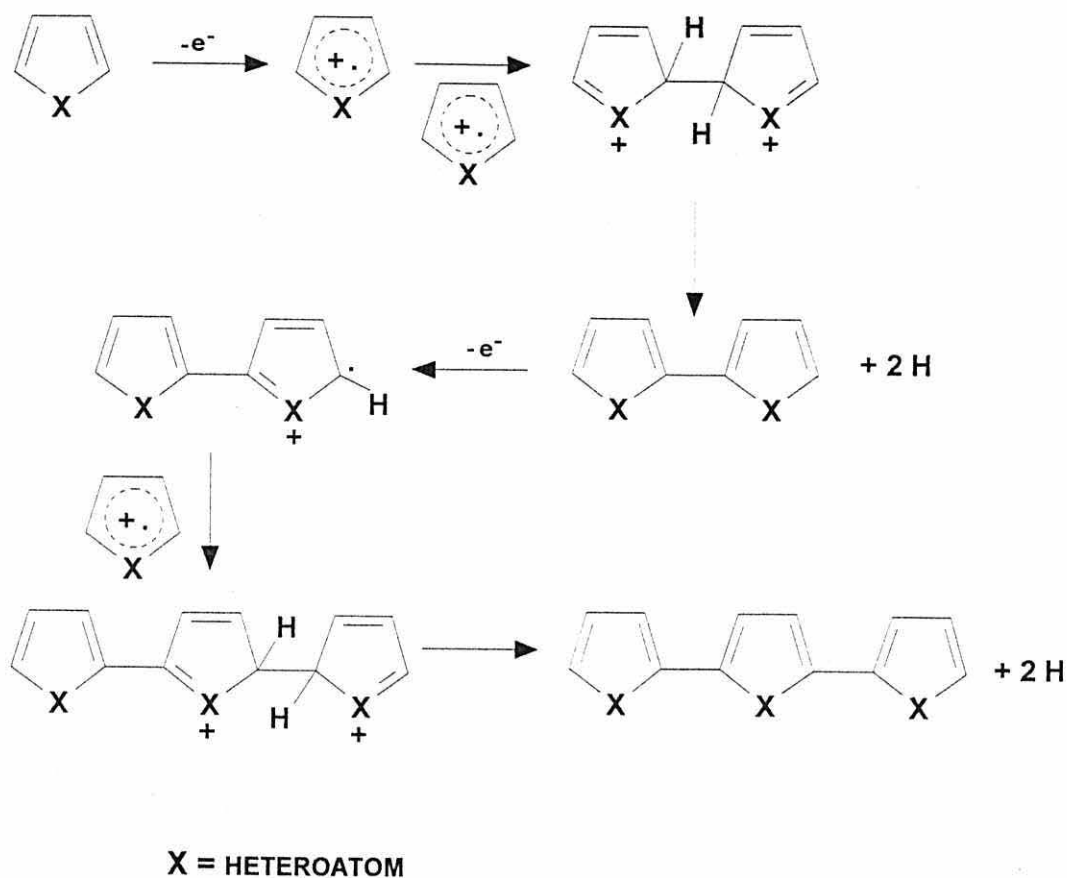
Scheme 4.1 : Mechanism of Polymerisation of Heterocycles

4.1.4 Substituted Polythiophenes

There are various strategies for the chemical modification of polythiophenes, but the polymerisation of monomers that have been modified by the introduction of functional groups is the simplest method of achieving control of the structure, electronic and electrochemical properties. If the functional group is to be interactive with the conjugated π-system, then the modification must be effected with the incorporation of the ligand π-system into the π-system of the polymer.

First synthesised in 1986, poly-3-alkyl thiophenes have attracted much attention due to the improved solubility associated with the presence of flexible alkyl chains on the conjugated polymer backbone [137 - 140]. The aryl derivatives of polythiophenes have been of interest because the phenyl groups are good anchoring sites for further functionalisation. There has been a considerable amount of work carried out on polypyrrole units [141], but there are very few examples of polythiophenes with a redox active functionalisation. This is due, in part, to the much higher oxidation potential of thiophene compared with pyrrole. Nevertheless, there are examples such as viologen [142, 143] and TTF [144] substituted thiophenes.

One of the governing factors in the synthesis of substituted polythiophenes is the functionalisation space, see Figure 4.2. The functionalisation space is defined as the volume into which a given substituent must be introduced in order to preserve the ability of the monomer to be polymerised and to result in an extended conjugation length in the polymer. The volume is determined by three parameters :

- the length of spacer needed to neutralise the electronic substituent effects (R)
- the limits of intra-chain distortion (α°)
- the limits of inter-chain distance (d)
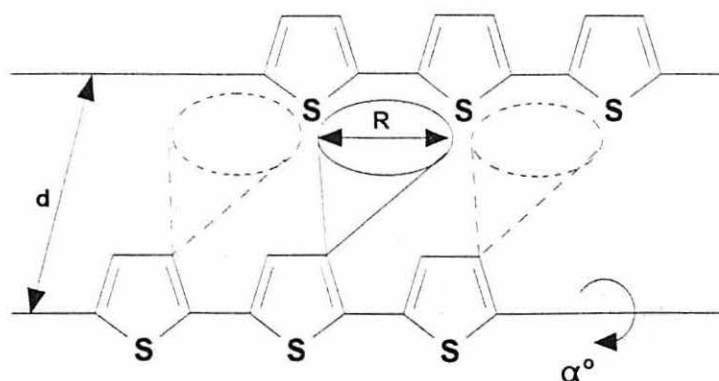
Figure 4.2 : Representation of the Functionalisation Space of Polythiophene

110

4.1.5 Attaching a Thiophene Moiety to a Transition Metal Centre

It was envisaged that by attaching a thiophene moiety to a redox-active metal centre, such as molybdenum or tungsten, then the physical and electrochemical properties of the thiophene, and ultimately the polythiophene, may be influenced by the oxidation state of the transition-metal centre.

Three ways of preparing compounds of this type have been investigated and will be described in detail later. They are as follows :

- attachment of the thiophene *via* an (η^6-aryl) linkage to a zero-valent metal centre (Section 4.2).

- attachment of thiophene *via* a nitrile linkage to a metal (II) cente (Section 4.3).

- attachment of thiophene *via* a nitrile linkage to a zero-valent metal centre (Section 4.5).

4.1.6 Molybdenum (II) and Tungsten(II) Complexes of Thiophene

Molybdenum and tungsten complexes are generally known to be redox active and can exist in oxidation states from -2 to +6. The complexes $[WI_2(CO)\{NCCH_2(3-SC_4H_3)\}(\eta^2-RC_2R)_2]$ $\{R = CH_3$ or Ph$\}$ and $[WI(CO)\{NCCH_2(3-C_4H_3S)\}(Ph_2P(CH_2)PPh_2)(\eta^2-MeC_2Me)][BF_4]$ have been prepared by the reaction of $[WI_2(CO)(NCMe)(\eta^2-RC_2R)_2]$ or $[WI(CO)(NCMe)(Ph_2P(CH)_2PPh_2)(\eta^2-MeC_2Me)][BF_4]$ with an equimolar amount of thiophene-3-acetonitrile, and the X-ray structure of the former when $\{R = Me\}$ has been elucidated [145], see Figure 4.3.
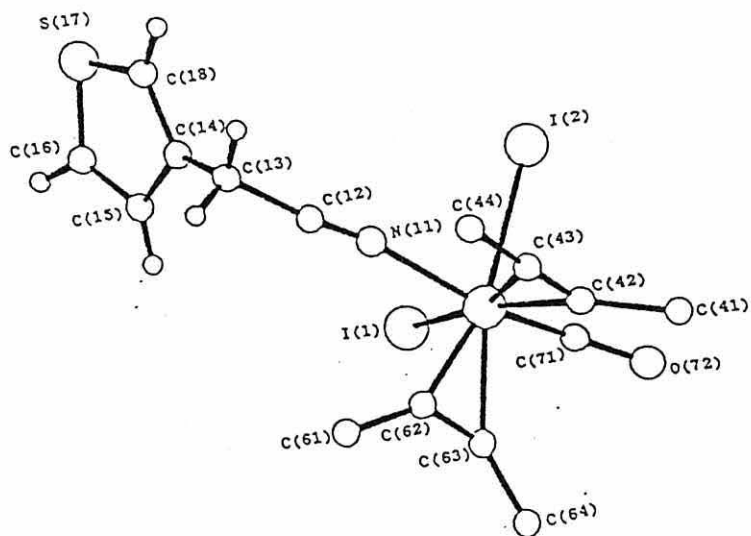
Figure 4.3 : X-ray Structure of $[WI_2(CO)\{NCCH_2(3\text{-}SC_4H_3)\}(\eta^2\text{-}MeC_2Me)_2]$

4.1.7   Molybdenum (0) and Tungsten (0) Complexes of Thiophene

As mentioned in Section 4.1.4, phenyl groups are a useful method of introducing a further functionality into a thiophene molecule. Previous studies have shown that the transition-metal complexes *fac*-$[M(CO)_3(NCMe)_3]$ {M = Mo or W} prepared *in situ* undergo substitution with an aryl ligand to give complexes of the type $[M(CO)_3(\eta^6\text{-}arene)]$ {M = Mo or W}[40 - 42].

Therefore, if an arene functionalised thiophene were to react with the metal complexes *fac*-$[M(CO)_3(NCMe)_3]$ {M = Mo or W} then a product such as $[M(CO)_3(\eta^6\text{-}arene\{3\text{-}SC_4H_3\})]$ may be expected, see Figure 4.4.

M = Mo(0) or W(0)
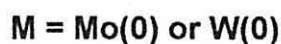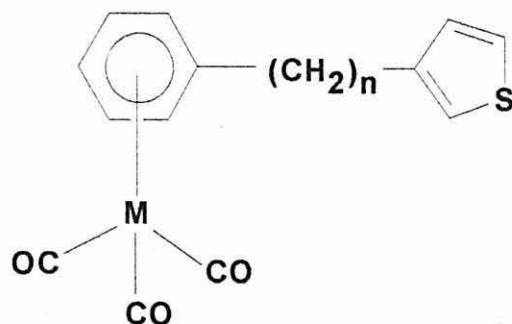
Figure 4.4 : A Thiophene Moiety Attached to a Zero-Valent Metal Centre

112

4.1.8 Polythiophene with Pendant Transition-Metal Functionalisations

It was envisaged that it may be possible to synthesise a polythiophene backbone substituted with transition-metal centres of the types described in Section 4.1.5, thereby creating a redox-active polymeric chain with pendant redox-active functional groups, see Figure 4.5.
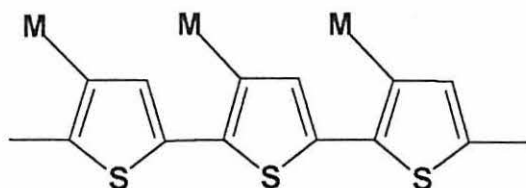
M = Mo (0) or W (0)

Figure 4.5 : Polythiophene with Pendant Redox-Active Functional Groups

4.2   ZERO-VALENT TRANSITION-METAL COMPLEXES OF THIOPHENES

The preparation of the zero-valent transition-metal complexes of arene-substituted thiophenes can be divided into two main steps. Firstly, the arene group has to be attached to the thiophene, and then the resulting complex reacted with the zero-valent transition-metal complex.

4.2.1   Synthesis of the Arene-Substituted Thiophene

Arene-substituted thiophenes of the type described in this section have been prepared by Roncali and co-workers [137] by reacting the Grignard product of the arene with 3-bromothiophene in tetrahydrofuran or diethyl ether using a nickel(II) catalyst, see Scheme 4.2.

113
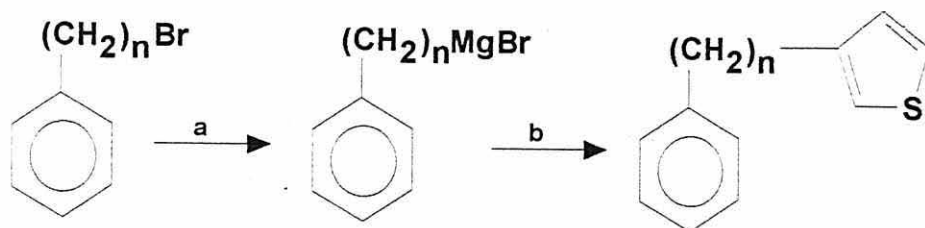
a : Mg turnings / Et$_2$O / I$_2$ crystal
b : 3-bromothiophene / Et$_2$O / NiCl$_2$(dppp)

Scheme 4.2 : Preparation of Aryl-substituted Thiophene

The work summarised in this chapter discusses the attempted synthesis of several different arene-functionalised thiophenes :

• 3-(phenylethyl)thiophene (C$_6$H$_5$(CH$_2$)$_2${3-SC$_4$H$_3$})

• 3-benzylthiophene (C$_6$H$_5$(CH$_2$){3-SC$_4$H$_3$})

• 3-(phenoxybutyl)thiophene (C$_6$H$_5$O(CH$_2$)$_4${3-SC$_4$H$_3$})

Attempts to synthesise the thiophenes that were required to react with the transition-metal complexes and the results, with the reaction conditions, are detailed in Table 4.2.

4.2.1.1 Synthesis of [3-(Phenylethyl)thiophene]

The procedure as described by Roncali [137] was followed. It was found that this reaction produced a mixture of products that on attempted separation by column chromatography, using a mixture of petrol and diethyl ether, gave unreacted 3-bromothiophene and a second component which was a mixture. The second constituent of the mixture was assumed to be the phenylethyl thiophene because the R$_f$ value of the second spot on the TLC plate did not correspond to either the 3-bromothiophene or phenylethane. The mixture was eluted through a silica column a number of times using different conditions, but the materials still proved to be inseparable. This suggested that the reaction between the 3-bromothiophene and the aryl magnesium bromide was incomplete, therefore the reaction mixture was gently refluxed for one hour prior to

stirring overnight. This produced a brown oil similar to that obtained when the reaction mixture was not heated. Half of the product was run through a silica column and the other half was distilled under vacuum. The portion of the mixture that was passed through the column gave a mixture as before. The distillation gave a colourless liquid that solidified upon slight cooling to a waxy, off-white solid that analysis showed to be phenylethane. Hence the synthesis of the required arene-thiophene had not been acheived.

The reaction mixture of 3-bromothiophene and phenylethyl magnesium bromide was refluxed for four hours and the resulting brown oil distilled under vacuum. The product was identified as a mixture of 3-bromothiophene and 3-(phenylethyl)thiophene. Further attempts at separation of the mixture proved to be unsuccessful. Purification of the mixture was attempted by column chromatography and resulted in an inseparable mixture as before. These reactions were attempted a number of times.

An Ullmann Coupling reaction was carried out in an effort to couple the two reagents together by using activated copper-bronze and heating the mixture of the two reagents to 200 °C in a sand bath. The resulting product was split into two parts one of which was eluted through a silica column and the other distilled under vacuum. Only 3-bromothiophene was obtained from the material that was passed through the column, but vacuum distillation gave 3-bromothiophene and the coupled product [PhC$_4$H$_8$Ph].

It was suggested that one of the main difficulties in preparing 3-(phenylethyl)thiophene could be that the length of the alkyl chain linking the thiophene and the phenyl moieties is too short. Roncali suggests that the optimum length for the alkyl spacer in this type of molecule is about four carbon atoms. This led to the attempted coupling of phenoxybutyl bromide and 3-bromothiophene.

4.2.1.2 Synthesis of [3-(Phenoxybutyl)thiophene]

The Grignard product of phenoxybutylbromide was formed and this was reacted with 3-bromothiophene. The coupling of the two reagents was first attempted by refluxing the

115

reaction mixture overnight. The product was shown by analysis to be phenoxybutane. Repeating the experiment, but stirring the reaction mixture at room temperature, resulted in the formation of phenoxybutane. This indicated that the Grignard reagent was hydrolysing at some point, either before the addition to the 3-bromothiophene or before the 3-bromothiophene had reacted with it. In order to discover at which point hydrolysis of the Grignard reagent took place, test reactions were carried out on the phenoxybutyl magnesium bromide and the results are presented in Table 4.1. It can be seen from the reaction with a simple ketone that the Grignard reagent produces the expected product. This demonstrates that no hydrolysis of the Grignard reagent has taken place. The reaction with bromobenzene was attempted to see if the Grignard reagent reacted with a simple aryl bromide. It was concluded that it worked partially since, in a chromatographic assessment of the reaction mixture, the first spot was bromobenzene and the R_f of the second spot did not correspond to that of phenoxybutane. It can be concluded from this that the Grignard product does react with alkyl halides, albeit in low yields, under the conditions of the reaction described above.

4.2.1.3 Synthesis of Benzylthiophene

The procedure described by Roncali [137] involving overnight stirring of the Grignard product of benzylbromide with 3-bromothiophene. This reaction gave a brown oil which was divided into two equal parts. One part was passesd through a silica column, whilst the other part was distilled under vacuum. As was observed with the phenylethyl derivative described in Section 4.2.1.1, a mixture of the 3-bromothiophene and benzyl thiophene was obtained. A chromatographic assessment of the products was carried out; the first spot corresponded to 3-bromothiophene and the second spot on the TLC was assumed to be benzyl thiophene for the same reasons as stated previously.

The reaction was repeated but instead of only stirring, the reaction mixture was refluxed overnight. In an attempt to separate the benzylthiophene from the unreacted 3-bromothiophene, a graduated column was run using petroleum ether / diethyl ether mixture as the eluent. A TLC of the fractions immediately after they had been eluted from

the column showed there to be separation of the product from the starting material
However, repeating the TLC an hour later revealed that the second fraction now showed
two spots, the new spot having the same R_f value as the 3-bromothiophene. From this it
was concluded that the product could be isolated immediately, however, it degrades quite
quickly when allowed to stand to a thiophene-based component and another unidentified
component. Immediate reaction with a metal complex would ensure that the minimum
amount of degradation took place.

Table 4.1 : Reagents and Results of the Test Reactions

Aryl Bromide	Reactant	Observations
Phenoxybutyl Bromide	Methyl Ethyl Ketone	3-Methyl-7-Phenoxyheptan-3-ol
Phenoxybutyl Bromide	Bromobenzene	•Brown oil •Two spots on TLC •Will not column •Assume that spots are bromobenzene and [PhOC$_4$H$_8$Ph]
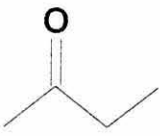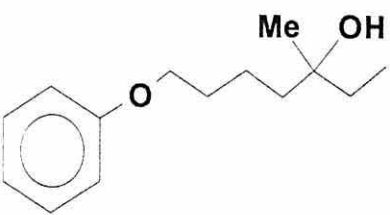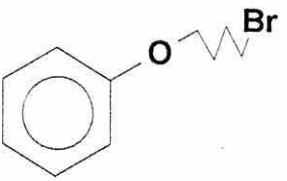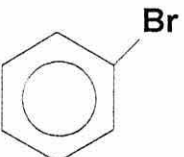
4.2.2 Investigations to Determine the Optimum Reaction Conditions for the Synthesis of Benzylthiophene

Reactions were carried out to ascertain the optimum conditions needed for the synthesis of benzylthiophene. The experiments, in the main, were to establish the length of time the reaction must reflux in order to produce the maximum amount of benzylthiophene. This was accomplished by removing 1 cm^3 aliquots from the refluxing reaction mixture at regular time intervals (1 minute, 30 minutes, 60 minutes etc.) and adding 2 cm^3 dilute hydrochloric acid to hydrolyse the mixture. The organic layer was then removed in three extractions, each of 1 cm^3 of diethyl ether, and the sample characterised by GC-MS. This indicated the amount of benzylthiophene present at the time the sample was taken, so that the optimum reflux time could be determined. It was found, by this and other experiments, that the optimum conditions for the reaction of benzyl magnesium bromide with 3-bromothiophene are :

- excess magnesium to prepare the Grignard reagent and refluxing for two hours.

- slow addition of the Grignard reagent to 3-bromothiophene and the nickel catalyst at 0 °C.

- refluxing the reaction mixture for one and a half to two hours before hydrolysis with dilute hydrochloric acid.

4.2.3 Preparation of the Metal Complexes

The reaction between arenes and molybdenum and tungsten complexes are reported in Comprehensive Organometallic Chemistry II Volume 3 [34]. Different reactions are described for each metal and these reactions were used as a basis for the conditions of the reactions between the transition metal complexes and the arene-thiophenes prepared.

Table 4.2 : Summary of the Aryl Bromide Reagents used, the Reaction Conditions and the Results

Aryl Bromide	Conditions	Purification	Isolated Product
	RT Stir 16 hours	Column	3-bromothiophene Mixture
	Reflux 1 hour	Column	Mixture
	RT Stir 16 hours	Vacuum Distillation	Phenylethane
	Reflux 4 hours	Vacuum Distillation	Mixture
	Ullmann Coupling	Column	3-bromothiophene
Phenyl Ethyl Bromide	Ullmann Coupling	Vacuum Distillation	3-bromothiophene 1,4-diphenylbutane
	RT Stir 16 hours	-	Phenoxybutane
Phenoxy Butyl Bromide	Reflux 16 hours	-	Phenoxybutane
	RT Stir 16 hours	Column	Mixture
	RT Stir 16 hours	Vacuum Distillation	Mixture
Benzyl Bromide	Reflux 16 hours	Column	Benzylthiophene? 3-Bromothiophene
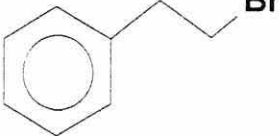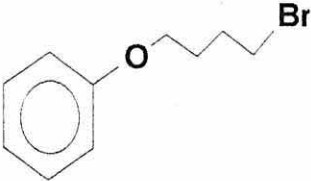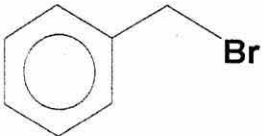
119

4.2.4 Zero-Valent Tungsten Complexes of (η^6-Arene)Thiophenes

The preparation of η^6-arene tungsten complexes can be accomplished by two methods. Firstly, is the reaction reported by E. O. Fischer and co-workers [40, 41] where the arene is heated directly with the tungsten hexacarbonyl. This, however, gives low yields (15 %) and is not a generally used route. The second reaction is that described by King and Fronzaglia in which they heat the arene with the tungsten tricarbonyl trisacetonitrile, fac-[W(CO)$_3$(NCMe)$_3$] [42]. The yields of this reaction are over 70 % and it is obviously the more favoured method of preparing η^6-arene tungsten complexes. The fac-[W(CO)$_3$(NCMe)$_3$] was prepared by refluxing tungsten hexacarbonyl in acetonitrile for 72 hours. After this time the arene was added and the mixture was refluxed for a further 24 hours.

As discussed previously, the thiophene substituted arenes had proved to be difficult to purify. However, it was envisaged that if 3-bromothiophene did not show any reaction with fac-[W(CO)$_3$(NCMe)$_3$] then this would dispense with the need to purify the thiophene product before reacting it with the tungsten complex. No reaction was observed when 3-bromothiophene was added to the fac-[W(CO)$_3$(NCMe)$_3$] and refluxed for 24 hours. Therefore the impure mixture containing the arene-thiophene was reacted with the complex without any further purification. The reaction between the tungsten complex and the corresponding non-thiophene containing arene was also carried out in both cases as a comparative reaction. The results are presented in Table 4.4.

4.2.5 Zero-Valent Molybdenum Complexes of (η^6-Arene)Thiophenes

The methods for preparing the molybdenum-arene complexes are not as simple as those of the tungsten analogues. E. O. Fischer et al described the preparation of the molybdenum complexes by heating the arene with molybdenum hexacarbonyl, however this, once more, gives low yields of between 5 and 10 % [40]. Price and Sørenson heated the arene with fac-[Mo(CO)$_3$(py)$_3$] in the presence of BF$_3$.OEt$_2$ to give the product in yields of 70 % [43]. Even though the best method of synthesising the [W(CO)$_3$(η^6-arene)

type complexes was to react the arene with *fac*-[W(CO)$_3$(NCMe)$_3$], no mention is made of how well the complex *fac*-[Mo(CO)$_3$(NCMe)$_3$] would react with arenes. It was decided to attempt to react benzyl thiophene with *fac*-[Mo(CO)$_3$(NCMe)$_3$] in a variety of solvents. The results of this are presented in Table 4.3. There is no reaction between benzylthiophene and *fac*-[Mo(CO)$_3$(NCMe)$_3$] when the solvent is acetonitrile, since there is an excess of acetonitrile this is the more favoured ligand. This implies that this reaction apparently can not be carried out *in situ*. However, by removing the acetonitrile to isolate *fac*-[Mo(CO)$_3$(NCMe)$_3$] and resolvating in another solvent, the reaction appears to proceed. The reaction in dichloromethane produces an oil, whereas the reactions in diethyl ether and hexane yield a powder. None of these products had satisfactory analyses.

Table 4.3 : The Solvents used in the Reaction between

fac-[Mo(CO)$_3$(NCMe)$_3$] and Benzylthiophene

Metal Complex	Thiophene Complex	Solvent	Observations
fac-[Mo(CO)$_3$(NCMe)$_3$]	Benzylthiophene	MeCN	No reaction
		CH$_2$Cl$_2$	Brown Oil No Analysis
		Et$_2$O	Brown Powder Poor Analysis
		Hexane	Brown Powder Poor Analysis
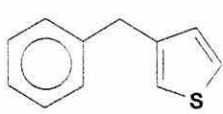
4.2.6 Conclusions about the Molybdenum and Tungsten Complexes of the Arene-thiophenes

- It is possible to prepare the arene derivatives of thiophene, but separation of the product from the unreacted 3-bromothiophene is difficult.

- 3-bromothiophene apparently does not react with the *fac*-[M(CO)$_3$(NCMe)$_3$] type complexes.

121

- The tungsten complexes containing arene-thiophenes can be synthesised with greater ease than the molybdenum analogues.

- The complexes [W(CO)$_3$(η^6-arene-thiophene)] were found to decompose slowly over time and hence were deemed unsuitable for polymerisation, therefore no further work was carried out on these materials.

Table 4.4 : Reaction of Different Arenes with *fac*-[W(CO)$_3$(NCMe)$_3$]

Tungsten Complex	Aryl Complex	Product
fac-[W(CO)$_3$(NCMe)$_3$]	Br (structure) 3-Bromothiophene	No reaction
	(structure) —CH$_3$ Toluene	W(CO)$_3$(η^6-toluene)
	(structure) —O—C$_4$H$_9$ Phenoxybutane	W(CO)$_3$(η^6-phenyoxybutane)
	(structure) —CH$_2$—(thiophene) 3-Benzylthiophene	W(CO)$_3$(η^6-benzylthiophene)
	(structure) —O—C$_4$H$_8$—(thiophene) Phenoxybutylthiophene	W(CO)$_3$(η^6-phenoxybutyl thiophene)
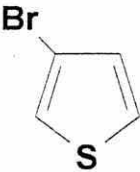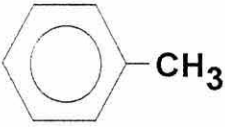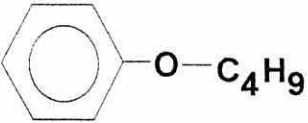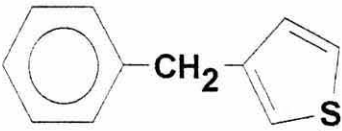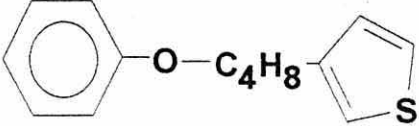
4.3 TUNGSTEN(II) COMPLEXES CONTAINING THIOPHENE-3-ACETONITRILE

The previous section contained a discussion of thiophene ligands attached to the metal centre by an arene functionality. Thiophenes can also be bound to transition-metal centres by co-ordination through a nitrile functionality as described in Section 4.1.5. The products formed by reacting thiophene-3-acetonitrile with seven co-ordinate complexes of tungsten(II) are discussed in the following section.

4.3.1 General Preparation

The complex $[WI_2(CO)_3(NCMe)_2]$, prepared as shown in Scheme 4.3, was dissolved in CH_2Cl_2 and reacted with either one equivalent of ligand L {L = PPh_3, AsPh_3 or P(OPh)_3}, followed by one equivalent of thiophene-3-acetonitrile (Section 4.3.2), or with two equivalents of thiophene-3-acetonitrile (Section 4.3.3). The analytical results of the product obtained are summarised in Table 4.5.

$$M(CO)_6 \xrightarrow{\text{a}} \textit{fac-}[M(CO)_3(NCMe)_3] \xrightarrow{\text{b}} [MI_2(CO)_3(NCMe)_2]$$

a : MeCN / reflux / 24 hours - Mo

72 hours - W

b : *in situ* I_2 / 0 °C / 20 minutes

M = Mo or W

Scheme 4.3 : Preparation of $[MI_2(CO)_3(NCMe)_2]$

123

Table 4.5 : Physical and Analytical Data of the Complexes [WI₂(CO)₃(L)(L')]

COMPLEX	COLOUR	%	C	H	N
[WI₂(CO)₃(NCCH₂{3-SC₄H₃})₂]	dark red/ brown powder	70.9	23.4 (23.4)	1.3 (1.3)	3.4 (3.6)
[WI₂(CO)₃(NCMe)(NCCH₂{3-SC₄H₃})]	brown oil	-	-	-	-
[WI₂(CO)₃(PPh₃)(NCCH₂{3-SC₄H₃})]	yellow powder	82.2	35.6 (35.7)	2.3 (2.2)	1.7 (1.5)
[WI₂(CO)₃(AsPh₃)(NCCH₂{3-SC₄H₃})]	yellow powder	77.8	34.0 (34.1)	2.2 (2.1)	1.5 (1.5)
Reaction between [WI₂(CO)₃(NCMe)(P(OPh)₃)] and (NCCH₂{3-SC₄H₃})	yellow oily solid	-	42.6 (34.0)	2.9 (2.1)	1.2 (1.5)

Calculated values in parentheses

4.3.2 Attempted Preparation of the Complexes [WI₂(CO)₃(L)(L')]
{L = NCMe, PPh₃, AsPh₃ or P(OPh)₃; L' = NCCH₂(3-SC₄H₃)}

The acetonitrile ligand is the most labile of the simple nitrile ligands. This is demonstrated by the relative ease with which it is displaced from the seven co-ordinate molybdenum and tungsten complexes by substituted nitrile ligands such as, NCR (R ≠ Me).

Initial attempts to prepare the complex [WI₂(CO)₃(NCCH₂{3-SC₄H₃})(NCMe)] yielded a dark brown intractable oil. This follows the trend amongst compounds of this type for the complex containing a nitrogen donor ligand to be much less stable than the phosphine derivatives. This may be supported by comparing the stability of the phosphine and the acetonitrile products discussed in Chapter 3, as well as numerous examples in the literature [59].

The complexes [WI₂(CO)₃(L)(L')] {L = PPh₃ or AsPh₃ ; L' = NCCH₂{3-SC₄H₃}} precipitate out of solution immediately upon formation. Subsequent attempts to resolvate

the precipitate in a variety of solvents were unsuccessful. To try to overcome this problem, triphenyl phosphite, was used since complexes of this ligand are known to be more soluble than those of PPh$_3$. The product formed was a very oily yellow solid. Elemental analysis results suggested the complex to be impure. No further characterisation was carried out on these complexes since the triphenylphosphine and triphenylarsine derivatives were completely insoluble a wide range of solvents and analysis of the triphenylphosphite derivative showed it to be impure.

4.3.3 Preparation of the Complex [WI$_2$(CO)$_3$(NCCH$_2${3-SC$_4$H$_3$})$_2$] (L) = (L')

Two methods for preparing the complex [WI$_2$(CO)$_3$(NCCH$_2${3-SC$_4$H$_3$})$_2$] were developed. Initially the complex [WI$_2$(CO)$_3$(NCMe)$_2$] was stirred with two equivalents of thiophene-3-acetonitrile in CH$_2$Cl$_2$ at room temperature overnight. This produced a dark shiny red-brown powder of [WI$_2$(CO)$_3$(NCCH$_2${3-SC$_4$H$_3$})$_2$], but only in a low yield. To enhance the amount of product obtained, the same procedure was followed, but the solution was warmed in a hot water bath for 90 minutes prior to further stirring for one hour. The yield was enhanced by approximately 50 %. The product, [WI$_2$(CO)$_3$(NCCH$_2${3-SC$_4$H$_3$})$_2$], was found to be soluble in acetonitrile and dichloromethane and was characterised in more detail.

4.4 CHARACTERISATION OF [WI$_2$(CO)$_3$(NCCH$_2${3-SC$_4$H$_3$})$_2$]

4.4.1 Infrared Studies of [WI$_2$(CO)$_3$(NCCH$_2${3-SC$_4$H$_3$})$_2$]

The infrared spectrum of the complex [WI$_2$(CO)$_3$(NCCH$_2${3-SC$_4$H$_3$})$_2$] was measured in solution as a thin film between NaCl plates and the data is presented in Table 4.6.

The absorption bands arising from the aliphatic and aromatic CH bonds are observed in the region 3200 - 2950 cm^{-1}. Absorption peaks corresponding to the nitrile and the CS bonds are seen at 2360 cm^{-1} and at 1044 cm^{-1} respectively. In addition to the peaks

125

attributed to thiophene-3-acetonitrile, carbonyl frequencies are observed at 2027 cm^{-1} and 1937 cm^{-1}. The peak at 2027 cm^{-1} may correspond to the capping carbonyl of this seven co-ordinate complex. This can be compared with the frequency of the capping carbonyl of the original complex [WI$_2$(CO)$_3$(NCMe)$_2$] which occurs at 2000 cm^{-1}. The absorption band at 1937 cm^{-1} is broad with a slight shoulder which indicates that there is a second absorption band underneath. This is comparable to the carbonyl bands observed in the infrared spectrum of [WI$_2$(CO)$_3$(NCMe)$_2$] which has bands at 2040 cm^{-1}, 1980 cm^{-1} and 1945 cm^{-1}.

Table 4.6 : Infrared Data for [WI$_2$(CO)$_3$(NCCH$_2$\{3-SC$_4$H$_3$\})$_2$]

ν (cm^{-1})^a	Bond
3019	C-H$_{ar}$
2977	C-H
2360	C$\equiv$N
2027 1937	C$\equiv$O
1044	C-S

^{a} measured in solution as a thin film between NaCl plates

The structure of the complex [WI$_2$(CO)$_3$(NCCH$_2$\{3-SC$_4$H$_3$\})$_2$] is likely to be capped octahedral, with a carbonyl ligand capping an octahedral face since the infrared spectral properties are similar to the complex [WI$_2$(CO)$_3$(NCMe)$_2$], which has a capped octahedral structure and is shown in Figure 1.6.

4.4.2   NMR Studies of [WI$_2$(CO)$_3$(NCCH$_2$\{3-SC$_4$H$_3$\})$_2$]

4.4.2.1 ^{1}H NMR Studies of [WI$_2$(CO)$_3$(NCCH$_2$\{3-SC$_4$H$_3$\})$_2$]

The proton NMR of the complex [WI$_2$(CO)$_3$(NCCH$_2$\{3-SC$_4$H$_3$\})$_2$] was obtained in CDCl$_3$ and the data is recorded in Table 4.7. Figure 4.6 identifies the protons that give rise to the signals in the ^{1}H NMR spectrum.
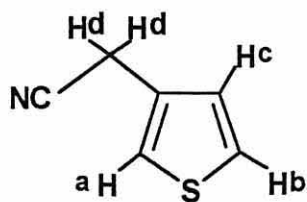
Figure 4.6 : Thiophene-3-Acetonitrile showing the a, b, c and d Protons

Table 4.7 : ^{1}H NMR Spectroscopic Data for [WI$_2$(CO)$_3$(NCCH$_2${3-SC$_4$H$_3$})$_2$]

δ (ppm)	H
7.4 (m, 1H)	CH^a
7.5 (m, 1H)	CH^b
7.1 (m, 1H)	CH^c
4.2 (s, 1H)	CH$_2^d$

m = multiplet
s = singlet

The proton NMR spectrum of [WI$_2$(CO)$_3$(NCCH$_2${3-SC$_4$H$_3$})$_2$] shows the same fundamental signals as that of the thiophene-3-acetonitrile since there are no protons in the complex except for those associated with this ligand. There are three signals observed in the phenyl region of the spectrum from 7.1 - 7.5 ppm which can be attributed to the protons in the thiophene ring. The sulphur atom adjacent to the protons **a** and **b** is electronegative and will result in deshielding of these protons. The signal at 7.5 ppm is due to the proton **b** and can be distinguished from proton **a**, seen at 7.4 ppm, by its more complicated signal due to splitting by proton **c** (seen at 7.1 ppm). These three signals would be expected to be quite simple (**a** singlet; **b** and **c** doublet), however there is evidence of long distance coupling from the other protons in the thiophene ring. The protons from the CH$_2$ group show a singlet resonance at 4.2 ppm.

4.4.2.2 ^{13}C NMR Studies of [WI$_2$(CO)$_3$(NCCH$_2${3-SC$_4$H$_3$})$_2$]

The ^{13}C NMR spectrum of [WI$_2$(CO)$_3$(NCCH$_2${3-SC$_4$H$_3$})$_2$] was recorded in CDCl$_3$ and the data is presented in Table 4.8. There are no signals observed for the carbonyl groups of the complex [WI$_2$(CO)$_3$(NCCH$_2${3-SC$_4$H$_3$})$_2$] in the spectrum due to the spectrum being too weak. The carbonyls are expected to show a signal at ca. 220 ppm. The spectrum is as expected for the thiophene-3-acetonitrile with the carbon of the nitrile group being much further downfield than the other carbon signals.

Table 4.8 : ^{13}C NMR Data for [WI$_2$(CO)$_3$(NCCH$_2${3-SC$_4$H$_3$})$_2$]

δ (ppm)	C
156 (s)	CN
126 (m)	(3-SC$_4$H$_3$)
20 (s)	CH$_2$

s = singlet
m = multiplet

4.4.3 Cyclic Voltammetric Studies of [WI$_2$(CO)$_3$(NCCH$_2${3-SC$_4$H$_3$})$_2$]

The cyclic voltammograms were all measured in a 0.1 M solution of [TBA][PF$_6$] in acetonitrile against either a standard calomel electrode or a silver/silver chloride electrode. The cyclic voltammetric results of the complex [WI$_2$(CO)$_3$(NCCH$_2${3-SC$_4$H$_3$})$_2$], both as the monomer and as a thin polymeric film, are presented in Table 4.9 together with the cyclic voltammetric results of related compounds.

The cyclic voltammogram of the ligand thiophene-3-acetonitrile has a large irreversible reduction peak at -1.3 V. The cyclic voltammogram of the complex [WI$_2$(CO)$_3$(NCMe)$_2$] comprises of three oxidation peaks at 0.3 V, 0.7 V and 1.1 V and three reduction peaks at 0.6 V, 0.0 V and -1.3 V. Previous studies on the cyclic voltammetry of seven co-

ordinate iodide complexes of tungsten(II) have shown that the two oxidation peaks at 0.3 V and 0.7 V arise from iodide based oxidative processes. The peak at 1.1 V is an irreversible oxidation which may be assigned to the oxidation of tungsten(II) to tungsten(III) by comparison with other studies, see Chapter 2. When the sample is scanned to this positive potential the resulting solution gives rise to a reduction peak not observed in the original solution at -1.3 V. This implies that the reduction wave corresponds to the reduction of a decomposition product generated in the oxidation of tungsten(II) to tungsten(III).

The cyclic voltammogram of the complex [WI$_2$(CO)$_3$(NCCH$_2${3-SC$_4$H$_3$})$_2$] is similar to that of [WI$_2$(CO)$_3$(NCMe)$_2$]. Comparable oxidation peaks at 0.4 V and 0.7 V are attributable to an iodide based oxidation. A peak was observed at 1.1 V due to the oxidation of the tungsten(II) as in the complex [WI$_2$(CO)$_3$(NCMe)$_2$]. A reduction peak is also observed at -1.2 V and could be due to the thiophene or to the reduction of a tungsten species. However, the peak is still observed if the potential is only taken to 0.8 V thus establishing that it is due to reduction of the thiophene ligand.

A thin film of the complex [WI$_2$(CO)$_3$(NCCH$_2${3-SC$_4$H$_3$})$_2$] was grown galvanostatically on a platinum electrode by holding the current at 10 mA for three minutes. Cyclic voltammetry was performed upon the resulting dark brown film using a silver/silver chloride electrode as a reference. An oxidation peak at 0 V and a reduction peak at -1.1 V were observed for the film. Both peaks were irreversible with the reduction peak being much larger than the oxidation peak.

Table 4.9 : Cyclic Voltammetric Data for $[WI_2(CO)_3(NCCH_2\{3\text{-}SC_4H_3\})_2]$ and Related Compounds

Material	Electrode	E (V)	Process
$[WI_2(CO)_3(NCCH_2\{3\text{-}SC_4H_3\})_2]$ monomer	SCE	0.4 0.7 1.1 0.6 0.1 -1.2	ox. red.
$[NCCH_2\{3\text{-}SC_4H_3\}]$ monomer	SCE	-1.3	red.
$[WI_2(CO)_3(NCMe)_2]$	SCE	0.3 0.7 1.1 0.6 0.0 -1.3	ox. red.
thiophene $[3\text{-}SC_4H_3]$ monomer	SCE	1.7	ox.
$[WI_2(CO)_3(NCCH_2\{3\text{-}SC_4H_3\})_2]$ polymer	Ag/AgCl	0.0 -1.1	ox. red.
thiophene $[3\text{-}SC_4H_3]$ polymer	Ag/AgCl	0.7 0.6 0.3	ox. red.

4.4.4 Conclusions

- The complex $[WI_2(CO)_3(NCCH_2\{3\text{-}SC_4H_3\})_2]$ can be prepared with a high degree of purity and in good yields.

- The complex is fairly stable in air and has a high solubility in dichloromethane and acetonitrile.

- The cyclic voltammetry indicates that there is an iodide based oxidation as well as an oxidation due to the tungsten and a reduction due to the thiophene moiety.

- The complex $[WI_2(CO)_3(NCCH_2\{3\text{-}SC_4H_3\})_2]$ can be electropolymerised, however, further studies are required to investigate this more thoroughly.

4.5   MOLYBDENUM(II) COMPLEXES CONTAINING THIOPHENE-3-ACETONITRILE

Reactions analogous to those described in Section 4.3.1 were attempted using the molybdenum derivative $[MoI_2(CO)_3(NCMe)_2]$. The majority of the products from these reactions were intractable oils. The powder obtained from the reaction between $[MoI_2(CO)_3(NCMe)_2]$ with triphenylphosphine, followed by addition of thiophene-3-acetonitrile gave a product which elemental analysis did not confirm to be $[MoI_2(CO)_3(PPh_3)(NCCH_2\{3\text{-}SC_4H_3\})]$.

4.6   ZERO-VALENT COMPLEXES OF MOLYBDENUM AND TUNGSTEN CONTAINING THIOPHENE-3-ACETONITRILE

4.6.1   Thiophene-3-Acetonitrile Complexes of Tungsten(0)

The preparation of tungsten(0) complexes of the type $[W(CO)_3(\eta^6\text{-arene-thiophene})]$ has already been discussed in Section 4.2.4. It was thought that complexes of the type $[W(CO)_2(NCCH_2\{3\text{-}SC_4H_3\})(\eta^6\text{-arene})]$ containing tungsten(0) might be prepared by replacing one of the carbonyl groups with thiophene-3-acetonitrile.

The arene complex $[W(CO)_3(\eta^6\text{-}C_6H_3(CH_3)_3)]$ ($\{C_6H_3(CH_3)_3\}$ = mesitylene) was prepared in the manner described in Section 4.2.4, by refluxing tungsten hexacarbonyl in acetonitrile for 72 hours and then adding mesitylene and refluxing for a further 12 hours. The resulting complex was then reacted *in situ* with trimethylamine N-oxide to remove a carbonyl group. The thiophene-3-acetonitrile was introduced and the dark green solution was left to stir. A dark green precipitate was isolated that did not analyse to be $[W(CO)_2(NCCH_2\{3\text{-}SC_4H_3\})(\eta^6\text{-}C_6H_3(CH_3)_3)]$, see Table 4.10. The precipitate was sensitive to air, changing colour within ten minutes of exposing it to the atmosphere. The resulting blue powder did not analyse for $[W(CO)_2(NCCH_2\{3\text{-}SC_4H_3\})(\eta^6\text{-arene})]$. The infrared spectrum contained the same characteristic aromatic CH and thiophene absorption frequencies as would be expected to be observed for the complex. The

carbonyl bands are present in the infrared spectrum, however they are of a slightly higher frequency than would be expected for the zero-valent complex. The similarity in the infrared spectrum and the blue colour of the precipitate suggest that the tungsten(0) complex has oxidised to tungsten(IV). The blue colour is likely to be due to tungsten(IV).

The preparation of the complex fac-[W(CO)$_3$(NCCH$_2$\{3-SC$_4$H$_3$\})$_3$] was also attempted. The complex fac-[W(CO)$_3$(NCMe)$_3$] was prepared and three equivalents of thiophene-3-acetonitrile was added. Stirring for one hour produced a pale green powder, however the analysis did not conform with the complex [W(CO)$_3$(NCCH$_2$\{3-SC$_4$H$_3$\})$_3$], see Table 4.10. Recrystallisation of this complex proved to be very difficult.

4.6.2 Thiophene-3-Acetonitrile Complexes Of Molybdenum(0)

The preparation of the molybdenum(0) complexes containing thiophene-3-acetonitrile was conducted in a similar way to that of the analogous tungsten(0) complexes. The reaction of [Mo(CO)$_3$(η^6-C$_6$H$_3$(CH$_3$)$_3$)] with trimethylamine N-oxide and thiophene-3-acetonitrile yielded a dark blue intractable oil.

The reaction of fac-[Mo(CO)$_3$(NCMe)$_3$] with three equivalents of thiophene-3-acetonitrile gave a brown powder which analysed to be [Mo(CO)$_3$(NCCH$_2$\{3-SC$_4$H$_3$\})$_3$], see Table 4.10. The infrared spectrum of the complex showed the expected absorption bands of thiophene-3-acetonitrile and the characteristic carbonyl stretches, see Table 4.11.

4.6.3 Conclusions About Molybdenum(0) and Tungsten(0) Complexes Containing Thiophene-3-Acetonitrile

- It was possible to prepare the complex fac-[Mo(CO)$_3$(NCCH$_2$\{3-SC$_4$H$_3$\})$_3$] and to characterise it by elemental analysis and infrared spectroscopy.

- Attempts to prepare the corresponding tungsten(0) complex were not successful, leaving a pale precipitate which is probably a mixture of

132

products.

- The reaction between thiophene-3-acetonitrile and $[W(CO)_3(\eta^6\text{-arene})]$ yields a powder that does not analyse to be the complex $[W(CO)_2(NCCH_2\{3\text{-}SC_4H_3\})(\eta^6\text{-arene})]$, however from the infrared spectrum it may be concluded that some oxidised product is isolated.

Table 4.10 : Physical and Analytical Data for Molybdenum(0) and Tungsten(0) Complexes Containing Thiophene-3-Acetonitrile

Complex	Colour	%	C	H	N
$Mo(CO)_2(T)(A)$	(blue oil)	-	-	-	-
$Mo(CO)_3(T)_3$	brown	<10	45.6 (45.9)	3.1 (2.7)	7.4 (7.7)
$W(CO)_2(T)(A)$	dark green	<10	33.0 (38.1)	2.4 (2.5)	4.8 (3.2)
$W(CO)_3(T)_3$	pale green	<5	42.6 (39.6)	3.0 (2.4)	7.2 (2.2)

$(A) = (\eta^6\text{-}C_6H_3(CH_3)_3)$
$(T) = (NCCH_2\{3\text{-}SC_4H_3\})$
Calculated values in parentheses

Table 4.11 : Infrared Data for the Complex $[Mo(CO)_3(NCCH_2\{3\text{-}SC_4H_3\})_3]$

ν (cm^{-1})[a]	Bond
3016	C=C-H
2990	C-C-H
2024	C≡N
1903 1864 1824	C≡O
1502	C-S

[a] measured in solution as a thin film between NaCl plates

133

4.7 GENERAL CONCLUSIONS

This chapter has described an extensive series of investigations carried out on the reactions of various derivatives of thiophenes with complexes of molybdenum and tungsten in either the zero or +2 oxidation states. A number of conclusions may be drawn from the observations made.

- A thiophene moiety can be attached to a molybdenum(0) or tungsten(0) centre *via* an aryl linkage.

- The aryl-thiophene molecule can be synthesised by reacting the Grignard derivative of the arylbromide with 3-bromothiophene. This produces a mixture of unreacted 3-bromothiophene and the aryl-thiophene.

- The unpurified aryl-thiophene can be reacted with *fac*-$[M(CO)_3(NCMe)_3]$ {M = Mo or W} to give the thiophene-substituted zero-valent metal complex $[M(CO)_3(\eta^6$-aryl-thiophene)].

- The nitrile group in thiophene-3-acetonitrile provides a versatile anchor point to link with molybdenum or tungsten complexes.

- Attempts to attach thiophene-3-acetonitrile to molybdenum(0) and tungsten(0) complexes were not highly successful. This is due, in part, to the tendency for aerial oxidation of these zero-valent metal complexes to occur.

- The tungsten(II) complexes $[WI_2(CO)_3(NCMe)_2]$ and $[WI_2(CO)_3(L)(NCMe)]$ {L = PPh_3 or $AsPh_3$} will react with thiophene-3-acetonitrile to give the complexes $[WI_2(CO)_3(NCCH_2\{3-SC_4H_3\})_2]$ and $[WI_2(CO)_3(L)(NCCH_2\{3-SC_3H_4\})]$ respectively.

- The complexes $[WI_2(CO)_3(L)(NCCH_2\{3-SC_3H_4\})]$ {L = PPh_3 or $AsPh_3$} are highly insoluble. The complex $[WI_2(CO)_3(L)(NCCH_2\{3-SC_3H_4\})]$ {L = $P(OPh)_3$} is difficult to purify and is an oily solid.

- The complex $[WI_2(CO)_3(NCCH_2\{3-SC_4H_3\})_2]$ can undergo galvanostatic polymerisation to grow as a thin film on a platinum electrode, and electrochemical investigations can be carried out on the film and the monomeric complex.

Chapter Five

Experimental

5.1 INSTRUMENTATION

Elemental Analysis..........................	Carlo Erba MOD 1106 Elemental Analyser.
Infrared Spectroscopy....................	Perkin Elmer 1600 FTIR.
^{1}H, ^{13}C and ^{31}P NMR......................	Bruker AC/250 NMR Spectrometer. ^{1}H and ^{13}C referenced to tetramethyl silane. ^{31}P referenced to 85% H_3PO_4.
Fluorometry...................................	Perkin Elmer LS3
NIR / reflectance spectroscopy........	Beckman DK-2A Ratio Recording Spectrophotometer.
FAB mass spectroscopy...................	VG-Autospec Instrument. Cs^+ ions at 25 kilovolts bombarded onto sample dissolved in 3-nitrobenzyl alcohol matrix target (E.S.P.R.C. MS unit, Swansea).
GC-MS..	Finnegan 1020 GC-MS.
Cyclic voltammetry........................	Hi-Tek Instruments Waveform Generator. MK2A 1993 Potentiostat. Lloyd Instruments XY plotter.
Crystallographic Studies.................	Mo-K_α radiation using a MAR Research Image Plate System.
THG...	10 pps Q-switch Nd:YAG laser operating at 1064 nm with a pulse duration of 10 nanoseconds. Beam focussed by 300 nm lens. Third harmonic beam at 354.6 nm detected using a photon multiplier in connection with a photon counter linked to a personal computer.

136

5.2 GENERAL EXPERIMENTAL

All experiments were carried out using standard Schlenk line techniques under nitrogen

5.2.1 Preparation of the Metal Tricarbonyl Trisacetonitrile
fac-[M(CO)₃(NCMe)₃] {M = Metal = Mo or W} [60]

Metal hexacarbonyl (metal = Mo, 2.64 g, 10 mmoles; W, 3.52 g, 10 mmoles) was refluxed in 250 cm³ acetonitrile for (t) hours under nitrogen (Mo, t = 24; W, t = 72). The resulting bright yellow solution of *fac*-[M(CO)₃(NCMe)₃] is assumed to be in 100 % yield.

5.2.2 Preparation of the Metal Di-iodide Tricarbonyl Bisacetonitrile
[MI₂(CO)₃(NCMe)₂] {M = Mo or W} [62]
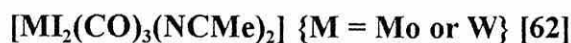
The metal hexacarbonyl (metal = Mo 2.64 g, 10 mmoles; W 3.52 g, 10 mmoles) was refluxed in 250 cm³ acetonitrile for (t) hours under nitrogen (Mo t = 24; W t = 72). The resulting solution was cooled to 0 °C and one equivalent of iodine, I₂ (2.54 g, 10 mmoles) was added. The mixture was stirred for twenty minutes at 0 °C and the solvent removed *in vacuo* to give in both cases a bright red powder of [MI₂(CO)₃(NCMe)₂] {M = Mo or W} in quantitative yield.

5.3 EXPERIMENTAL FOR CHAPTER TWO

5.3.1 Preparation of the Fluorescent Ligand, C₂₃H₁₇N₃O₂ [93]

To 4-cyanoacetophenone (4.35 g; 0.03 mole) in 20 cm³ ethanol was added 4-carboxybenzaldehyde (4.14 g; 0.03 mole). A solution of sodium hydroxide (1.80 g; 0.045 mole) in 10 cm³ water was added dropwise and the mixture stirred for three hours at room temperature. To the yellow mixture was added 5 M hydrochloric acid (ca. 20 cm³), with

cooling, until precipitation of a pale yellow solid was complete. The pale yellow precipitate of $C_{17}H_{11}NO_3$ was filtered off and dried.

Yield = 6.23 g, 72.1 %.

To glacial acetic acid (5 cm^3) was added the pale yellow product (2.21 g; 8 mmole) and the mixture heated over a water bath until the solid dissolved completely. To the deep orange red solution was added phenyl hydrazine (3.64 g; 0.02 mole) dropwise with rapid stirring and the mixture heated for three hours. The mixture was cooled and ethanol (5 cm^3) added. Further cooling in ice and the addition of ethanol and water yielded a bright yellow precipitate of $C_{23}H_{17}N_3O_2$. This was recrystallised from ethanol.

Yield = 1.70 g, 58.1 %

$C_{23}H_{17}N_3O_2$	Calc %	C : 75.2	H : 4.6
	Found %	C : 73.8	H : 4.2

5.3.2 Reaction of [Mo(CO)$_6$] with $C_{23}H_{17}N_3O_2$

To molybdenum hexacarbonyl (1.0 g; 3.7 mmole) in 100 cm^3 toluene was added one equivalent of the fluorescent ligand, $C_{23}H_{17}N_3O_2$ (1.39 g; 3.7 mmoles). The mixture was refluxed for four hours and the brown solution stored at 0 °C for a week. A brown powder precipitated which analysed to be [Mo(CO)$_5$($C_{23}H_{17}N_3O_2$)]. See Table 2.1 for analytical data.

Yield = 1.3 g, 58.7 %

5.3.3 Reaction of [W(CO)$_6$] with $C_{23}H_{17}N_3O_2$

To tungsten hexacarbonyl (1.0 g; 2.8 mmole) in 100 cm^3 toluene was added one equivalent of the fluorescent ligand, $C_{23}H_{17}N_3O_2$ (1.04 g; 2.8 mmoles). The mixture was refluxed for seven hours and the brown solution stored at 0 °C for a week. A yellow green powder was precipitated which did not analyse to be [W(CO)$_5$($C_{23}H_{17}N_3O_2$)].

138

5.3.4 Reaction of [MI$_2$(CO)$_3$(NCMe)$_2$] with C$_{23}$H$_{17}$N$_3$O$_2$

To a stirred solution of [MI$_2$(CO)$_3$(NCMe)$_2$] {M = Mo 0.67 g, 1.3 mmoles; M = W 0.78g, 1.3 mmoles) in dry degassed dichloromethane, was added two equivalents of C$_{23}$H$_{17}$N$_3$O$_2$ (0.95 g; 2.6 mmoles). The solution was stirred for 20 hours, filtered and the solvent removed to leave a brown powder. The product was recrystallised from dichloromethane and hexane. See Table 2.1 for analytical data.

Yield = [MoI$_2$(CO)$_3$(C$_{23}$H$_{17}$N$_3$O$_2$)$_2$]   0.73 g, 69.8 %

　　　　[WI$_2$(CO)$_3$(C$_{23}$H$_{17}$N$_3$O$_2$)$_2$]   0.77 g, 66.4 %

5.4 EXPERIMENTAL FOR CHAPTER THREE

5.4.1 Preparation of [WI$_2$(CO)$_3$(PPh$_3$)$_2$] [49]

To a solution of [WI$_2$(CO)$_3$(NCMe)$_2$] (0.5 g, 0.8 mmole) in 20 cm^3 dry, degassed CH$_2$Cl$_2$ under dinitrogen was added triphenylphosphine (0.44 g, 1.7 mmole). After the addition the reaction was left to stir for one minute. The solution was filtered and the solvent removed *in vacuo* to yield a dark yellow powder of [WI$_2$(CO)$_3$(PPh$_3$)$_2$].
Yield = 1.39 g, 80.3 %

C$_{39}$H$_{30}$O$_3$P$_2$WI$_2$　　　Calc %　　　C : 44.7 H : 2.9

　　　　　　　　　　Found %　　　C : 44.4 H : 2.7

5.4.2 Preparation of [WI$_2$(CO)$_3$(PEt$_3$)$_2$] [146]

To a suspension of [WI$_2$(CO)$_3$(NCMe)$_2$] (0.54 g, 0.9 mmole) in 50 cm^3 dry, degassed diethyl ether was added triethyl phosphine (1.79 cm^3, 1.8 mmole). Dry, degassed CH$_2$Cl$_2$ (30 cm^3) was added and the reaction stirred for 20 minutes. The yellow solution was filtered, the solvent was removed *in vacuo* and the product left under vacuum to dry. The

yellow solid was recrystallised from CH_2Cl_2 and hexane to give yellow-orange crystals of $[WI_2(CO)_3(PEt_3)_2]$.

Yield = 0.53 g, 78.2 %

Single crystals of $[WI_2(CO)_3(PEt_3)_2]$ were grown by dissolving the yellow-orange crystals in a mixture of CH_2Cl_2 and hexane (80:20) and storing the solution at 0 °C.

$C_{15}H_{24}O_3P_2WI_2$	Calc %	C : 37.8 H : 2.6
	Found %	C : 37.2 H : 2.3

5.4.3 Preparation of $[WI_2(CO)_3(AsPh_3)_2]$ [49]

To a stirred solution of $[WI_2(CO)_3(NCMe)_2]$ (0.5 g, 0.8 mmole) in dry, degassed CH_2Cl_2 (30 cm³) was added $AsPh_3$ (0.51 g, 1.7 mmole). After stirring for 3 minutes, the solution was filtered through Celite and the solvent removed *in vacuo*. The dark yellow, oily product was washed several times in hexane to give a yellow powder of $[WI_2(CO)_3(AsPh_3)_2]$.

Yield = 0.60 g, 64.3 %

$C_{39}H_{30}O_3As_2WI_2$	Calc %	C : 41.3	H : 2.6
	Found %	C : 40.1	H : 2.3

5.4.4 Preparation of $[WI_2(CO)_3(dppe)]$

To a suspension of $[WI_2(CO)_3(NCMe)_2]$ (0.6 g, 1.0 mmole) in 50 cm³ dry, degassed CH_2Cl_2 was added bis(diphenylphosphino)ethane (0.39 g, 1.0 mmole). After the addition, the reaction was left to stir for 10 minutes. The solution was filtered and the solvent removed *in vacuo*. The dark yellow powder was recrystallised from CH_2Cl_2 and hexane to give a yellow powder of $[WI_2(CO)_3(dppe)]$.

Yield = 0.76 g, 85.7 %

$C_{29}H_{24}O_3P_2WI_2$ Calc %   C : 37.8   H : 2.6

                     Found %   C : 37.6   H : 2.4

5.4.5 Preparation of [WI$_2$(CO)$_3$(dppm)]

The procedure for the preparation of [WI$_2$(CO)$_3$(dppe)] was followed [Section 5.4.4], but bis(diphenylphosphino)methane was used in place of dppe. A dark yellow powder of [WI$_2$(CO)$_3$(dppm)] was obtained .

Yield = 0.89 g, 83.1 %

$C_{28}H_{22}O_3P_2WI_2$ Calc %   C : 37.1   H : 2.4

                     Found %   C : 38.1   H : 2.1

5.4.6 Preparation of [WI$_2$(CO)(NCMe)(η^2-PhC$_2$Ph)$_2$] [147]

To a stirred solution of [WI$_2$(CO)$_3$(NCMe)$_2$] (0.5 g, 0.8 mmole) at 0 °C in CH$_2$Cl$_2$ for 10 minutes, was added diphenyl acetylene (0.3 g, 1.7 mmole). The solution was allowed to reach room temperature and stirred for 16 hours. The yellow solution was filtered and stored at 0 °C to give yellow crystals of [WI$_2$(CO)(NCMe)(η^2-PhC$_2$Ph)$_2$].

Yield = 55.9 g, 73.1 %

$C_{31}H_{23}ONWI_2$ Calc %   C : 43.1   H : 2.7

                 Found %   C : 42.5   H : 2.3

5.4.7 Preparation of [MoI$_2$(CO)$_3$(PPh$_3$)$_2$]

To a solution of [MoI$_2$(CO)$_3$(NCMe)$_2$] (1.0 g, 1.9 mmole) in dry, degassed CH$_2$Cl$_2$ was added triphenyl phosphine (1.02 g, 3.9 mmole). After stirring for one minute, the solution was filtered and the solvent removed *in vacuo*. The dark red oily solid was recrystallised from dichloromethane and hexane to give a dark red powder of [MoI$_2$(CO)$_3$(PPh$_3$)$_2$].

Yield = 1.45 g, 78.1 %

141

$C_{39}H_{30}O_3P_2MoI_2$ Calc %   C : 45.1   H : 3.1

Found %   C : 44.3   H : 2.7

5.4.8   Reaction of $Na_2(dmit)$ with $[WI_2(CO)_3(L)]$

To sodium metal (0.032 g, 1.4 mmole) dissolved in dry ethanol was added dmit thiol ester (0.28 g, 0.3 mmole) with stirring under a stream of dinitrogen. The mixture was left to stir for 45 minutes. The deep red solution was added dropwise with stirring to a solution of $[WI_2(CO)_3(L)]$ (0.7 mmole, L = (PPh_3)_2 0.72 g, (PEt_3)_2 0.52 g or (dppe) 0.63 g) in 10 cm^3 acetonitrile and the mixture stirred for 16 hours. The solvent was removed *in vacuo* and the dark, oily powder resolvated in dry, degassed CH_2Cl_2, filtered and the solvent removed. This procedure was repeated several times to ensure removal of sodium iodide. The oily product was recrystallised from dry dichloromethane and hexane to give $[W(dmit)(CO)_2(L)]$. See Table 3.2 for analytical data.

Yield = [W(dmit)(CO)_2 (PPh_3)_2]   0.52 g, 77.6 %

[W(dmit)(CO)_2 (PEt_3)_2]   0.37 g, 79.2 %

[W(dmit)(CO)_2 (dppe)]   0.28 g, 48.1 %

Single crystals of $[W(dmit)(CO)_2(PEt_3)_2]$ were grown by dissolving the product in a mixture of CH_2Cl_2 and hexane (ca.80:20) at 0 °C.

5.4.9   Reaction of $H_2(bdt)$ with $[WI_2(CO)_2(L)]$

To a stirred suspension of $H_2(bdt)$ (0.04 g, 0.3 mmole) in 5 cm^3 acetonitrile was added dropwise a solution of $WI_2(CO)_3(L)$ (0.3 mmole : L = (PPh_3)_2 0.29 g, (PEt_3)_2 0.21 g or (dppe) 0.26 g) in 10 cm^3 acetonitrile. The reaction was stirred for 16 hours, filtered and the solvent removed *in vacuo*. The product was recrystallised from acetonitrile to yield $[W(bdt)(CO)_2(L)]$. See Table 3.2 for analytical data.

Yield = [W(bdt)(CO)_2 (PPh_3)_2]   0.13 g, 46.9 %

[W(bdt)(CO)_2 (PEt_3)_2]   0.09 g, 49.9 %

[W(bdt)(CO)_2 (dppe)]   0.10 g, 43.5 %

Single crystals of $[W(bdt)(CO)_2(PEt_3)_2]$ and $[W(bdt)(CO)_2(dppe)]$ were grown from a solution in CH_2Cl_2 and hexane (ca. 80:20) and stored at 0 °C.

5.4.10 Reaction of $Na_2(mnt)$ with $[WI_2(CO)_3(L)]$

To a stirred solution of $[WI_2(CO)_3(L)]$ (2.7 mmole, L = $(PPh_3)_2$ 2.81 g, $(PEt_3)_2$ 2.04 g or (dppe) 2.47 g) in 10 cm^3 acetonitrile was added a solution of $Na_2(mnt)$ (0.5 g, 2.7 mmole) in 20 cm^3 acetonitrile, dropwise under dinitrogen. The mixture was stirred for four hours and the solvent removed *in vacuo*. The dark brown oily product was resolvated in dry dichloromethane, filtered and the solvent removed. This was repeated several times. The product was recrystallised from acetonitrile to give $[W(mnt)(CO)_2(L)]$. See Table 3.2 for analytical data.

Yield = $[W(mnt)(CO)_2 (PPh_3)_2]$ 1.59 g, 65.3 %

          $[W(mnt)(CO)_2 (PEt_3)_2]$ 1.17 g, 70.1 %

          $[W(mnt)(CO)_2 (dppe)]$ 1.44 g, 68.6 %

5.4.11 Reaction of $[WI_2(CO)_3(AsPh_3)_2]$ with $Na_2(dmit)$

The procedure for the reaction of $Na_2(dmit)$ with $[WI_2(CO)_3(L)]$ {L = $(PPh_3)_2$, $(PEt_3)_2$ or dppe} was followed (Section 5.4.8), except that the reactant was $[WI_2(CO)_3(AsPh_3)_2]$. The black brown powder did not analyse as $[W(dmit)(CO)_2(AsPh_3)_2]$. See Table 3.1 for analytical data.

5.4.12 Reaction of $[WI_2(CO)_3(dppm)]$ with $Na_2(dmit)$

The procedure for the reaction of $Na_2(dmit)$ with $[WI_2(CO)_3(L)]$ {L = $(PPh_3)_2$, $(PEt_3)_2$ or dppe} was followed (Section 5.4.8), except that the reactant was $[WI_2(CO)_3(dppm)]$. The brown powder did not analyse as $[W(dmit)(CO)_2(dppm)]$. See Table 3.1 for analytical data.

5.4.13 Reaction of [WI$_2$(CO)(NCMe)(η^2-PhC$_2$Ph)$_2$] with Na$_2$(dmit)

The procedure for the reaction of Na$_2$(dmit) with [WI$_2$(CO)$_3$(L)] {L = (PPh$_3$)$_2$, (PEt$_3$)$_2$ or dppe} was followed (Section 5.4.8), except that the reactant was [WI$_2$(CO)(NCMe)(η^2-PhC$_2$Ph)$_2$] (0.25 g, 0.3 mmole). The brown powder analysed as [W(dmit)(CO)(NCMe)(η^2-PhC$_2$Ph)$_2$] (see Table 3.1). However, on attempted recrystallisation the product decomposed to give a dark brown oily solid.

Yield = 0.06g, 23.1 %

[W(dmit)(CO)(NCMe)(η^2-PhC$_2$Ph)$_2$]	C	H	S	N
Calculated %	50.7	2.9	19.9	1.7
Before Recrystallisation %	59.2	3.2	10.9	0.0
After Recrystallisation %	7.2	2.8	10.2	0.0

5.4.14 Reaction of [MoI$_2$(CO)$_3$(PPh$_3$)$_2$] with Na$_2$(dmit)

The procedure for the reaction of Na$_2$(dmit) with [WI$_2$(CO)$_3$(L)] {L = (PPh$_3$)$_2$, (PEt$_3$)$_2$ or dppe} was followed (Section 5.4.8), except that the reactant was [MoI$_2$(CO)$_3$(PPh$_3$)$_2$]. The brown powder did not analyse as [Mo(dmit)(CO)$_2$(PPh$_3$)$_2$]. See Table 3.1 for analytical data.

5.4.15 Reaction of [WI$_2$(CO)$_3$(PPh$_3$)$_2$] with Cs$_4$(TTFS$_4$)

To a solution of CsOH.2H$_2$O (0.97 g, 5.2 mmole) in thf was added TTFS$_4$(EtCN)$_4$ (0.35 g, 0.6 mmole). After stirring for two hours the resulting red solution was added dropwise to a solution of [WI$_2$(CO)$_3$(PPh$_3$)$_2$] (1.41 g, 1.4 mmole) in acetonitrile. The mixture was stirred for a further four hours after which time the dark brown solution was filtered and the solvent removed *in vacuo*. The dark brown oily solid was resolvated in CH$_2$Cl$_2$, filtered and the solvent removed *in vacuo*. This procedure was repeated several times to ensure removal of caesium iodide. The solid was then recrystallised from CH$_2$Cl$_2$ and hexane to give a dark brown powder of [{W(CO)$_2$(PPh$_3$)$_2$}$_2$(TTFS$_4$)], see Table 3.2 for analytical data.

Yield = 0.48g, 18.4 %

5.4.16 Reaction of [WI$_2$(CO)$_3$(PPh$_3$)$_2$] with Na$_2$(tdas)

To a solution of sodium sulphite nonahydrate (0.46 g, 1.9 mmole) in 30 cm^3 degassed water was added 3,4-dichloro-1,2,5-thiadiazole (TDACl$_2$) (0.17 g, 0.9 mmole) and the solution stirred for 2 hours. After this time the yellow solution was added dropwise to a solution of [WI$_2$(CO)$_3$(PPh$_3$)$_2$] (1.0 g, 0.9 mmole) in 20 ml acetonitrile and the solution stirred for three hours. The solution developed into a opaque brown solution with a trace of a pale brown precipitate, see Table 3.1 for analytical data.

5.5   EXPERIMENTAL FOR CHAPTER FOUR

5.5.1   Preparation of the Grignard Products

To a solution of aryl bromide (10 mmole) in 70 cm^3 dry degassed diethyl ether was added dried magnesium turnings (0.36 g, 15 mmole) and one crystal of iodine. The mixture was gently refluxed under nitrogen for 2 hours.

Aryl Bromide	Amount(g)	mmoles
Benzyl Bromide	1.72	10
Phenylethyl Bromide	1.86	10
Phenoxybutyl Bromide	2.30	10

5.5.2   Reaction of Grignard Product with 3-Bromothiophene [137]

To a solution of 3-bromothiophene (1.64 g, 10 mmole) in 30 cm^3 dry degassed diethyl ether with nickel dichlorobis(diphenylphosphino)propane [NiCl$_2$(dppp)] as a catalyst, was added the Grignard product of the aryl bromide at 0 °C, with stirring, dropwise over an hour. The solution was allowed to reach room temperature and then refluxed for times varying from 90 minutes to two hours under nitrogen. After this time, the reaction was cooled in an ice bath and 50 cm^3 0.1 M HCl acid added slowly. The organic layer was extracted several times with diethyl ether, dried and the solvent removed on the rotary

evaporator.

Product	Appearance
(together with 3-bromothiophene)	
3-Benzylthiophene	golden brown liquid
Phenylethyl thiophene	golden brown liquid
Phenoxybutyl thiophene	brown liquid

5.5.3 Attempted Reaction of 3-Bromothiophene with Tungsten Tricarbonyl Trisacetonitrile

To the bright yellow solution of fac-[W(CO)$_3$(NCMe)$_3$] (prepared in $situ$) was added 3-bromothiophene (1.64 g, 10 mmoles) and the mixture was refluxed for 24 hours. After this time no reaction had taken place. This was confirmed by thin layer chromatography.

5.5.4 Preparation of Tungsten Tricarbonyl (η^6-mesitylene) [W(CO)$_3$(η^6-C$_6$H$_3$(CH$_3$)$_3$)] [42]

To the bright yellow solution of fac-[W(CO)$_3$(NCMe)$_3$] was added one equivalent of mesitylene (1.2 g, 10 mmoles) and the solution refluxed for 12 hours. After this time the solvent was removed in $vacuo$ to leave a brown powder which was shown by its infrared spectrum to have the correct absorption peaks for the complex [W(CO)$_3$(η^6-C$_6$H$_3$(CH$_3$)$_3$)]. The analysis showed it to be impure.

Yield = 1.24 g, 31.9 %

C$_{12}$H$_{12}$O$_3$W	Calc %	C : 37.1	H : 3.1
	Found %	C : 34.5	H : 2.1

5.5.5 Reaction of Tungsten Tricarbonyl Trisacetonitrile with Unsubstituted Arenes

To the bright yellow solution of fac-[W(CO)$_3$(NCMe)$_3$] was added one equivalent of the unsubstituted arene (toluene (C$_6$H$_5$CH$_3$) 0.92 g; phenoxybutane (C$_6$H$_5$OC$_4$H$_9$) 1.50 g) and

the solution refluxed for 12 hours. After this time the solution was filtered and the solvent removed *in vacuo* to yield the product [W(CO)$_3$(η^6-arene)].

Product	Colour	%	C	H
[W(η^6-C$_6$H$_5$CH$_3$)(CO)$_3$]	brown	30-40	31.0 (33.3)	2.8 (2.2)
[W(η^6-C$_6$H$_5$OC$_4$H$_9$)(CO)$_3$]	brown	20-30	29.6 (37.3)	2.4 (3.4)

Calculated values in parentheses

5.5.6 Reaction of the Arylthiophene / 3-Bromothiophene Mixture with Tungsten Tricarbonyl Trisacetonitrile

To the bright yellow solution of *fac*-[W(CO)$_3$(NCMe)$_3$] was added an excess of the mixture of 3-benzylthiophene and the aryl thiophene (benzylthiophene (C$_6$H$_5$CH$_2${3-SC$_4$H$_3$}) 5.22 g; phenoxybutylthiophene (C$_6$H$_5$OC$_4$H$_8${3-SC$_4$H$_3$}) 6.96 g) obtained from the reaction of the 3-bromothiophene with the Grignard product of the aryl bromide and the solution was refluxed for twelve hours. After this time the reaction mixture was filtered and the solvent removed *in vacuo*.

An excess of the arylthiophene / 3-bromothiophene mixture was deemed to be the comparable quantity of three equivalents of the arylthiophene (30 mmoles).

Product	Colour	%	C	H	S
[W(η^6-C$_6$H$_5$CH$_2${3-SC$_4$H$_3$})(CO)$_3$]	brown	15-20	36.6 (38.0)	3.3 (2.3)	6.4 (7.2)
[W(η^6-C$_6$H$_5$OC$_4$H$_8${3-SC$_4$H$_3$})(CO)$_3$]	brown	10-20	37.6 (42.1)	3.5 (3.1)	5.6 (6.6)

Calculated values in parentheses

147

5.5.7 Reaction of Molybdenum Tricarbonyl Trisacetonitrile with Thiophene-3-Acetonitrile

To the solution of *fac*-[Mo(CO)$_3$(NCMe)$_3$] (10 mmole) was added three equivalents of thiophene-3-acetonitrile (3.69 g, 30 mmoles). After stirring for one hour at room temperature, the solution was filtered and the solvent removed *in vacuo* to leave an oily brown solid. The solid was washed with hexane to give a brown powder that analysed to be [Mo(CO)$_3$(NCCH$_2${3-SC$_4$H$_3$})$_3$]. See Table 4.10. for physical and analytical data. Yield =0.39 g, 7.1 %

5.5.8 Reaction of Tungsten Tricarbonyl Trisacetonitrile with Thiophene-3-Acetonitrile

The same procedure was carried out as described in Section 5.5.7, except using [W(CO)$_3$(NCMe)$_3$]. The solvent was removed and a green oily solid was obtained. After washing the oily solid with hexane, a green powder of [W(CO)$_3$(NCCH$_2${3-SC$_4$H$_3$})$_3$] was obtained. See Table 4.10 for physical and analytical data.
Yield = 0.27 g, 4.2 %

5.5.9 Preparation of [M(CO)$_2$(NCCH$_2${3-SC$_4$H$_3$})(η^6-C$_6$H$_3$(CH$_3$)$_3$)]

To a solution of *fac*-[M(CO)$_3$(NCMe)$_3$] was added one equivalent of mesitylene (1.2 g, 10 mmoles). The mixture was stirred for 30 minutes and the solvent reduced to half the volume *in vacuo*. One equivalent of trimethylamine-N-oxide was added followed by one equivalent of thiophene-3-acetonitrile (1.23 g, 10 mmoles) and the reaction mixture stirred for 45 minutes. After this time the solution was filtered and the solvent removed *in vacuo*. In the case of molybdenum, a blue intractable oil was yielded. The analogous tungsten complex gave a dark green powder. See Table 4.10 for physical and analytical data
Yield = [W(CO)$_2$(NCCH$_2${3-SC$_4$H$_3$})(η^6-C$_6$H$_3$(CH$_3$)$_3$)]   0.57g, 8.9 %

5.5.10 Preparation of the Complexes [MI$_2$(CO)$_3$(L)(NCCH$_2${3-SC$_4$H$_3$})]

To a solution of [MI$_2$(CO)$_3$(NCMe)$_2$] {M = Mo or W} (1.5 g, 2.5 mmoles) in 15 cm^3 CH$_2$Cl$_2$ was added one equivalent of ligand L {L = PPh$_3$, AsPh$_3$ or P(OPh)$_3$} (2.5 mmoles) with stirring. After time (t) the solution was filtered into a second Schlenk tube containing one equivalent of thiophene-3-acetonitrile (0.31 g, 0.28 cm^3, 2.5 mmoles) in 10 cm^3 CH$_2$Cl$_2$ and stirred for 30 minutes. The solvent was removed *in vacuo* and to yield, in the case of the tungsten derivative, the yellow product [WI$_2$(CO)$_3$(L)(NCCH$_2${3-SC$_4$H$_3$})]. See Table 4.5 for physical and analytical data. The corresponding molybdenum compounds [MoI$_2$(CO)$_3$(L)(NCCH$_2${3-SC$_4$H$_3$})] were obtained as intractable oils.

Yield = [WI$_2$(CO)$_3$(PPh$_3$)(NCCH$_2${3-SC$_4$H$_3$})]   1.86 g, 82.2 %

[WI$_2$(CO)$_3$(AsPh$_3$)(NCCH$_2${3-SC$_4$H$_3$})]   1.85 g, 77.8 %

Ligand (L)	Amount (g)	mmoles	Time (t)
PPh$_3$	0.65	2.5	1 min.
AsPh$_3$	0.78	2.5	3 min.
P(OPh)$_3$	0.77	2.5	15 min.

5.5.11 Preparation of [WI$_2$(CO)$_3$(NCCH$_2${3-SC$_4$H$_3$})$_2$]

To a solution of [WI$_2$(CO)$_3$(NCMe)$_2$] (5.0 g, 20 mmoles) in 50 cm^3 of CH$_2$Cl$_2$ was added thiophene-3-acetonitrile (2.46 g, 40 mmoles). The solution was stirred in a warm water bath for 90 minutes and then for a further hour at room temperature. After this time the mixture was filtered and the solvent removed *in vacuo* to leave a brown oily product. This was resolvated in CH$_2$Cl$_2$ and diethyl ether and stored at 0 °C. The resulting dark red-brown crystalline powder analysed to be [WI$_2$(CO)$_3$(NCCH$_2${3-SC$_4$H$_3$})$_2$]. See Table 4.10 for physical and analytical data.

Yield = 1.36 g, 70.9 %

5.6   PREPARATION OF THIN FILMS FOR THG MEASUREMENT

To 5 cm³ chlorobenzene was added the host polymer polymethylmethacrylate (PMMA) and approximately 10% weight ratio of the sample with stirring and warming. Using a syringe fitted with a filter, a small amount of the solution was dropped onto a sterilised glass slide and spread into a film over the surface of the slide using the filter and by rocking the slide. The solvent was allowed to evaporate. Only one side of the slide was covered. Precipitation of the sample occurred in some cases and this was overcome by using a lower weight percent ratio of sample to polymer. The thickness of the films was calculate using the formula in Section 2.6.

Chapter Six

Conclusions and Scope for Further Work

6.1   GENERAL DISCUSSION AND CONCLUSIONS

The work embodied in this thesis has covered three general areas :

- Molybdenum and tungsten complexes containing a fluorescent ligand.
- Multisulphur donor complexes of tungsten.
- Molybdenum and tungsten complexes with a thiophene moiety.

These areas are linked by the fact that they are all centred around six or seven co-ordinate complexes of molybdenum or tungsten. Chapter 2 and Chapter 4 consider the metal in oxidation states of zero and +2, and Chapter 3 discusses the metal in the +2 oxidation state.

The prevailing question throughout this work was whether the presence of the transition-metal centre would affect the inherent overall properties of the ligand and *vice versa*. The secondary objective was how the properties of the complex would be affected by changing the oxidation state of the metal.

Firstly, the possibility of attaching the three types of ligand to the metal centre has been investigated. In general, it was found to be possible to synthesise most of the complexes proposed.

- The fluorescent ligand contained a nitrile group and as a result directly replaced the acetonitrile groups on the seven co-ordinate metal(II) complex, $[MI_2(CO)_3(NCMe)_2]$. It was also possible to react the fluorescent ligand with the zero-valent molybdenum species to give a six co-ordinate molybdenum(0) complex. However, it was not possible to synthesise the zero-valent tungsten product.
- The dianionic 1,2-dithiolenes were found to react with seven co-ordinate tungsten(II) complexes to eliminate the iodide ligands and form the six co-ordinate neutral tungsten(II) complexes. Attempts to synthesise the molybdenum analogues proved to be unsuccessful.

151

- A thiophene ring with a phenyl substituent reacted immediately with the complex *fac*-[W(CO)$_3$(NCMe)$_3$] to give a six co-ordinate complex with the metal in the zero-valent oxidation state.

- A thiophene was attached *via* a nitrile linkage directly to the metal centre. This worked very well with tungsten(II) complexes with direct substitution of existing nitrile groups taking place in the complex. In some cases, the thiophene can also be complexed to a zero-valent metal *via* a nitrile linkage although these complexes appear to be very susceptible to oxidation.

6.2 FLUORESCENT COMPLEXES OF MOLYBDENUM AND TUNGSTEN

The ligand, $C_{23}H_{17}N_3O_2$, exhibits a fluorescence of its own. It was thought that by combining the ligand with a redox-active centre, such as a tungsten or molybdenum complex, the fluorescence may become controllable by altering the oxidation state of the metal.

The complexes [Mo(CO)$_5$(C$_{23}$H$_{17}$N$_3$O$_2$)] and [MI$_2$(CO)$_3$(C$_{23}$H$_{17}$N$_3$O$_2$)$_2$] {M = Mo or W} discussed in Chapter 2 exhibited some fluorescence. However the complexation of the ligand with either a zero-valent molybdenum and tungsten centre or a complex with the metal in an oxidation state of +2 did not significantly affect the fluorescence. This implies that there is no noticeable perturbation of the energy levels in the ligand by the metal centre in either case. It was expected that by binding a metal centre that will readily accept electrons to a fluorescent ligand that is electron-rich it would alter the energies of molecular orbitals of the ligand, thereby altering the fluorescent properties. This is not the case, and therefore it can be concluded that the nitrile group, although a suitable linking group, does not communicate effectively between the ligand and the metal centre. This suggests that a linking group that will allow more communication between the two active parts of the molecule (the metal centre and the centre of the fluorescence) would lead to the effects of reduction and oxidation being transmitted through the fluorescence more effectively.

Additional studies on these complexes indicated that the complexes [Mo(CO)$_5$(C$_{23}$H$_{17}$N$_3$O$_2$)] and [MoI$_2$(CO)$_3$(C$_{23}$H$_{17}$N$_3$O$_2$)$_2$] show third harmonic generation effects and have measurable $\chi^{(3)}$ values. The fluorescent ligand, C$_{23}$H$_{17}$N$_3$O$_2$ also shows a THG signal, but the introduction of a molybdenum centre reduces the third-order effect.

The THG studies on the complex [MoI$_2$(CO)$_3$(C$_{23}$H$_{17}$N$_3$O$_2$)$_2$] were inconsistent and further measurements are being done to determine an accurate $\chi^{(3)}$ coefficient.

Further investigations into the third-order effects of these model complexes and other similar complexes such as [MoI$_2$(CO)$_3$(C$_{23}$H$_{17}$N$_3$O$_2$)(L)] {L = nitrile or phosphine} or even [MoX(CO)$_3$(C$_{23}$H$_{17}$N$_3$O$_2$)$_2$] {X = Cl$_2$, Br$_2$ or other anionic ligand} could give a valuable insight into the structural and other requirements for enhanced values of $\chi^{(3)}$. There is a wide range of fluorescent ligands similar to the one described in Chapter 2 and therefore there are many compounds similar that might be exploited before other systems such as anthracene-based ligands are even considered.

6.3   TUNGSTEN-1,2-DITHIOLENES

Dithiolene-type complexes have the potential to display many interesting solid state properties. The combination of two redox active centres i.e. a dithiolene ligand and a tungsten centre, was envisaged as having the potential to exhibit some unusual electrochemical properties or intermolecular interactions leading to bulk material properties.

The reaction between the seven co-ordinate tungsten complexes and the divalent dithiolene ligands resulted in the substitution of the iodide ligands and the elimination of a carbonyl group to leave a neutral six co-ordinate complex. The crystal structures of three of the products, [W(X)(CO)$_2$(L)] {X = bdt, L = (PEt$_3$)$_2$ or dppe; X = dmit, L = (PEt$_3$)$_2$} were determined together with the structure of the initial complex [WI$_2$(CO)$_3$(PEt$_3$)$_2$]. The reintroduction of a third carbonyl group can be effected by

153

bubbling carbon monoxide gas through a solution of the six co-ordinate complex, $[W(dmit)(CO)_2(PPh_3)_2]$. The product appears to be a dimer and is unstable, rapidly losing the third carbonyl group.

The first objectives of a continuation of this investigation should be steered towards an explanation of how the capping carbonyl in the original tungsten complex is lost when reacted with the dithiolene. A second question is how the carbonyl re-enters the complex when the complex is in solution saturated with carbon monoxide gas.

The direct implications of the results of Chapter 3 indicate that efforts should be channelled towards synthesising complexes such as $[A][WI(X)(CO)_y(L)]$ {A = anion; X = dithiolene; y = 1-3; L = monodentate or bidentate phosphine}. If the tungsten-dithiolene complex is a charged species, then the possibilities for exploitation of the redox properties are greatly expanded.

6.4 REDOX-ACTIVE METAL CENTRES ATTACHED TO THIOPHENES

Polythiophene can, under certain conditions, conduct electrical currents. The polymeric film has to be 'doped' which, from a simplistic point of view, involves introducing a charge into the film to allow the conduction of a current. Preparation of a molybdenum or tungsten complex containing a thiophene moiety should allow a polymeric film of thiophene to be synthesised with pendant redox-active transition metal groups attached. The oxidation of the transition metal groups should affect the properties of the polythiophene film and hence the conductivity of the film would be changed. Molybdenum and tungsten are easily oxidised or reduced, depending upon the initial oxidation state of the metal. In order for the redox properties of the metal complexes to be exploited with regard to altering the conductivity of the polythiophene, it would be necessary for the oxidations or reductions taking place to :

- be completely reversible
- result in a relatively air-stable complex

154

In Chapter 4, the complexes of tungsten(II) with thiophene attached *via* a nitrile group electropolymerise to give a film on an electrode. Electrochemical studies on $[WI_2(CO)_3(NCCH_2\{3\text{-}SC_4H_3\})_2]$ (Section 4.4) have shown the electrochemical process that take place in both the monomer and the polymer to be irreversible. The products of the electro-oxidation of the monomer appear to be unstable since a different reduction wave is observed in the cyclic voltammogram when the sweep is reversed. The irreversibility together with the instability of the product made any further investigation unproductive.

The complexes of molybdenum(0) and tungsten(0) with thiophene attached *via* an aryl group to the metal centre can be synthesised, however, these complexes are relatively unstable in air and decompose over time. These complexes were deemed unsuitable for further investigation.

These findings have helped to demonstrate the key requirements for the synthesis of redox-active complexes containing thiophene moieties. If this avenue of research were to be pursued in the future, then a more stable, reversible redox-active centre should be used, such as ferrocene.

6.5 CONCLUSIONS

In conclusion, this thesis has dealt with compounds which combine the redox chemistry of molybdenum and tungsten complexes with a variety of redox-active ligands. In some cases it is clear that there is no significant interaction between the metal centre and the 'active' ligand, so that the properties of the metal centre and ligand are unaffected on complexation. Some of the paths have provided a deeper insight into the chemistry of the systems involved. It is hoped that the work in this thesis goes some way to explaining the chemistry of these systems and that the knowledge gained may be of use in the future.

References

References

1. A. E. Underhill, *Chem. in Brit.*, London, 1991, 708.

2. P. Day, D. D. C. Bradley and D. Bloor, *Materials Chemistry for Electronics*, London : Royal Society, 1990.

3. J. Ferraris, D. O. Cowan, V. Walatka and J. H. Perlstein, *J. Am. Chem. Soc.*, 1973, **95**, 948.

4. P. W. Atkins, *Physical Chemistry*, 1987, 3rd. Ed., Oxford University Press, London.

5. M. R. Bryce, *Chem. in Brit.*, London, 1988, 781.

6. A. E. Underhill, *Comprehensive Coordination Chemistry*, 1987, **6**, 133.

7. R. E. Peierls, *Quantum Theory of Solids*, 1955, Oxford University Press, London.

8. D. Jerome, A. Mazaud, M. Ribault and K. Bechgaard, *J. Phys. Lett.*, 1980, **41**, L95.

9. A. Kobayashi, R. Kato, A. Miyamoto, T. Naito, H. Kobayashi, R. A. Clark and A. E. Underhill, *Chem. Lett.*, 1991, 2163.

10. K. Bange and T. Gambke, *Adv. Mater.*, 1990, **2**, 10.

11. H. G. Heller, *I.E.E. Proc.*, 1983, **130**, 209.

12. T. Gambke and B. Metz, *Glastech. Ber.*, 1989, **62**, 38.

13. M. Green and K. Kang, *Solid State Ionics 3 & 4*, 1981, 141 .

14. F. G. K. Bauke, K. Bange and T. Gambke, *Displays 10*, 1988, 179.

15. C. M. Lampert, *Sol. Energy Mater.*, 1984, **11**, 1.

16. H. Tamaki, Z. J. Zhong, N. Matsumoto, S. Kida, M. Koikawa, N. Achiwa, Y. Hashimoto and H. Okawa, *J. Am. Chem. Soc.*, 1992, **114**, 6974.

17. H. Okawa, N. Matsumoto, H. Tamaki and M. Ohba, *Mol. Cryst. Liq. Cryst.*, 1993, **233**, 257.

18. D. Gatteschi, *Adv. Mater.*, 1994, **6**, 644.

19. A. R. Dias, M. H. Garcia, M. P. Robalo, M. L. H. Green, K. K. Lai, A. J. Pulham, S. M. Klueber and G. Balavoine, *J. Organomet. Chem.*, 1993, **453**, 241.

20. A. S. Dhinsda, A. E. Underhill, S. Oliver and S. Kershaw, *J. Mater. Chem.*, 1995, **5**.

21.   K. L. Wolf, F. Frahm and H. Harms, *Z. Phys. Chem.*,1937, **B37**, 17.

22.   J-M. Lehn, *Angew. Chem., Int. Ed. Engl.*, 1988, **27**, 89.

23.   G. M. Whitesides, J. P. Mathias and C. T. Seto, *Science*, 1991, **254**, 1312.

24.   V. Goulle, Ph.D. Thesis, Strasbourg, France, 1992.

25.   L. R. Melby, *Inorg. Chem.*, 1969,**8**, 349.

26.   C. L. Rollinson, *Comprehensive Inorganic Chemistry*, 1973, **3**, 623.

27.   F. A. Cotton and G. Wilkinson, *Advanced Inorganic Chemistry*, 5th Ed., 804, Wiley Interscience.

28.   M. J. Wovkulich and J. D. Atwood, *Inorg. Synth.*, 1985, **23**, 37.

29.   H. Kunkely and A. Volger, *Organometallics*, 1992, **11**, 3172.

30.   W. Buchner and W. A Schenk, *Inorg. Chem.*, 1984, **23**, 132.

31.   F. R. Hartley (ed.), *Chemistry of Organophosphorus Compounds*, Wiley New York, 1990, **1**.

32.   O. J. Scherer, *Angew. Chem., Int. Ed. Engl.*, 1985, **24**, 924.

33.   M. Regitz and O. J. Scherer, *Multiple Bonds and Low Co-ordination in Phosphorus Chemistry*, G. Thierne Verlag, Germany, 1990.

34.   W. D. Covey and T. L Brown, *Inorg. Chem.*, 1973, **12**, 2820.

35.   F. A. Cotton, D. J. Darensbourg, S. Klein and B. W. S. Kolthammer, *Inorg. Chem.*, 1982, **21**, 2661.

36.   D. J. Darensbourg and C. J. Bischoff, *Inorg. Chem.*, 1993, **32**, 47.

37.   M. L. Boyles, D. V. Brown, D. A. Drake, C. K. Hostetler, C. K. Maves and J. A. Mosbo, *Inorg. Chem.*, 1985, **24**, 3126.

38.   G. M. Bancroft, L. Dignard-Bailey and R. D. Puddephatt, *Inorg. Chem.*, 1986, **25**, 3675.

39.   S. Woodward, *Comprehensive Organometallic Chemistry II*, 1995, **5**, 215.

40.   E. O. Fischer, K. Öfele, H. Essler, W. Fröhlich, J. Mortensen and W. Semmlinger, *Chem. Ber.*, 1958, **91**, 2763.

41.   E. O Fischer, K. Öfele, H. Essler, W. Fröhlich, J. Mortensen and W. Semmlinger, *Z. Naturforsch., Teil B.*, 1958, **13**, 458.

42.   R. B. King and A. Fronzaglia, *Inorg. Chem.*, 1966, **5**, 1837.

43.   J. T. Price and T. S. Sørenson, *Can. J. Chem.*, 1968, **46**, 515.

44. M. W. Anker, R. Colton and I. B. Tomkins, *Pure Appl. Chem.*, 1986, **18**, 23.

45. R. Colton, *Coord. Chem. Rev.*, 1971, **6**, 269.

46. M. G. B. Drew, *Prog. Inorg. Chem.*, 1977, **23**, 67.

47. M. Melník and P. Sharrock, *Coord. Chem. Rev.*, 1985, **65**, 49.

48. P. K. Baker, *Adv. Organomet. Chem.*, In Press, 1996.

49. H. L. Nigam and R. S. Nyholm, *Proc. Chem. Soc.*, 1957, 321.

50. A. C. Filippou and W. Grünleiter, *J. Organomet. Chem.*, 1990, **398**, 99.

51. S. C. Tripathi, S. C. Srivastava and R. P. Mani, *J. Organomet. Chem.*, 1976, **105**, 239.

52. S. C. Tripathi, S. C. Srivastava and A. K Shrimal, *Inorg. Chim. Acta*, 1976, **18**, 231.

53. S. C. Tripathi, S. C. Srivastava and D. P. Pandey, *Transition-Met. Chem.*, 1977, **2**, 52.

54. P. Umland and H. Varenkamp, *Chem. Ber.*, 1982, **115**, 3555.

55. P. Umland and H. Varenkamp, *Chem. Ber.*, 1982, **115**, 3565.

56. J. Lewis and R. Whyman, *J. Chem. Soc.*, 1965, 5486.

57. R. Colton and J. J. Howard, *Aus. J. Chem.*, 1970, **23**, 223.

58. J. A. Connor, G. K. McEwen and C. J. Rix, *J. Less-Chem Met.*, 1974, **36**, 204.

59. J. A. Connor, G. K. McEwen and C. J. Rix, *J. Chem. Soc., Dalton Trans.*, 1974, 589.

60. D. P. Tate, W. R. Knipple and J. M. Augl, *Inorg. Chem.*, 1962, **1**, 433.

61. A. D. Westland and N. Muriithi, *Inorg. Chem.*, 1972, **11**, 2971.

62. P. K. Baker, S. G. Fraser and E. M. Keys, *J. Organomet. Chem.*, 1986, **309**, 319.

63. M. G. B. Drew, P. K. Baker, E. M. Keys and S. G. Fraser, *Polyhedron*, 1988, **7**, 245.

64. P. K. Baker, M. B. Hursthouse, A. I. Karaulov, A. J. Lavery, K. M. A. Malik, D. J. Muldoon and A. Shawcross, *J. Chem. Soc., Dalton. Trans.*, 1994, 3493.

65. P. K. Baker, M. E. Harman, M. B. Hursthouse, A. I. Karaulov, A. J. Lavery, K. M. A. Malik, D. J. Muldoon and A. Shawcross, *J. Organomet. Chem.*, 1995, **494**, 205.

66. P. K. Baker and S. G. Fraser, *Transition-Met. Chem.*, 1987, **12**, 560.

67. P. K. Baker and S. G. Fraser, *Transition-Met. Chem.*, 1988, **13**, 284.

68. P. K. Baker and S. G. Fraser, *Inorg. Chem. Acta*, 1986, **116**, L1.

69. P. K. Baker, S. G. Fraser and M. G. B. Drew, *J. Chem. Soc., Dalton Trans.*, 1988, 2729.

70. P. K. Baker, K. R. Flower, H. M. Naylor and K. Voight, *Polyhedron*, 1993, **12**, 357.

71. P. K. Baker and S. G. Fraser, *Polyhedron*, 1987, **6**, 2081.

72. P. K. Baker, K. R. Flower and S. M. L. Thompson, *Transition. Met. Chem.*, 1987, **12**, 349.

73. P. K. Baker and S. G. Fraser, *J. Organomet. Chem.*, 1986, **299**, C23.

74. S. D. Harris, Ph.D. Thesis, University of Wales, 1995.

75. J. Kim and D. C. Rees, *Nature*, 1992, **360**, 553.

76. J. Kim and D. C. Rees, *Science*, 1992, **257**, 1677.

77. P. K. Baker, S. D. Harris, M. C. Durrant, D. L. Hughes and R. L. Richards, *J. Chem. Soc., Dalton Trans.*, 1994, 1401.

78. M. C. Durrant, D. L. Hughes, R. L. Richards, P. K. Baker and S. D. Harris, *J. Chem. Soc., Dalton Trans.*, 1992, 3399.

79. P. K. Baker, M. C. Durrant, B. Goerdt, S. D. Harris, D. L. Hughes and R. L. Richards, *J. Organomet. Chem.*, 1994, **469**, C22.

80. P. K. Baker and D. ap Kendrick, *Polyhedron*, 1991, **10**, 433.

81. P. K. Baker and S. G. Fraser, *Transition-Met. Chem.*, 1986, **11**, 273.

82. P. K. Baker, S. G. Fraser and D. ap Kendrick, *J. Chem. Soc., Dalton Trans.*, 1991, 131.

83. E. L. Muetterties and C. M. Wright, *Quart. Rev. Chem.*, 1967, **21**, 109.

84. D. K. Smith and H. W. Newkirk, *Acta Cryst.*, 1965, **18**, 983.

85. H. Barnighausen, H. Patow and H. P. Beck, *Z. Anorg. Allg. Chem.*, 1974, **40.**

86. A. P. de Silva and K. R. A. S. Sandanayake, *J. Chem. Soc., Chem. Commun.*, 1989, 1183.

87. A. P. de Silva and K. R. A. S. Sandanayake, *Tetrahedron Lett.*, 1991, **32**, 421.

88. A. P. de Silva, H. Q. N. Gunaratne and K. R. A. S. Sandanayake, *Tetrahedron*

Lett., 1990, **31**, 5193.

89.   A. P. de Silva, S. A. de Silva, A. S. Dissanayake and K. R. A. S. Sandanayake, *J. Chem. Soc.,Chem. Commun.*, 1989, 1054.

90.   A. P. De Silva and K. R. A. S. Sandanayake, *Angew. Chem., Int. Ed. Engl.*, 1990, **29**, 1173.

91.   A. P. De Silva, S. A. De Silva, A. S. Dissanayake and K. R. A. S. Sandandyake, *J. Chem. Soc., Chem. Commun.*, 1985, 1669.

92.   A. P. de Silva, H. Q. N. Gunaratne and C. P. McCoy, *Nature*, 1993, **364**, 42.

93.   Personal correspondence, A. P. de Silva.

94.   A. Yariv and R. A. Fisher, "Optical Phase Conjugation", Academic Press, Inc., 1983, 1.

95.   D. M. Pepper and Y. Yariv "Optical Phase Conjugation", Academic Press, Inc., 1983, 24.

96.   M. Sheik-Behae, A. A. Said and E. W. van Stryland, *Opt. Lett.*,1989, **14**, 955.

97.   C. S. Winter, S. R. Oliver, R. J. Manning, J. D. Rush, C. A. S. Hill and A. E. Underhill, *J. Mater. Chem.*, 1992, **2**, 443.

98.   NLO Human Capital and Mobility Network Meeting, Cambridge, 1994.

99.   A. R. Dias, M. H. Garcia, J. C. Rodrigues, J. C. Petersen, T. Bjørnholm and T. Geisler, *J. Mater. Chem.*, 1995, **5**, 1861.

100.   V. K. Shah and W. J. Brill, *Proc. Natl. Acad. Sci., U.S.A.*, 1990, **38**,1.

101.   H. B. Abrahamson, M. L. Freeman, M. B. Hussain and D. Van der Helm, *Inorg. Chem.*, 1984, **23**, 2286.

102.   R. Colton, G. R. Scollary and I. B. Tomkins, *Aust. J. Chem.*, 1968, **21**, 15.

103.   J. L. Templeton and B. C. Ward, *J. Am. Chem. Soc.*, 1980, **102**, 6560.

104.   M. Bonamico, G. Dessy and V. Fares, *J. Chem. Soc., Dalton Trans.*, 1977, 2315.

105.   R. E. D. Clarke, *Analyst*, 1936, **60**, 242.

106.   W. H. Mills and R. E. D. Clarke, *J. Chem. Soc.*, 1936, 175.

107.   G. Bähr and G. Schleitzer, *Chem. Ber.*, 1957, **88**, 438.

108.   G. N. Schrauzer and V. P. Mayweg, *J. Am. Chem. Soc.*, 1962, **84**, 3221.

109.   T. W. Gilbert Jnr. and E. B. Sandell, *J. Am. Chem. Soc.*, 1960, **82**, 1087.

110.   P. Cassoux, L. Valade, H. Kobayashi, A. Kobayashi, R. A. Clark and A. E.

Underhill, *Coord. Chem. Rev.*, 1991, **110**, 115.

111. R. B. King, *J. Am. Chem. Soc.*, 1963, **85**, 1587.

112. J. A. McCleverty, T. A. James, E. J. Wharton and C. J. Winscom, *J. Chem. Soc.,
Chem. Commun.*, 1966, 677.

113. J. Locke and J. A. McCleverty, *Inorg. Chem.*, 1966, **5**, 1157.

114. H. W. Baird and B. M. White, *J. Am. Chem. Soc.*, 1966, **88**, 4744.

115. J. R. Knox and C. K. Prout, *J. Chem. Soc., Chem. Commun.*, 1966, 1277.

116. R. Eisenberg, *Prog. Inorg. Chem.*, 1970, **12**, 295.

117. R. Colton and J. Kevekordes, *Aust. J. Chem.*, 1982, **35**, 895.

118. B. Mann, *Adv. Organomet. Chem.*, 1974, **12**, 135.

119. P. S. Braterman, D. W. Milne, E. W. Randall and E. Rosenberg, *J. Chem. Soc.,
Dalton Trans.*, 1973, 1027.

120. T. Ito, H. Shirakawa and S. Ikeda, *J. Polym. Sci., Polym. Chem. Ed.*, 1974, **12**,
11.

121. C. K. Chiang, Y. W. Park, A. J. Heeger, H. Shirakawa, E. J. Louis and A. G.
McDiarmid, *Phys. Rev. Lett.*, 1977, **39**, 1098.

122. J. Roncali, *Chem. Rev.*, 1992, **92**, 711.

123. W. Steinkopt, R. Leitsmann and K. H. Hofmann, *Liebigs Ann. Chem.*, 1941, **546**,
180.

124. H. J. Kooreman and H. Wynberg, *Recl. Trav. Chim. Pays-Bas*, 1967, **86**, 37.

125. H. Wynberg and J. Metselaar, *J. Synth. Commun.*, 1984, **14**, 1.

126. J. Kagan and S. Arora, *Tetrahedron Lett.*, 1983, **24**, 4043.

127. A. Berlin, G. A. Pagani and F. Sannicolo, *J. Chem. Soc., Chem. Commun.*, 1986,
1663.

128. T. Yamamoto, K. Sanechika and A. J. Yamamoto, *J. Polym. Sci., Polym. Lett.
Ed.*, 1980, **18**, 9.

129. J. W. P. Lin and L. P. Dudek, *J. Polym. Sci.*, 1980, **18**, 2869.

130. D. D.Cunningham, L. Laguren-Davidson, H. B. Mark, C. V. Pharm and H.
Zimmer, *J. Chem. Soc., Chem. Commun.*, 1987, 1021.

131. G. Zotti and G. Schiavon, *J. Electroanal. Chem.*, 1984, **163**, 395.

132. Z. Xu, G. Horowitz and F. Garnier, *J. Electroanal. Chem.*, 1988, **246**, 467.

133. A. F. Diaz, *Chem. Scr.*, 1981, **17**, 142.

134. G. Tourillon and F. Garnier, *J. Electroanal. Chem.*, 1985, **135**, 173.

135. R. J. Waltman and J. Bargon, *Can. J. Chem.*, 1986, **64**, 76.

136. S. Hotta, T. Hosaka and W. Shimotsuma, *J. Chem. Phys.*, 1984, **80**, 954.

137. M. Lemaire, R. Garreau, D. Delabouglise, J. Roncali, H. K. Youssoufi and F. Garnier, *New J. Chem.*, 1990, **14**, 359.

138. M. Sato, S. Tanaka and K. Kaeriyama, *J. Chem. Soc., Chem. Commun.*, 1986, 873.

139. M. Lemaire, J. Roncali, F. Garnier, R. Garreau and E. Hannecart, French Pat. 86.04744, 4.4.86.

140. K. Y. Jen, G. G. Miller and R. L. Elsenbaumer, *J. Chem. Soc., Chem. Commun.*, 1986, 1346.

141. J. Grimshaw and S. D. Perera, *J. Electroanal. Chem.*, 1990, **278**, 287.

142. P. Baüerle and K. U. Gaudl, *Adv. Mater.*, 1990, **2**, 185.

143. D. Ofer, R. M. Crooks and M. S. Wrighton, *J. Am. Chem. Soc.*, 1990, **112**, 7869.

144. M. R. Bryce, A. D. Chissel, J. Gopal, P. Kathirgamanathan and D. Parker, *Synth. Met.*, 1991, **39**, 397.

145. P. K. Baker, M. G. B. Drew, S. J. Edge and S. D. Ridyard, *J. Organomet. Chem.*, 1991, **409**, 207.

146. Personal correspondence, A. I. Clark.

147. E. M. Armstrong, P. K. Baker and M. G. B. Drew, *Organometallics*, 1988, **7**, 319.

Appendix One

$$[WI_2(CO)_3(PEt_3)_2]$$

$$[WI_2(CO)_3(PEt_3)_2]$$
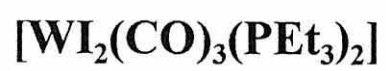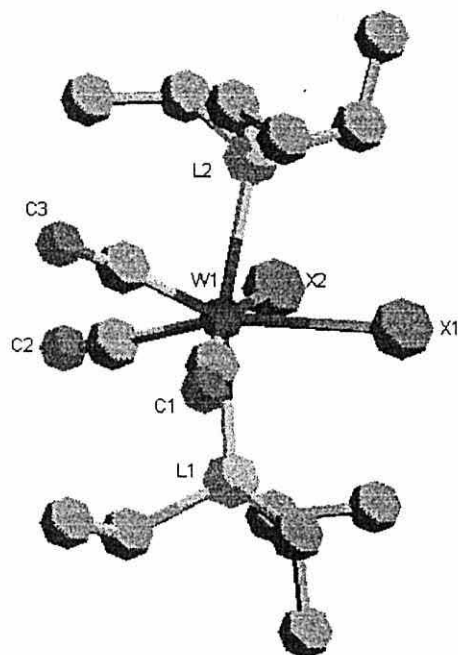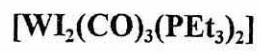
Appendix 1

THE CRYSTAL DATA AND STRUCTURE REFINEMENT FOR

$WI_2(CO)_3(PEt_3)_2$
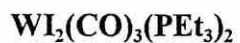
EMPIRICAL FORMULA	$C_{15}H_{27}I_2O_3P_2W$
FORMULA WEIGHT	754.96
TEMPERATURE	293 (2) K
WAVELENGTH	0.71070 Å
CRYSTAL SYSTEM	monoclinic
SPACE GROUP	P21/c
UNIT CELL DIMENSIONS	a = 14.907 (7) Å
	b = 10.799 (7) Å
	c = 14.645 (7) Å
	β = 104.100 (10) °
VOLUME	2287 (2) Å^3
Z	4
DENSITY (CALCULATED)	2.193 Mg/m^3
ABSORPTION COEFFICIENT	7.901 mm^{-1}
F (000)	1404
Θ RANGE FOR DATA COLLECTION	2.37 to 23.82 °
INDEX RANGES	$-16 \leq h \leq 16$
	$0 \leq k \leq 12$
	$-16 \leq l \leq 16$
R	0431

ATOMIC CO-ORDINATES (x 10⁴)

Equivalent Displacement Parameters (Å^2 x 10^3) for 1

U(eq) = ⅓ of trace of orthogonalised U_{ij} tensor

ATOM	x	y	z	U(eq)
W (1)	2603(1)	118(1)	3162(1)	30(1)
I (1)	1823(1)	-1173(1)	4083(1)	46(1)
I (2)	1305(1)	-439(1)	1421(1)	49(1)
C (11)	1748 (12)	3195(14)	3688(14)	64(4)
C (12)	2691(16)	3598(18)	4304(16)	87(6)
C (13)	292(11)	1642(15)	2865(12)	63(4)
C (14)	-304(11)	486(17)	2959(15)	75(5)
C (15)	1256(11)	1280(16)	4805(10)	56(4)
C (16)	553(12)	2117(16)	5119(11)	65(4)
P (2)	3383(2)	-1717(3)	2549(2)	37(1)
C (21)	2713(11)	-3103(14)	2308(15)	66(5)
C (22)	3150(14)	-4196(19)	2028(18)	90(7)
C (23)	3658(12)	-1473(16)	1443(11)	62(4)
C (24)	4254(19)	-418(19)	1323(16)	90(6)
C (25)	4479(8)	-2163(18)	3290(10)	59(4)
C (26)	4471(13)	-2517(20)	4259(12)	74(5)
C (1)	3161(7)	483(13)	4509(9)	39(3)
O (32)	3512(8)	691(11)	5270(7)	64(3)
C (2)	2640(10)	1623(11)	2377(10)	45(3)
O (34)	2662(10	2435(10)	1944(7)	67(3)
C (35)	3855(7)	599(9)	3294(7)	27(2)
O (36)	4605(7)	982(12)	3422(8)	68(3)

BOND LENGTHS (Å)

BOND	BOND LENGTH (Å)
W (1) - C (35)	1.901(10)
W (1) - C (1)	1.985(13)
W (1) - C (2)	1.999(13)
W (1) - P (2)	2.568(3)
W (1) - P (1)	2.581(3)
W (1) - I (1)	2.847(61)
W (1) - I (2)	2.864(31)
P (1) - C (11)	1.79(2)
P (1) - C (15)	1.80(2)
P (1) - C (13)	1.82(2)
C (11) - C (12)	1.54(3)
C (13) - C (14)	1.56(3)
C (15) - C(16)	1.54(2)
P (2) - C (21)	1.786(14)
P (2) - C (23)	1.78(2)
P (2) - C (25)	1.793(13)
C (21) - C (22)	1.45(2)
C (23) - C (24)	1.48(3)
C (25) - C(26)	1.47(2)
C (1) - O (32)	1.13(2)
C (2) - O (34)	1.09(2)
C (35) - O (36)	1.16(2)

BOND ANGLES (degrees)

ATOMS	ANGLE
C (35) - W (1) - C (1)	71.4(5)
C (35) - W (1) - C (2)	70.9(5)
C (1) - W (1) - C (2)	110.3(5)
C (35) - W (1) - P (2)	74.3(3)
C (1) - W (1) - P (2)	112.6(4)
C (2) - W (1) - P (2)	110.4(4)
C (35) - W (1) - P (1)	120.9(3)
C (1) - W (1) - P (1)	75.3(3)
C (2) - W (1) - P (1)	77.1(4)
P (2) - W (1) - P (1)	164.85(10)
C (35) - W (1) - I (1)	130.7(3)
C (1) - W (1) - I (1)	78.0(4)
C (2) - W (1) - I (1)	158.0(4)
P (2) - W (1) - I (1)	83.32(9)
P (1) - W (1) - I (1)	85.87(8)
C (35) - W (1) - I (2)	125.5(3)
C (1) - W (1) - I (2)	162.8(3)
C (2) - W (1) - I (2)	76.5(4)
P (2) - W (1) - I (2)	78.01(8)
P (1) - W (1) - I (2)	91.49(8)
I (1) - W (1) - I (2)	90.34(4)
C (11) - P (1) - C (15)	104.7(8)
C (11) - P (1) - C (13)	100.3(8)
C (15) - P (1) - C (13)	105.6(8)
C (11) - P (1) - W (1)	114.6(5)
C (15) - P (1) - W (1)	114.6(5)
C (13) - P (1) - W (1)	115.5(5)
C (12) - C(11) - P (1)	118.7(13)
C (14) - C (13) - P (1)	112.7(12)
C (16) - C (15) - P (1)	116.2(12)
C (21) - P (2) - C (23)	100.7(8)

ATOMS	ANGLE
C (21) - P (2) - C (25)	106.1(9)
C (23) - P (2) - C (25)	102.2(7)
C (21) - P (2) - W (1)	115.9(5)
C (23) - P (2) - W (1)	115.3(6)
C (25) - P (2) - W (1)	114.8(6)
C (22) - C (21) - P (2)	118.0(12)
C (24) - C (23) - P (2)	119.9(13)
C (26) - C (25) - P (2)	115.6(11)
O (32) - C (1) - W (1)	177.3(11)
O (34) - C (2) - W (1)	179.3(12)
O (36) - C (35) - W (1)	173.9(10)

Appendix Two

[W(dmit)(CO)$_2$(PEt$_3$)$_2$]

[W(dmit)(CO)₂(PEt₃)₂]
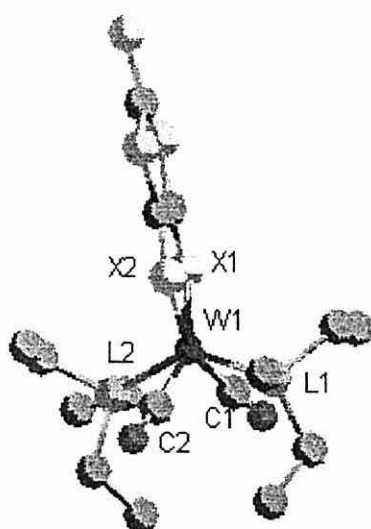
APPENDIX 2

THE CRYSTAL DATA AND STRUCTURE REFINEMENT FOR

$W(dmit)(CO)_2(PEt_3)_2$

EMPIRICAL FORMULA	$C_{17} H_{30} O_2 P_2 S_6 W$
FORMULA WEIGHT	673.59
TEMPERATURE	293 (2) K
WAVELENGTH	0.71070 Å
CRYSTAL SYSTEM	triclinic
SPACE GROUP	P-1
UNIT CELL DIMENSIONS	a = 11.117 Å
	b = 12.776 Å
	c = 17.901 Å
	α = 91.95 °
	β = 91.09 °
	γ = 94.06 °
VOLUME	2534 Å^3
Z	4
DENSITY (CALCULATED)	1.766 Mg/m^3
ABSORPTION COEFFICIENT	5.127 mm^{-1}
F (000)	1332
ϴ RANGE FOR DATA COLLECTION	5.46 to 24.72 °
INDEX RANGES	-13 ≤ h ≤ 12
	-14 ≤ k ≤ 14
	0 ≤ l ≤ 20
R	0547

ATOMIC CO-ORDINATES (x 10⁴)

Equivalent Displacement Parameters (Å² x 10³) for l

$$U(eq) = \frac{1}{3} \text{ of trace of orthogonalised } U_{ij} \text{ tensor}$$

ATOM	x	y	z	U(eq)
W (1)	1478(1)	1809(1)	1292(1)	31(1)
P (1)	-589(4)	1668(3)	1770(2)	35(1)
C (111)	-1755(25)	960(24)	1167(16)	74(8)
C (112)	-2999(24)	818(38)	1408(41)	148(28)
C (113)	-1283(18)	2876(13)	2049(12)	45(5)
C (114)	-1513(22)	3652(15)	1423(15)	59(6)
C (115)	-598(21)	960(18)	2617(13)	58(6)
C (116)	192(27)	1387(17)	3234(14)	59(6)
S (2)	3191(4)	1214(3)	1927(3)	45(1)
C (13)	3119(15)	-127(11)	1709(10)	36(4)
S (141)	2460(4)	-1949(3)	1084(3)	47(1)
S (1)	1110(4)	-2 (3)	897(3)	41(1)
C (14)	2327(17)	-588(12)	1272(10)	42(5)
S (131)	4284(4)	-870(3)	2045(3)	49(1)
C (15)	3790(16)	-2051(11)	1592(12)	43(5)
S (16)	4437)6)	-3135(4)	1709(4)	69(2)
P (2)	2954(4)	3029(3)	699(3)	39(1)
C (121)	4129(21)	3678(18)	1305(15)	61(7)
C (122)	5190(22)	4277(22)	982(19)	73(8)
C (123)	2461(18)	4084(14)	146(11)	41(4)
C (124)	1766(38)	4878(22)	583(28)	105(15
C (125)	3734(34)	2332(20)	-16(19)	76(8)
C (126)	4414(74)	1541(52)	80(52)	162(34)
C (2)	1582(17)	3009(16)	2027(11)	46(5)
O (17)	1667(18)	3659(12)	2476(10)	70(5)
C (1)	548(23)	2235(16)	432(12)	56(6)
O (18)	-3(17)	2414(15)	-96 (10)	72(6)
W (2)	1675(1)	3457(1)	6258(1)	32(1)
P (21)	-354(4)	3295(3)	6781(2)	37(1)

ATOM	x	y	z	U(eq)
C (211)	-1545(19)	3872(17)	6264(11)	49(5)
C (212)	-2772(20)	3855(21)	6602(16)	67(7)
C (213)	-1040(17)	1985(15)	7028(14)	51(5)
C (214)	-1315(25)	1256(23)	6342(23)	85(11)
C (215)	-375(22)	4005(16)	7723(11)	55(6)
C (216)	406(25)	3593(18)	8259(14)	57(6)
P (22)	3111(4)	2395(3)	5589(3)	43(1)
C (221)	2513(20)	1215(19)	5064(12)	62(7)
C (222)	1896(26)	363(19)	5520(20)	73(8)
C (223)	4317(16)	1905(11)	6164(10)	38(4)
C (224)	5290(23)	1435(22)	5790(22)	92(12)
C (225)	3843(29)	3163(19)	4836(23)	82(11)
C (226)	3180(60)	3691(46)	4419(28)	114(17)
S (23)	1212(4)	5160(3)	5856(3)	44(1)
C (23)	2389(15)	5993(11)	6181(10)	35(4)
S (231)	2477(4)	7330(3)	5974(3)	44(1)
S (24)	3401(4)	4405(3)	6849(3)	45(1)
C (24)	3287(15)	5702(12)	6613(10)	35(4)
S (241)	4384(4)	6677(3)	6907(3)	45(1)
C (25)	3800(18)	7689(12)	6459(11)	43(4)
S (25)	4416(6)	8901(4)	6493(4)	65(2)
C (27)	685(15)	2864(14)	5421(12)	45(5)
O (27)	116(15)	2567(14)	4879(9)	67(5)
C (26)	1903(17)	2348(15)	6943(13)	49(6)
O (26)	2013(16)	1699(12)	7375(10)	64(5)

BOND LENGTHS (Å)

BOND	BOND LENGTH (Å)
W (1) - C (1)	1.95(2)
W (1) - C (2)	1.98(2)
W (1) - S (2)	2.384(3)
W (1) - S (1)	2.400(4)
W (1) - P (2)	2.462(5)
W (1) - P (1)	2.464(5)
P (1) - C (115)	1.79(2)
P (1) - C (113)	1.83(2)
P (1) - C (111)	1.84(3)
C (111) - C (112)	1.46(6)
C (113) - C (114)	1.55(3)
C (115) - C (116)	1.46(4)
S (2) - C (13)	1.739(14)
C (13) - C (14)	1.27(2)
C (13) - S (131)	1.768(12)
S (141) - C (15)	1.74(2)
S (141) - C (14)	1.777(14)
S (2) - C (14)	1.728(13)
S (131) - C (15)	1.74(2)
C (15) - S (16)	1.623(13)
P (2) - C (125)	1.81(3)
P (2) - C (123)	1.81(2)
P (2) - C (121)	1.82(2)
C (121) - C (122)	1.50(4)
C (123) - C (124)	1.52(5)
C (125) - C (126)	1.32(6)
C (2) - O (17)	1.13(2)
C (1) - O (18)	1.16(2)
W (2) - C (26)	1.93(2)
W (2) - C (27)	1.94(2)
W (2) - S (23)	2.401(3)

BOND	BOND LENGTH (Å)
W (2) - S (24)	2.403(4)
W (2) - P (21)	2.457(5)
W (2) - P (22)	2.468(4)
P (21) - C (211)	1.81(2)
P (21) - C (213)	1.86(2)
P (21) - C (215)	1.89(2)
C (211) - C (212)	1.50(3)
C (213) - C (214)	1.53(4)
C (215) - C (216)	1.42(3)
P (22) - C (221)	1.83(2)
P (22) - C (223)	1.833(14)
P (22) - C (225)	1.86(3)
C (221) - C (222)	1.52(5)
C (223) - C (224)	1.44(3)
C (225) - C (226)	1.28(5)
S (23) - C (23)	1.71(2)
C (23) - C (24)	1.33(2)
C (23) - S (231)	1.757(14)
S (231) - C (25)	1.72(2)
S (24) - C (24)	1.74(2)
C (24) - S (241)	1.74(2)
S (241) - C (25)	1.704(14)
C (25) - S (25)	1.65(2)
C (27) - O (27)	1.18(3)
C (26) - O (26)	1.16(3)

BOND ANGLES (degrees)

ATOMS	ANGLES
C (1) - W (1) - P (2)	78.5(8)
C (2) - W (1) - P (2)	78.9(7)
S (2) - W (1) - P (2)	84.8(2)
S (1) - W (1) - P (2)	123.3(2)
C (1) - W (1) - P (1)	78.5(8)
C (2) - W (1) - P (1)	79.9(6)
S (2) - W (1) - P (1)	124.4(2)
S (1) - W (1) - P (1)	86.02(14)
P (2) - W(1) - P (1)	142.42(12)
C (115) - P (1) - C (113)	102.7(9)
C (115) - P (1) - C (111)	105.0(2)
C (113) - P (1) - C (111)	103.3(10)
C (115) - P (1) - W (1)	109.0(7)
C (113) - P (1) - W (1)	118.55(8)
C (111) - P (1) - W (1)	116.9(10)
C (112) - C (111) - P (1)	121.0(3)
C (114) - C (113) - P (1)	117.0(2)
C (116) - C (115) - P (1)	118.0(2)
C (13) - S (13) - W (1)	104.0(5)
C (14) - C (13) - S (13)	123.5(10)
C (14) - C (13) - S (131)	117.7(10)
S (13) - C (13) - S (131)	118.6(9)
C (15) - S (141) - C (14)	97.1(7)
C (14) - S (14) - W (1)	103.4(6)
C (13) - C (14) - S (14)	124.6(11)
C (13) - C (14) - S (141)	116.4(10)
S (14)- C (14) - S (141)	119.0(10)
C (15) - S (131) - C (13)	96.8(7)
S (16) - C (15) - S (141)	124.9(10)
S (16) - C (15) - S (131)	122.9(9)
S (141) - C (15) - S (131)	111.9(7)

ATOMS	ANGLES
C (125) - P (2) - C (123)	98.7(12)
C (125) - P (2) - C (121)	106.0(2)
C (123) - P (2) - C (121)	103.2(9)
C (125) - P (2) - W (1)	109.6(11)
C (123) - P (2) - W (1)	120.8(7)
C (121) - P (2) - W (1)	116.7(9)
C (122) - C (121) - P (2)	121.0(2)
C (124) - C (123) - P (2)	114.0(2)
C (126) - C (125) - P (2)	127.0(5)
O (17) - C (2) - W (1)	176.2(13)
O (18) - C (1) - W (1)	175.0(2)
C (26) - W (2) - C (27)	107.8(8)
C (26) - W (2) - S (23)	157.8(6)
C (27) - W (2) - S (23)	87.5(5)
C (26) - W (2) - S (24)	87.7(6)
C (27) - W (2) - S (24)	155.7(6)
S (23) - W (2) - S (24)	83.78(12)
C (26) - W (2) - P (21)	80.9(6)
C (27) - W (2) - P (21)	77.1(6)
S (23) - W (2) - P (21)	87.25(14)
S (24) - W (2) - P (21)	125.0(2)
C (26) - W (2) - P (22)	77.8(6)
C (27) - W (2) - P (22)	78.4(5)
S (23) - W (2) - P (22)	122.0(2)
S (24) - W (2) - P (22)	87.0(2)
P (22) - W (2) - P (21)	140.55(14)
C (211) - P (21) - C (213)	104.0(10)
C (211) - P (21) - C (215)	102.6(9)
C (213) - P (21) - C (215)	99.8(11)
C (211) - P (21) - W (2)	117.0(8)
C (213) - P (21) - W (2)	120.1(6)
C (215) - P (21) - W (2)	110.8(9)

ATOMS	ANGLES
C (212) - C (211) - P (21)	118.0(2)
C (214) - C (213) - P (21)	113.0(2)
C (216) - C (215) - P (21)	112.7(12)
C (221) - P (22) - C (223)	102.6(7)
C (221) - P (22) - C (225)	101.0(2)
C (223) - P (22) - C (225)	107.3(12)
C (221) - P (22) - W (2)	118.1(7)
C (223) - P (22) - W (2)	115.9(6)
C (225) - P (22) - W (2)	110.2(7)
C (222) - C (221) - P (22)	116.0(2)
C (224) - C (223) - P (22)	118.0(2)
C (226) - C (225) - P (22)	118.0(3)
C (23) - S (23) W (2)	105.1(4)
C (24) - C (23) - S (23)	123.9(12)
C (24) - C (23) - S (231)	114.9(14)
S (23) - C (23) - S (231)	121.1(8)
C (25) - S (231) - C (23)	97.4(7)
C (24) - S (24) - W (2)	105.0(6)
C (23) - C (24) - S (24)	122.0(2)
C (23) - C (24) - S (241)	116.9(13)
S (24) - C (24) - S (241)	121.0(8)
C (25) - S (241) - C (24)	97.3(8)
S (25) - C (25) - S (241)	123.9(12)
S (25) - C (25) - S (231)	122.6(9)
S (241) - C (25) - S (231)	113.4(10)
O (27) - C (27) - W (2)	175.0(2)
O (26) - C (26) - W (2)	177.0(2)

Appendix Three

$[W(bdt)(CO)_2(PEt_3)_2]$

[W(bdt)(CO)$_2$(PEt$_3$)$_2$]
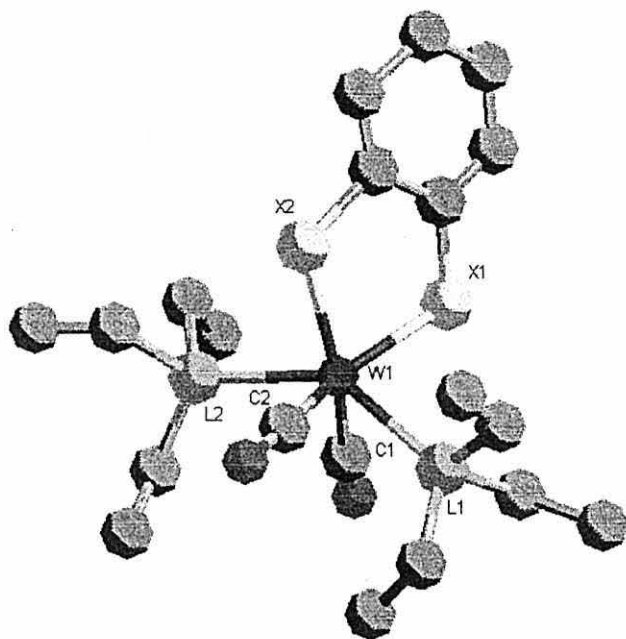
APPENDIX 3

THE CRYSTAL DATA AND STRUCTURE REFINEMENT FOR $W(bdt)(CO)_2(PEt_3)_2$

EMPIRICAL FORMULA	$C_{20} H_{37} O_2 P_2 S_2 W$
FORMULA WEIGHT	309.70
TEMPERATURE	293 (2) K
WAVELENGTH	0.71070 Å
CRYSTAL SYSTEM	triclinic
SPACE GROUP	P-1
UNIT CELL DIMENSIONS	a = 7.881 Å
	b = 10.672 Å
	c = 13.944 Å
	α = 97.259 °
	β = 101.242 °
	γ = 98.427 °
VOLUME	1123.3 Å^3
Z	2
DENSITY (CALCULATED)	1.831 Mg/m^3
ABSORPTION COEFFICIENT	5.484 mm^{-1}
F (000)	618
θ RANGE FOR DATA COLLECTION	2.27 to 24.64 °
INDEX RANGES	$0 \leq h \leq 9$
	$-12 \leq k \leq 12$
	$-14 \leq l \leq 14$
R	073

ATOMIC CO-ORDINATES (x 10⁴)

Equivalent Displacement Parameters (Å² x 10³) for 1

$U(eq) = ⅓$ of trace of orthogonalised U_{ij} tensor

ATOM	x	y	z	U(eq)
W (1)	1483(1)	3260(1)	2449(1)	43(1)
P (2)	2670(11)	2397(8)	3880(6)	46(2)
C (31)	1423(83)	1297(8)	4420(49)	94(14)
C (32)	579(121)	238(81)	3725(66)	124(22)
C (33)	4683(65)	1688(49)	3695(42)	77(11)
C (34)	5798(67)	1612(49)	4744(38)	78(11)
C (35)	3405(68)	3526(50)	4923(39)	78(11)
C (36)	2269(70)	4288(53)	5233(43)	82(11)
P (1)	-864(10)	2755(7)	1010(6)	46(2)
C (41)	-1837(48)	1198(36)	653(31)	60(8)
C (42)	-3117(69)	596(50)	1150(42)	83(12)
C (43)	-8(45)	3319(34)	-27(27)	53(7)
C (44)	1025(96)	2435(67)	-548(58)	95(17)
C45)	-2649(59)	3683(44)	928(42)	66(10)
C (46)	-4041(56)	3466(42)	221(34)	29(8)
S (2)	4352(10)	4161(6)	2543(6)	48(2)
S (1)	1040(11)	5342(8)	2404(7)	56(2)
C (11)	2971(35)	6366(28)	2452(24)	41(6)
C (12)	4550(44)	5721(32)	2474(27)	54(7)
C (13)	5946(46)	6450(33)	2557(28)	58(8)
C (14)	6109(76)	7672(60)	2442(48)	86(14)
C (15)	4669(61)	8307(45)	2422(37)	70(10)
C (16)	2938(73)	7523(48)	2329(42)	79(12)
C (1)	-455(35)	2950(26)	3036922)	42(6)
O (100)	-1758(33)	2698(24)	3340(20)	58(5)
C (2)	1918(49)	1649(36)	1873(32)	60(8)
O (200)	2284(33)	814(24)	1530(20)	59(6)

BOND LENGTHS (Å)

BOND	BOND LENGTH (Å)
W (1) - C (2)	1.91(4)
W (1) - C (1)	1.88(3)
W (1) - S (1)	2.306(9)
W (1) - S (2)	2.296(7)
W (1) - P (2)	2.387(8)
W (1) - P (1)	2.393(8)
P (2) - C (31)	1.76(6)
P (2) - C (35)	1.71(5)
P (2) - C (33)	1.90(5)
C (31) - C (32)	1.38(11)
C (33) - C (34)	1.57(7)
C (35) - C (36)	1.39(8)
P (1) - C (41)	1.69(4)
P (1) - C (45)	1.83(4)
P (1) - C (43)	1.84(4)
C (41) - C (42)	1.45(7)
C (43) - C (44)	1.54(8)
C (45) - C (46)	1.29(7)
S (2) - C (12)	1.67(3)
S (1) - C (11)	1.72(3)
C (11) - C(16)	1.27(6)
C (11) - C (12)	1.50(4)
C (12) - C (13)	1.23(5)
C (13) - C (14)	1.32(8)
C (14) - C (15)	1.40(7)
C (15) - C (16)	1.47(7)
C (1) - O (100)	1.19(4)
C (2) - O (200)	1.06(4)

BOND ANGLES (degrees)

ATOMS	BOND ANGLE
C (2) - W (1) - C (1)	108.0(2)
C (2) - W (1) - S (1)	153.1(13)
C (1) - W (1) - S (1)	89.6(8)
C (2) - W (1) - S (2)	89.9(12)
C (1) - W (1) - S (2)	150.7(9)
S (1) - W (1) - S (2)	82.8(3)
C (2) - W (1) - P (2)	78.2(13)
C (1) - W (1) - P (2)	77.4(9)
S (1) - W (1) - P (2)	126.4(3)
S (2) - W (1) - P (2)	84.4(3)
C (1) - W (1) - P (1)	79.7(12)
C (2) - W (1) - P (1)	79.5(9)
S (1) - W (1) - P (1)	84.3(3)
S (2) - W (1) - P (1)	127.5(3)
P (1) - W (1) - P (2)	140.8(3)
C (31) - P (2) - C (35)	96.0(3)
C (31) - P (2) - C (33)	107.0(3)
C (35) - P (2) - C (33)	105.0(2)
C (31) - P (2) - W (1)	124.0(2)
C (35) - P (2) - W·(1)	113.0(2)
C (33) - P (2) - W (1)	110.0(2)
C (32) - C (31) - P (2)	111.0(6)
C (34) - C (33) - P (2)	108.0(4)
C (36) - C (35) - P (2)	120.0(4)
C (41) - P (1) - C (45)	106.0(2)
C (41) - P (1) - C (43)	108.0(2)
C (45) - P (1) - C (43)	96.0(2)
C (41) - P (1) - W (1)	117.5(14)
C (45) - P (1) - W (1)	119.0(2)
C (43) - P (1) - W (1)	107.7(12)
C (461) - P (1) - W (1)	101.0(2)

ATOMS	BOND ANGLE
C (42) - C (41) - P (1)	122.0(3)
C (44) - C (43) - P (1)	116.0(4)
C (46) - C (45) - P (1)	125.0(4)
C (12) - S (2) - W (1)	111.3(12)
C (11) - S (1) - W (1)	111.7(10)
C (16) - C (11) - C (12)	125.0(3)
C (16) - C (11) - S (1)	120.0(3)
C (12) - C (11) - S (1)	115.0(2)
C (13) - C (12) - C (11)	115.0(3)
C (13) - C (12) - S (2)	125.0(3)
C (11) - C (12) - S (2)	120.0(2)
C (12) - C (13) - C (14)	125.0 (4)
C (15) - C (14) - C (13)	120.0(5)
C (14) - C (15) - C (16)	118.0(5)
C (11) - C (16) - C (15)	115.0(4)
O (100) - C (1) - W (1)	175.0(3)
O (200) - C (2) - W (1)	174.0(4)

Appendix Four

$[W(bdt)(CO)_2(dppe)]$
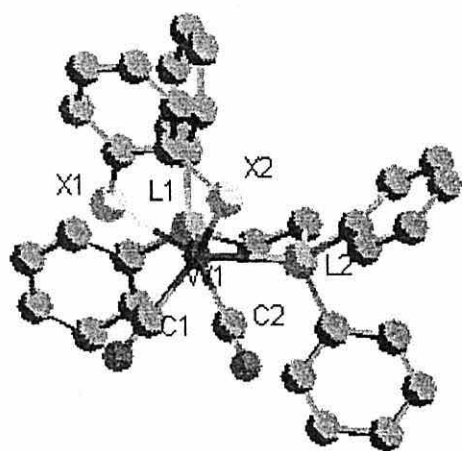
[W(bdt)(CO)₂(dppe)]

APPENDIX 4

THE CRYSTAL DATA AND STRUCTURE REFINEMENT FOR
W(bdt)(CO)$_2$(dppe)

EMPIRICAL FORMULA	$C_{34.5} H_{29} Cl O_2 P_2 S_2 W$
FORMULA WEIGHT	820.94
TEMPERATURE	293 (2) K
WAVELENGTH	0.71070 Å
CRYSTAL SYSTEM	monoclinic
SPACE GROUP	P21/n
UNIT CELL DIMENSIONS	a = 8.047 Å
	b = 18.581 Å
	c = 23.070 Å
	β = 93.22 °
VOLUME	3444.0 Å^3
Z	4
DENSITY (CALCULATED)	1.583 Mg/m^3
ABSORPTION COEFFICIENT	3.675 mm^{-1}
F (000)	1620
θ RANGE FOR DATA COLLECTION	2.08 to 25.20 °
INDEX RANGES	$0 \le h \le 9$
	$-21 \le k \le 21$
	$-27 \le l \le 27$
R	0663

ATOMIC CO-ORDINATES (x 10⁴)

Equivalent Displacement Parameters (Å² x 10³) for 1

U(eq) = ⅓ of trace of orthogonalised U_{ij} tensor

ATOM	x	y	z	U(eq)
W (1)	1257(1)	1231(1)	1715(1)	64(1)
C (1)	87(21)	1956(8)	2180(7)	67(4)
O (11)	-676(17)	2342(7)	2418(6)	102(4)
C (2)	697(22)	1990(9)	1154(8)	77(5)
O (12)	260(18)	2419(8)	821(6)	113(5)
P (1)	3045(6)	1233(2)	2622(2)	66(1)
P (2)	4019(5)	1651(2)	1398(2)	65(1)
S (1)	1009(6)	370(2)	957(2)	74(1)
C (11)	69(19)	-398(8)	1220(7)	70(4)
C (12)	-556(19)	-384(8)	1773(7)	71(4)
S (2)	-383(5)	375(2)	2207(2)	73(1)
C (3)	-182(23)	-1014(9)	875(8)	80(5)
C (4)	-897(27)	-1616(11)	1076(9)	97(6)
C (5)	-1495(27)	-1617(10)	1623(9)	99(6)
C (6)	-1255(22)	-1010(10)	1979(9)	86(5)
C (7)	4981(22)	1724(9)	2549(7)	76(4)
C (8)	5625(21)	1472(10)	1964(7)	78(1)
C (31)	3881(21)	357(8)	2806(7)	73(4)
C (32)	3842(24)	-207(9)	2426(8)	85(5)
C (33)	4597(27)	-890(11)	2558(9)	96(6)
C (34)	5346(27)	-976(12)	3095	99(6)
C (35)	5423(31)	-421(11)	3477(9)	111(7)
C (36)	4679(28)	240(11)	3346(9)	103(6)
C (41)	2155(21)	1554(8)	3278(7)	71(4)
C (42)	2457(28)	2249(10)	3471(8)	104(7)
C (43)	1627(38)	2550(13)	3903(11)	143(10)
C (44)	588(34)	2071(14)	4190(10)	126(8)
C (45)	325(39)	1392(13)	4019(11)	140(11)
C (46)	1018(30)	1125(10)	3540(9)	107(7)

ATOM	x	y	z	U(eq)
C (51)	4785(19)	1249(7)	748(6)	62(4)
C (52)	3851(21)	1331(9)	234(7)	72(4)
C (53)	4485(25)	1099(10)	-282(7)	85(5)
C (54)	5907(23)	740(9)	-288(7)	74(4)
C (55)	6872(25)	648(10)	219(8)	91(6)
C (56)	6373(23)	900(9)	744(6)	75(4)
C (61)	4422(18)	2593(8)	1293(7)	65(4)
C (62)	3587(22)	3123(8)	1596(7)	75(4)
C (63)	3993(29)	3846(10)	1568(11)	109(7)
C (64)	5239(34)	4060(12)	1175(11)	125(8)
C (65)	6020(26)	3550(10)	860(9)	95(6)
C (66)	5630(23)	2826(10)	914(7)	90(6)
Cl (1)	2606(21)	-270(9)	4927(7)	159(5)
C (2)	3380(65)	-1132(23)	4855(22)	117(14)
Cl (2A)	5127(42)	-1367(14)	5291(12)	125(8)
Cl (2B)	3965(33)	-1443(12)	5301(10)	102(6)

BOND LENGTHS (Å)

BOND	BOND LENGTH (Å)
W (1) - C (2)	1.95(2)
W (1) - C (1)	1.99(2)
W (1) - S (1)	2.368(4)
W (1) - S (2)	2.394(4)
W (1) - P (1)	2.472(4)
W (1) - P (2)	2.505(4)
C (1) - O (11)	1.11(2)
C (2) - O (12)	1.15(2)
P (1) - C (31)	1.80(2)
P (1) - C (41)	1.81(2)
P (1) - C (7)	1.82(2)
P (2) - C (61)	1.801(14)
P (2) - C (8)	1.82(2)

BOND	BOND LENGTH (Å)
P (2) - C (51)	1.813(14)
S (1) - C (1)	1.74(2)
C (1) - C (3)	1.40(2)
C (1) - C (2)	1.40(2)
C (2) - C (6)	1.39(2)
C (2) - S (2)	1.73(2)
C (3) - C (4)	1.35(2)
C (4) - C (5)	1.37(3)
C (5) - C (6)	1.40(3)
C (7) - C (8)	1.54(2)
C (31) - C (32)	1.37(2)
C (31) - C (36)	1.39(2)
C (32) - C (33)	1.43(2)
C (33) - C (34)	1.36(3)
C (34) - C (35)	1.36(3)
C (35) - C (36)	1.39(3)
C (41) - C (42)	1.38(2)
C (41) - C (46)	1.38(2)
C (42) - C (43)	1.35(3)
C (43) - C (44)	1.41(3)
C (44) - C (45)	1.33(3)
C (45) - C (46)	1.36(3)
C (51) - C (52)	1.38(2)
C (51) - C (56)	1.43(2)
C (52) - C (53)	1.39(2)
C (53) - C (54)	1.32(2)
C (54) - C (55)	1.38(2)
C (55) - C (56)	1.38(2)
C (61) - C (66)	1.41(2)
C (61) - C (62)	1.40(2)
C (62) - C (63)	1.38(2)
C (63) - C (64)	1.45(3)

BOND	BOND LENGTH (Å)
C (64) - C (65)	1.37(3)
C (65) - C (66)	1.39(2)
Cl (1) - C (2)	1.73(4)
C (2) - Cl (2B)	1.25(5)
C (2) - Cl (2A)	1.74(6)

BOND ANGLES (degrees)

ATOMS	BOND ANGLES
C (2) - W (1) - C (1)	76.6(7)
C (2) - W (1) - S (1)	89.6(5)
C (1) - W (1) - S (1)	146.2(5)
C (2) - W (1) - S (2)	133.1(6)
C (1) - W (1) - S (2)	84.5(4)
S (1) - W (1) - S (2)	82.84(14)
C (2) - W (1) - P (1)	131.4(5)
C (1) - W (1) - P (1)	79.2(5)
S (1) - W (1) - P (1)	130.3(2)
S (2) - W (1) - P (1)	84.85(14)
C (2) - W (1) - P (2)	75.8(5)
C (1) - W (1) - P (2)	113.5(4)
S (1) - W (1) - P (2)	92.02(13)
S (2) - W (1) - P (2)	150.3(2)
P (1) - W (1) - P (2)	76.26(14)
O (11) - C (1) - W (1)	175(2)
O (12) - C (2) - W (1)	175(2)
C (31) - P (1) - C (41)	105.0(8)
C (31) - P (1) - C (7)	99.5(8)
C (41) - P (1) - C (7)	107.1(7)
C (31) - P (1) - W (1)	112.9(6)
C (41) - P (1) - W (1)	118.0(6)
C(7) - P (1) - W (1)	112.5(6)

ATOMS	BOND ANGLES
C (61) - P (2) - C (8)	98.5(8)
C (61) - P (2) -C (51)	102.5(7)
C (8) - P (2) - C (51)	105.0(7)
C (61) - P (2) - W (1)	120.9(5)
C (8) - P (2) -W (1)	109.9(5)
C (51) - P (2) -W (1)	117.5(5)
C (1) - S (1) - W (1)	108.5(6)
C (3) - C (1) - C (2)	119.0(14)
C (3) - C (1) - S (1)	121.6(13)
C (2) - C (1) - S (1)	119.2(12)
C (6) - C (2) - C (1)	118(2)
C (6) - C (2) - S (2)	120.4(14)
C (1) - C (2) - S (2)	121.4(11)
C (2) - S (2) - W (1)	107.3(5)
C (4) - C (3) - C (1)	122(2)
C (3) - C (4) - C (5)	120(2)
C (6) - C (5) - C (4)	120(2)
C (2) - C (6) - C (5)	121(2)
C (8) - C (7) - P (1)	105.1(11)
C (7) - C (8) - P(2)	108.3(2)
C (32) - C (31) - (36)	11792)
C (32) - C (31) - P (1)	123.1(13)
C (36) - C (31) - P (1)	12.1914)
C (31) - C (32) - C (33)	123(2)
C (34) - C (33) - C (32)	118(2)
C (33) - C (34) - C (35)	120(2)
C (34) - C (35) - C (36)	122(2)
C (35) - C (36) - C (31)	120(2)
C (42) - C (41) - C (46)	121(2)
C (42) - C (41) - P (1)	120.3(13)
C (46) - C (41) - P (1)	118.7(12)
C (43) - C (42) - C (41)	123(2)

ATOMS	BOND ANGLES
C (42) - C (43) - C (44)	115(2)
C (45) - C (44) - C (43)	123(2)
C (46) - C (45) - C (44)	121(2)
C (45) - C (46) - C (41)	117(2)
C (52) - C (51) - C (56)	119.3(13)
C (52) - C (51) - P (2)	118.2(11)
C (56) - C (51) - P (2)	122.4(12)
C (53) - C (52) - C (51)	120(2)
C (54) - C (53) - C (52)	122(2)
C (53) - C (54) - C (55)	120(2)
C (54) - C (55) - C (56)	122(2)
C (55) - C (56) - C (51)	118(2)
C (66) - C (61) - C (62)	117.4(14)
C (66) - C (61) - P (2)	121.2(12)
C (62) - C (61) - P (2)	121.4(11)
C (63) - C (62) - C (61)	123(2)
C (62) - C (63) - C (64)	118(2)
C (65) - C (64) - C (63)	120(2)
C (64) - C (65) - C (66)	121(2)
C (61) - C (66) - C (65)	121(2)
Cl (2B) - C (2) - Cl (1)	118(4)
Cl (1) - C (2) - Cl (2A)	117(3)